Spring 5-16-2014

Analysis of Fault location methods on transmission lines

Sushma Ghimire
University Of New Orelans, sghimir1@uno.edu

Analysis of Fault Location Methods on Transmission Lines

A Thesis

Submitted to the Graduate Faculty of the
University of New Orleans
in partial fulfillment of the
requirements for the degree of

Master of Science
in
Engineering
Electrical

by
Sushma Ghimire

B.S. Tribhuvan University, 2006

May, 2014

ACKNOWLEDGEMENT

I would like to express my gratitude to my husband to support me throughout my academic career.

My sincere appreciation and gratitude goes to my professor Dr Parviz Rastagoufard, Dr Ittiphong Leevongwat and my friend Rastin Rastagoufard for his valuable advice, help and guidance throughout the course of this research. I am heartily thankful to the UNO faculty members who made this thesis possible.

I would like to thank my family members, particularly my father (Uttam Prasad Ghimire) and my mother (Subhadra Ghimire), and my closest friends, who have been a constant source of inspiration and encouragement.

Table of Contents

List of Figures

List of Tables

ABSTRACT

Analysis of different types of fault is an important and complex task in a power system. Accurate fault analysis requires models that determine fault distances in a transmission line. The mathematical models accurately capture behavior of different types of faults and location in a timely manner, and prevents damaging power system from fault energy. The purpose of this thesis is to use two methods for determining fault locations and their distance to the reference end buses connected by the faulted transmission line. The two methods used in this investigation are referred to as *impedance-based* and *traveling wave* methods. To analyze both methods, various types of faults were modeled and simulated at various locations on a two-bus transmission system using EMTP program. Application and usefulness of each method is identified and presented in the thesis. It is found that Impedance-based methods are easier and more widely used than traveling-wave methods.

Key words: Impedance based method, traveling wave method

Chapter 1

Introduction

Electricity produced by a power plant is delivered to load centers and electricity consumers through transmission lines held by huge transmission towers. During normal operation, a power system is in a balanced condition. Abnormal scenarios occur due to faults. Faults in a power system can be created by natural events such as falling of a tree, wind, and an ice storm damaging a transmission line, and sometimes by mechanical failure of transformers and other equipment in the system. A power system can be analyzed by calculating system voltages and currents under normal and abnormal scenarios [1].

A fault is define as flow of a large current which could cause equipment damage. If the current is very large, it might lead to interruption of power in the network. Moreover, voltage level will change, which can affect equipment insulation. Voltage below its minimum level could sometimes cause failure to equipment.

It is important to study a power system under fault conditions in order to provide system protection. *Analysis of Faulted Power System* by Paul Anderson and *Power System Analysis* by Arthur R.Bergen and Vijay Vittal offer extensive analysis in fault studies and calculations.

Background

The purpose of this research is to provide the overview of different methods to calculate the fault distance on a transmission line. Different methods based on two principles – impedance theory and traveling-wave theory are discussed throughout this paper. Widely used methods from both theories were implemented on a test system to calculate a fault distance under different types of faults. A comparative analysis was performed to compare the calculation errors in the implemented methods. In order to understand how to calculate the fault distance on a transmission line, the following topics need to be explained:

1.1. Symmetrical Components

1.2. Types of Fault

1.3. Use of Symmetrical components for fault analysis

1.4. Wave on Transmission Lines

1.1. Symmetrical Components [1]

Power systems are always analyzed using per-phase representation because of its simplicity. Balanced three-phase power systems are solved by changing all delta connections to equivalent wye connections and solving one phase at a time. The remaining two phases differ from the first by 120°. To analyze an unbalanced system, the system is transformed into its symmetrical components for per-phase analysis.

Charles Legeyt Fortescue developed a theory which suggests that an unbalanced system can be well defined using the symmetrical components. These three symmetrical components are positive sequence, negative sequence and zero sequence. They are represented by "+", "-", and "0" or "1", "2", and "0" for positive, negative and zero sequence respectively.

1.1.1. Positive Sequence: It consists of three phasors with equal magnitudes and 120° apart from each other. The phase sequence are in the same order of original phasors.

1.1.2. Zero Sequence: It consists of three phasors with equal magnitudes and zero phase displacement.

1.1.3. Negative Sequence: It consists of three phasors with equal magnitudes and 120° apart from each other. The phase sequence are in the opposite order of original phasors.

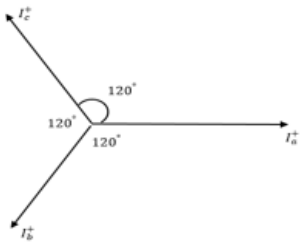

Figure 1.1: Positive Sequence

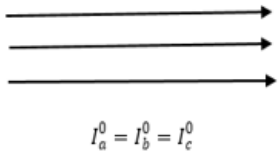

Figure 1.2: Zero Sequence

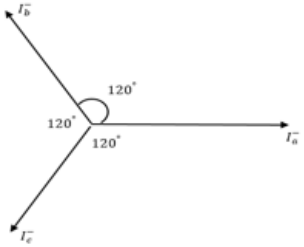

Figure 1.3: Negative Sequence

Let's take an arbitrary set of three phasors I_a, I_b, and I_c. It can be represented in terms of nine symmetrical components as follows:

$$I_a = I_a^0 + I_a^+ + I_a^- \quad (1.1)$$
$$I_b = I_b^0 + I_b^+ + I_b^-$$
$$I_c = I_c^0 + I_c^+ + I_c^-$$

Where I_a^0, I_b^0, and I_c^0 are a zero sequence set; I_a^+, I_b^+, and I_c^+ are a positive sequence set; and I_a^-, I_b^-, and I_c^- are a negative sequence set. The zero sequence set has equal magnitude phasors with zero phase displacement and carries the following property:

$$I_a^0 = I_b^0 = I_c^0 \tag{1.2}$$

A matrix form of equation (1.1) is written as equation (1.3).

$$\begin{bmatrix} I_a \\ I_b \\ I_c \end{bmatrix} = \begin{bmatrix} I_a^0 \\ I_b^0 \\ I_c^0 \end{bmatrix} + \begin{bmatrix} I_a^+ \\ I_b^+ \\ I_c^+ \end{bmatrix} + \begin{bmatrix} I_a^- \\ I_b^- \\ I_c^- \end{bmatrix} \tag{1.3}$$

Let $\mathbf{I}$ be the current vector having components I_a, I_b and I_c. Therefore $\mathbf{I}^0, \mathbf{I}^+$ and $\mathbf{I}^-$ are the zero sequence set, positive sequence set, and negative sequence set respectively.

Vector notation of equation (1.3) is

$$\mathbf{I} = \mathbf{I}^0 + \mathbf{I}^+ + \mathbf{I}^-$$

Now to find the nine symmetrical components, taking $\alpha = e^{\frac{j2\pi}{3}} = 1\angle 120°$. Multiplying complex number $\mathbf{I}$ by α gives the magnitude unchanged but increased the angle by $120°$. That means it rotates $\mathbf{I}$ by positive angle of $120°$. So, only three of the nine symmetrical components may be chosen independently. Taking I_a^0, I_a^+ and I_a^- as independent variables and expressing other terms as lead variables. Applying to equation (1.4), we get

$$\begin{bmatrix} I_a \\ I_b \\ I_c \end{bmatrix} = I_a^0 \begin{bmatrix} 1 \\ 1 \\ 1 \end{bmatrix} + I_a^+ \begin{bmatrix} 1 \\ \alpha^2 \\ \alpha \end{bmatrix} + I_a^- \begin{bmatrix} 1 \\ \alpha \\ \alpha^2 \end{bmatrix} \tag{1.4}$$

Where,

$a = 1\angle 120° = -0.5 + j0.866$

$a^2 = 1\angle 240° = -0.5 - j0.866$

Equation (1.4) is equivalent to:

$$\begin{bmatrix} I_a \\ I_b \\ I_c \end{bmatrix} = \begin{bmatrix} 1 & 1 & 1 \\ 1 & \alpha & \alpha^2 \\ 1 & \alpha^2 & \alpha \end{bmatrix} \begin{bmatrix} I_a^0 \\ I_a^+ \\ I_a^- \end{bmatrix} = A \begin{bmatrix} I_a^0 \\ I_a^+ \\ I_a^- \end{bmatrix} \tag{1.5}$$

Then,

$$\begin{bmatrix} I_a^0 \\ I_a^+ \\ I_a^- \end{bmatrix} = \frac{1}{3} \begin{bmatrix} 1 & 1 & 1 \\ 1 & \alpha & \alpha^2 \\ 1 & \alpha^2 & \alpha \end{bmatrix} \begin{bmatrix} I_a \\ I_b \\ I_c \end{bmatrix} = A^{-1} \begin{bmatrix} I_a \\ I_b \\ I_c \end{bmatrix} \tag{1.6}$$

Now, we get

$$I_a^0 = \frac{1}{3}\,(I_a + I_b + I_c) \tag{1.7}$$

$$I_a^+ = \frac{1}{3}\,(I_a + \alpha I_b + \alpha^2 I_c) \tag{1.8}$$

$$I_a^- = \frac{1}{3}\,(I_a + \alpha^2 I_b + \alpha I_c) \tag{1.9}$$

Equations (1.7), (1.8) and (1.9) presents the zero sequence, the positive and the negative sequence current respectively. Similarly, the zero sequence, the positive sequence and the negative sequence voltage is presented by equations (1.10), (1.11) and (1.12) respectively.

$$V_a^0 = \frac{1}{3}\,(V_a + V_b + V_c) \tag{1.10}$$

$$V_a^+ = \frac{1}{3}\,(V_a + \alpha V_b + \alpha^2 V_c) \tag{1.11}$$

$$V_a^- = \frac{1}{3}\,(V_a + \alpha^2 V_b + \alpha V_c) \tag{1.12}$$

Equations (1.10), (1.11) and (1.12) can be written in matrix form as

$$\begin{bmatrix} V_a^0 \\ V_a^+ \\ V_a^- \end{bmatrix} = \frac{1}{3}\begin{bmatrix} 1 & 1 & 1 \\ 1 & \alpha & \alpha^2 \\ 1 & \alpha^2 & \alpha \end{bmatrix}\begin{bmatrix} V_a \\ V_b \\ V_c \end{bmatrix} \tag{1.13}$$

1.2. Types of faults

There are two types of faults which can occur on any transmission lines; balanced fault and unbalanced fault also known as symmetrical and asymmetrical fault respectively. Most of the faults that occur on the power systems are unbalanced faults. In addition, faults can be categorized as shunt faults and series faults [1]. Series faults are those type of faults which occur in impedance of the line and does not involve neutral or ground, nor does it involves any interconnection between the phases. In this type of faults there is increase of voltage and frequency and decrease of current level in the faulted phases. Example: opening of one or two lines by circuit breakers. Shunt faults are the unbalance between phases or between ground and phases. This research only consider shunt fault. In this type of faults there is increase of current and decrease of frequency and voltage level in the faulted phases. The shunt faults can be classified into four types [1]:

1.2.1 Phase to ground fault

In this type of fault, any one line makes connection with the ground.

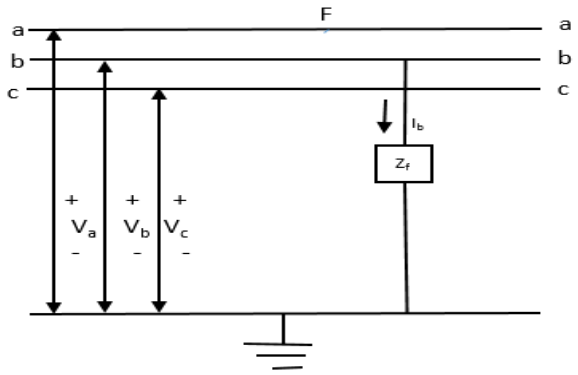

Figure 1.4: Single Phase to ground fault

1.2.2 Phase to Phase fault

In this type of fault, there established the connection between the phases.

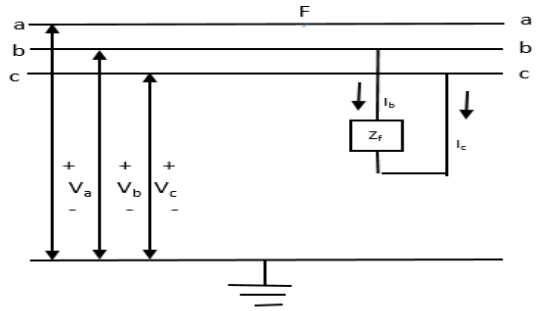

Figure 1.5: Phase to Phase fault

1.2.3. Double Phase to ground fault

In this type of fault, two phases established the connection with the ground.

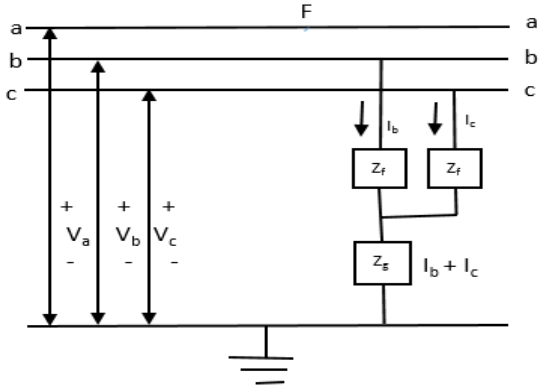

Figure 1.6: Double phase to ground fault

1.2.4. Three phase fault

In this type of fault, three phase makes connection with the ground. This is severe fault.

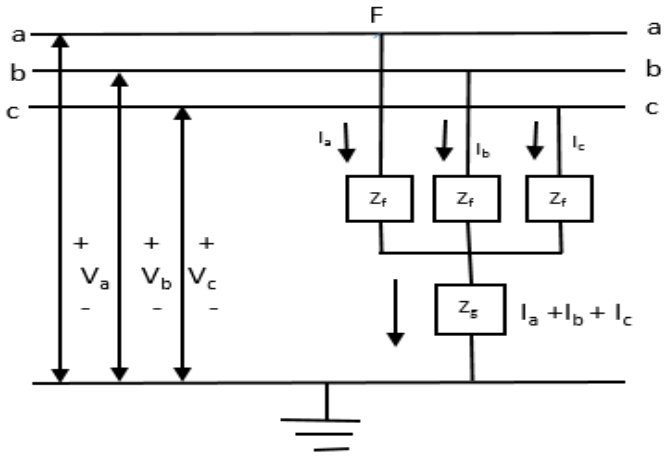

Figure 1.7: 3phase fault

1.3. Use of Symmetrical components for fault analysis [2]

Faulted power systems do not have three phase symmetry, so it cannot be solved by per phase analysis. To find fault currents and fault voltages, it is first transformed into their symmetrical components. This can be done by replacing three phase fault current by the sum of a three phase zero sequence source, a three phase positive sequence source and a three phase negative sequence source. Each circuit is solved by per phase analysis called a *sequence network*.

The voltage equations and current equations in sequence components are already discussed in section 1.1. In this section, all the sequence components of fault voltages and currents for all faults types are determined.

1.3.1 Sequence Network for Single Phase to Ground Fault

Assuming that fault current (I_f)occurred on the phase a with fault impedance (Z_f) . The voltages and currents at the point of fault are $V_a = Z_f I_a, I_b = 0, I_c = 0$

Voltage equation similar to equation (1.1) is

$$V_a = V_a^0 + V_a^+ + V_a^-$$
$$= Z_f I_a$$

Since fault current in the phase b and the phase c is zero, equation (1.6) will be,

$$\begin{bmatrix} I_a^0 \\ I_a^+ \\ I_a^- \end{bmatrix} = \frac{1}{3}\begin{bmatrix} 1 & 1 & 1 \\ 1 & \alpha & \alpha^2 \\ 1 & \alpha^2 & \alpha \end{bmatrix}\begin{bmatrix} I_a = I_f \\ I_b = 0 \\ I_c = 0 \end{bmatrix}$$

$$I_a^0 = I_a^+ = I_a^- = \frac{I_f}{3} \quad (1.14)$$

It implies that the sequence current are equal and sequence network must be connected in series. The sequence voltage add to $3Z_f I_a^+$

$$I_a^0 = I_a^+ = I_a^- = \frac{V_f}{Z_0+Z_1+Z_2+3Z_f} \quad (1.15)$$

Where,

Z_0, Z_1, Z_2 are a zero, a positive and a negative sequence impedance.

Equation (1.15) is used to find out sequence fault voltage.

1.3.2 Sequence Network for Double phase to ground fault

Assuming the phase b and the phase c are connected to the ground through the fault impedance (Z_f).

So, fault current on phase a, $I_a = 0$

Since the phase b and the phase c make connection, fault voltages at phase b and phase c are

$$V_b = V_c = Z_f(I_b + I_c) \quad (1.16)$$

Fault currents is present in the phase b and the phase c, equation (1.6) will be

$$\begin{bmatrix} I_a^0 \\ I_a^+ \\ I_a^- \end{bmatrix} = \frac{1}{3}\begin{bmatrix} 1 & 1 & 1 \\ 1 & \alpha & \alpha^2 \\ 1 & \alpha^2 & \alpha \end{bmatrix}\begin{bmatrix} I_a = 0 \\ I_b \\ I_c \end{bmatrix}$$

We get, $I_a^0 = \frac{1}{3}(I_b + I_c)$ (1.17)

$$V_b = V_c = Z_f 3I_a^0 \quad (1.18)$$

$$\begin{bmatrix} V_a^0 \\ V_a^+ \\ V_a^- \end{bmatrix} = \frac{1}{3}\begin{bmatrix} 1 & 1 & 1 \\ 1 & \alpha & \alpha^2 \\ 1 & \alpha^2 & \alpha \end{bmatrix}\begin{bmatrix} V_a \\ 0 \\ 0 \end{bmatrix} \quad (1.19)$$

Equation (1.19) implies that

$$V_a^0 = V_a^+ = V_a^-$$

$$I_a^0 + I_a^+ + I_a^- = 0$$

Since the zero, the positive and the negative sequence voltages are equal which imply that the sequence networks must be in parallel.

$$V_a^0 = \frac{1}{3}(V_a + V_b + V_c) \quad (1.20)$$

Since $V_b = V_c$

$$3V_a^0 = (V_a + 2V_b) = V_a^0 + V_a^+ + V_a^- + 2\left(Z_f 3I_a^0\right) \quad (1.21)$$

From (1.18), we get, $V_a^+ = V_a^-$

$$3V_a^0 = V_a^0 + 2V_a^+ + 2\left(Z_f 3I_a^0\right) \quad (1.22)$$

$$2V_a^0 - 2\left(Z_f 3I_a^0\right) = 2V_a^+ \quad (1.23)$$

$$\therefore V_a^+ = V_a^0 - \left(3Z_f I_a^0\right) \quad (1.24)$$

Fault current, $I_a^+ = \frac{V_f}{Z_1 + \left[\frac{Z_2\left(Z_0 + 3Z_f\right)}{Z_2 + Z_0 + 3Z_f}\right]}$ (1.25)

$$I_a^0 = -\frac{Z_2}{Z_2 + Z_0 + 3Z_f} I_a^+ \quad (1.26)$$

$$I_a^- = -\frac{Z_0 + Z_f}{Z_2 + Z_0 + 3Z_f} I_a^+ \quad (1.27)$$

In this way sequence current and voltage are calculated for double phase to ground fault.

1.3.3 Sequence Network for Phase to Phase Fault

Assume fault current (I_f) occur when the phase b and the phase c make connection with each other and taking Z_f as the fault impedance.

$$V_b - V_c = I_b Z_f \quad (1.28)$$

Since the phase c makes connection the phase b, at point of connection $V_b = V_c$

Equation (1.13) can be written as

$$\begin{bmatrix} V_a^0 \\ V_a^+ \\ V_a^- \end{bmatrix} = \frac{1}{3}\begin{bmatrix} 1 & 1 & 1 \\ 1 & \alpha & \alpha^2 \\ 1 & \alpha^2 & \alpha \end{bmatrix}\begin{bmatrix} V_a \\ V_b = V_c \\ V_c \end{bmatrix} \quad (1.29)$$

Equation (1.29) implies that

$$V_a^+ = V_a^- \quad (1.30)$$

Since fault current is present in the phase b and the phase c only, equation (1.6) will be

$$\begin{bmatrix} I_a^0 \\ I_a^+ \\ I_a^- \end{bmatrix} = \frac{1}{3}\begin{bmatrix} 1 & 1 & 1 \\ 1 & \alpha & \alpha^2 \\ 1 & \alpha^2 & \alpha \end{bmatrix}\begin{bmatrix} 0 \\ I_f \\ -I_f \end{bmatrix} \quad (1.31)$$

Equation (1.31) implies that

$$\mathrm{I_a^0} = 0 \text{ and } \mathrm{I_a^+} = -\mathrm{I_a^-} \quad (1.32)$$

From Equation (1.24) we get,

$$I_a^+ = \frac{1}{3}(\alpha - \alpha^2)I_f = \frac{jI_f}{\sqrt{3}}$$

$$\therefore I_f = -j\sqrt{3}\, I_a^+ \tag{1.33}$$

In this way sequence voltages and currents are calculated for the phase to phase fault.

1.4 Waves on Transmission Lines [2]

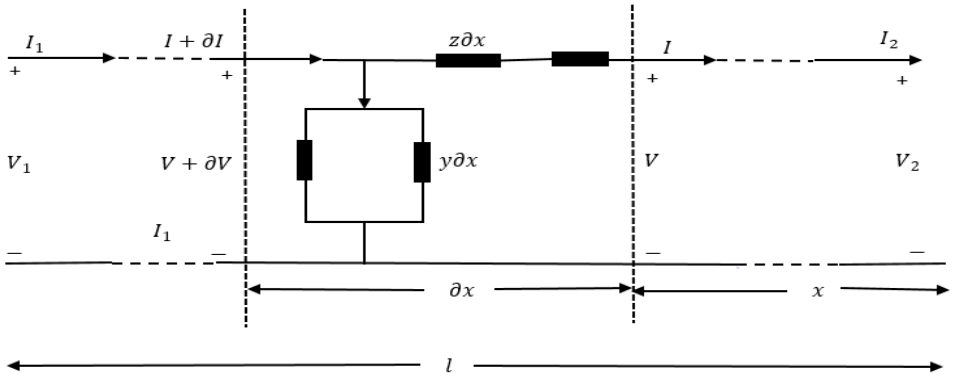

Figure 1.8: Transmission Line

Considering the above transmission line in the sinusoidal steady state. Assuming series impedance per meter and shunt admittance per meter to neutral are

$$z = r + j\omega l \tag{1.34}$$

$$y = g + j\omega c \tag{1.35}$$

From figure 1.8, V_1, I_1 are the per phase terminal voltages and currents at left and V_2, I_2 are the per phase terminal voltage and current at right. Considering a small section of line length ∂x .Taking the series impedance and the shunt admittance of ∂x are $z\partial x \; and \; y\partial x$ respectively. The receiving end at right side is located at x=0 and the sending end at left side is at x=l. Applying Kirchhoff's voltage law and Kirchhoff's current law to ∂x

$$\partial V = Iz\partial x \tag{1.36}$$

$$\partial I = (V + \partial V)y\partial x \approx Vy\partial x \tag{1.37}$$

Equations (1.36) and (1.37) are rewritten as

$$\frac{\partial V}{\partial x} = Iz \tag{1.38}$$

$$\frac{\partial I}{\partial x} = Vy \tag{1.39}$$

Second-order of equations (1.38) and (1.39) are written as

$$\frac{\partial^2 V}{\partial x^2} = yzV = \gamma^2 V \tag{1.40}$$

$$\frac{\partial^2 I}{\partial x^2} = yzI = \gamma^2 I \tag{1.41}$$

$\gamma \triangleq \sqrt{yz}$, where γ called the propagation constant, it is complex value.

The characteristic roots of the characteristic equation $s^2 - \gamma^2 = 0$ are

$$s_1, s_2 = \pm\gamma$$

The general solution for V is,

$$V = k_1 e^{\gamma x} + k_2 e^{-\gamma x} \tag{1.42}$$

$$= (k_1 + k_2)\frac{e^{\gamma x} + e^{-\gamma x}}{2} + (k_1 - k_2)\frac{e^{\gamma x} - e^{-\gamma x}}{2} \tag{1.43}$$

$$= K_1 \cosh \gamma x + K_2 sinh\gamma \tag{1.44}$$

Where,

$$K_1 = k_1 + k_2,\ K_2 = k_1 - k_2 \tag{1.45}$$

Similar equation for current I

$$I = K_1 \cosh \gamma x + K_2 sinh\gamma x \tag{1.46}$$

From figure 1.8, at $x = 0, V = V_2, I = I_2$ which implies that $K_1 = V_2$

Applying this to equation (1.38) and (1.39), we get

$$\frac{\partial \mathrm{V(x=0)}}{\partial \mathrm{x}} = \mathrm{I_2 z} \tag{1.47}$$

$$\frac{\partial \mathrm{I(x=0)}}{\partial \mathrm{x}} = \mathrm{V_2 y} \tag{1.48}$$

Differentiating equation (1.45) and (1.46) with respect to ∂x

$$\frac{\partial V}{\partial x} = -K_1 \gamma \sinh \gamma x + K_2 \gamma cosh\gamma x \tag{1.49}$$

$$\frac{\partial I}{\partial x} = -K_1 \gamma \sinh \gamma x + K_2 \gamma cosh\gamma x \tag{1.50}$$

Equating (1.49) with (1.47), we get

$$\mathrm{K_2 = \frac{z}{\gamma} I_2 = \frac{z}{\sqrt{yz}} I_2 = \sqrt{\frac{z}{y}} I_2 = Z_c I_2} \tag{1.51}$$

Equating (1.50) with (1.48), we get

$$K_2 = \frac{y}{\gamma} V_2 = \frac{y}{\sqrt{yz}} V_2 = \sqrt{\frac{y}{z}} V_2 = \frac{V_2}{Z_c} \tag{1.52}$$

Where,

$Z_c \triangleq \sqrt{\frac{z}{y}}$ is called the characteristic impedance of the line

Placing the value of K_2 in (1.44) and (1.46), we get

$$V = V_2 \cosh \gamma x + Z_c I_2 sinh\gamma \quad (1.53)$$

$$I = I_2 \cosh \gamma x + \frac{V_2}{Z_c} sinh\gamma x \quad (1.54)$$

When $x = l$, the per phase voltages and the per phase currents at the end of transmission lines are

$$V_1 = V_2 \cosh \gamma l + Z_c I_2 sinh\gamma l \quad (1.55)$$

$$I_1 = I_2 \cosh \gamma l + \frac{V_2}{Z_c} sinh\gamma l \quad (1.56)$$

In the figure 1.8, right side is load and equation (1.55) and (1.56) gives us voltage and current of supply side i.e. left side in the fig 1.8 to satisfy load requirement.

From equation (1.42), we see that the phasor voltage V has two terms $k_1 e^{\gamma x}$ and $k_2 e^{-\gamma x}$. The first term $k_1 e^{\gamma x}$ is actually a voltage wave traveling to the right (incident wave) and $k_2 e^{-\gamma x}$ is a voltage wave traveling to the left. The wave traveling to the left is the reflected wave. The propagation constant and the characteristic impedance are important parameters of the transmission line in terms of incident waves and reflected waves.

Propagation constant $(\gamma) \triangleq \alpha + j\beta$

Where,

α is the attenuation constant which has an influence on amplitude of the traveling wave and $\alpha \geq 0$.

β is the phase constant and it has influence on phase shift of the traveling wave.

Substituting γ in (1.42) and finding the instantaneous voltage as a function of t and x,

$$v(t,x) = \sqrt{2} Re k_1 e^{\alpha x} e^{j(\omega t + \beta x)} + \sqrt{2} Re k_1 e^{-\alpha x} e^{j(\omega t - \beta x)} \quad (1.57)$$

$$= v_1(t,x) + v_2(t,x) \quad (1.58)$$

If we take a small length of line we can neglect α and taking only $v_2(t,x)$, v_2 is a sinusoidal function of t for fixed value of x and also sinusoidal function of x for fixed value of t. As t increases, the voltage v_2 at points x also increases with following formula.

$$\omega t - \beta x = constant \quad (1.59)$$

Here v_2 remains constant. A voltage wave traveling to the left with a velocity

$$\frac{\partial x}{\partial t} = \frac{\omega}{\beta} = \frac{\omega}{Im\sqrt{zy}} \quad (1.60)$$

The reason the wave is travelling to the left is that increasing x means moving from right to left. The effect of the neglected term $e^{-\alpha x}$ is to attenuate the wave when it moves to the left. This wave is the reflected wave.

Similarly, if we consider a line of infinite length, $\alpha > 0$ that means there is no reflected wave.

1.4.1 Wavelet Transform [41]

Wavelet transform is a linear transformation like fourier transform. It decomposes the signal into different frequency and also can locate the time of each frequency. In power systems there are many non-periodic signals that may contain sinusoidal and impulse transient components. For such types of signals time-frequency resolution is needed. The spectrum of those signals cannot be extracted by fast fourier transform. To overcome the limitation of fast fourier transform, wavelet analysis is used. Wavelet Transform is suited for wideband signals. It has a multi resolution property that it will adjust time-widths to its frequency. Higher frequency wavelets will narrow, and lower frequency will widen. Due to this property it is useful for analyzing high frequency superposed on power frequency signals.

Continuous Wavelet Transform of signal $f\ (t)$ is given by

$$WT(f, a, b) = \frac{1}{\sqrt{a}} \int_{\infty}^{\infty} f(t)\, \Psi^* \left(\frac{t-b}{a}\right) \partial t \quad (1.61)$$

Where,

a is the scaling (dilation) constant and b is time shift constant.

Ψ is the mother wavelet function, and asterisk tells us that it is complex conjugate.

In continuous wavelet transform, the mother wavelet is continuously dilated and translated. This will produce substantial redundant information. Scaling parameter a is inversely proportional to frequency. If a is large, mother wavelet is low frequency, and if a is small, mother wavelet is high frequency. From figure 1.9 it is clear that high scales provide global information of the wave whereas low scales provide the detail information of the wave.

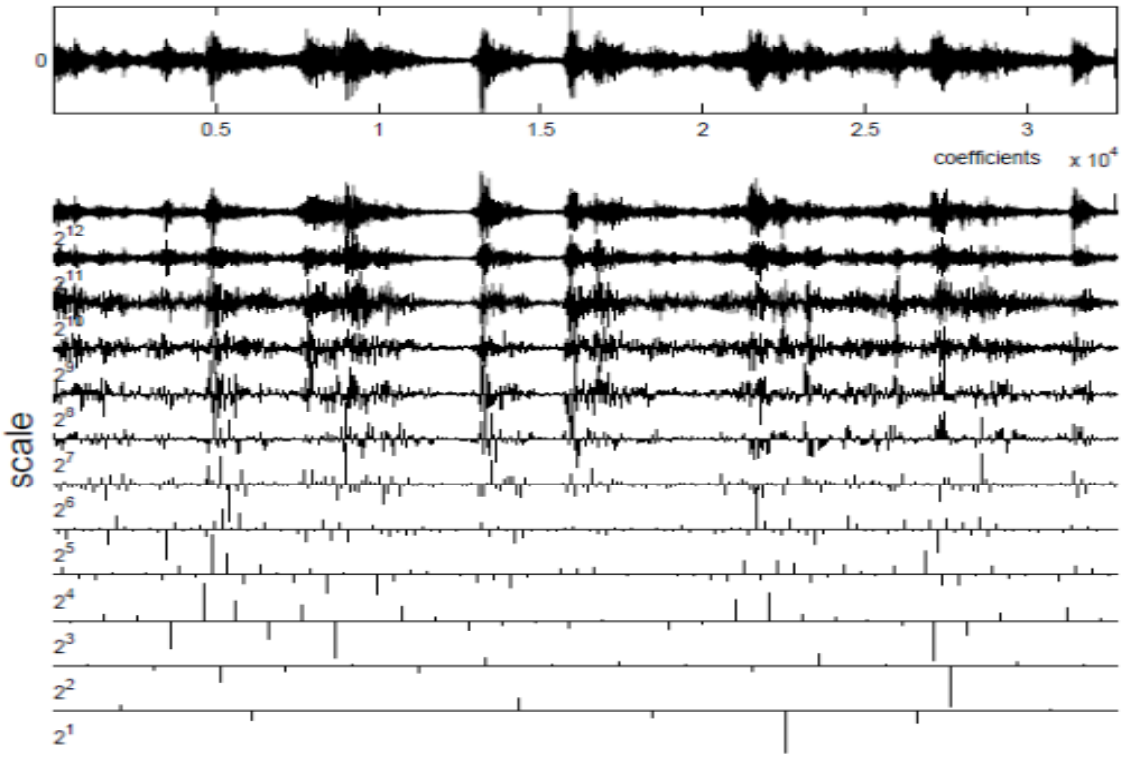

Figure 1.9: The top figure is the original signal. The figures below demonstrate the detail wavelet coefficients at different scaling levels [14]

Discrete wavelet transform is used to find wavelet transform of samples waveforms.

Corresponding Discrete wavelet transform (DWT) is given by

$$DWT(f,m,n) = \frac{1}{\sqrt{a_o^m}} \sum_m f(m)\, \Psi^* \left(\frac{n - k a_o^m}{a_o^m} \right) \qquad (1.62)$$

Where,

a , b of (1.61) are replaced by a_o^m and $k a_o^m$ respectively.

k , m are the integers.

a_0 , b_0 fixed constant and $a_0 > 1 \; and \; b_0 > 0$.

Discrete wavelet transform based on filter bank is shown in figure 1.10.

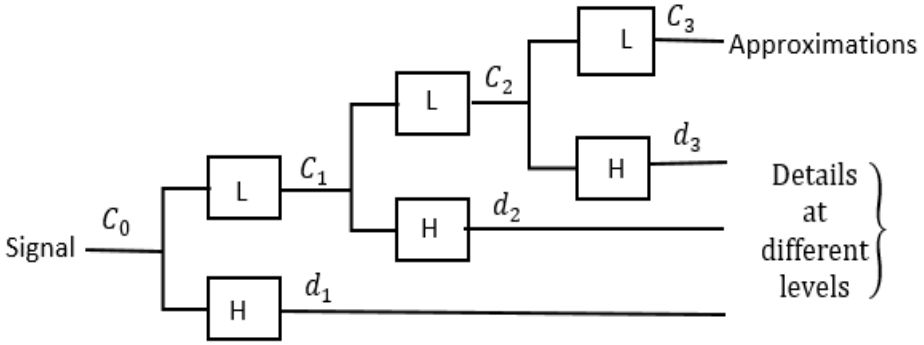

Figure 1.10: Filter bank interpretation of discrete wavelet transform [41]

Figure 1.10 shows that discrete wavelet transform has band-pass and low-pass filters at each scaling stage. Signal C_0 is decomposed by high pass and low pass filters into two signals C_1 and d_1 at scale1. C_1 is a smoothed version of the original signal. It contains only low frequency components. Wavelet transform coefficient d_1 is a detailed version of original signal [41]. Since it is filtered by a band pass filter it has higher frequency components. $d_1$is also the difference between the original signals C_0 and C_1. The number of samples in C_1 and $d_1$are half that of C_0 for the same observation period because high pass and low pass filters decomposed a signal by the factor two [41]. Signal d_1 has detail occurrence of disturbance. Scale 2 decomposition is done in same way to the signal C_1[41]. Similarly, C_2 is a smoothed version of C_1 and C_3 is a smoothed version of C_2. The number of samples at scale 2 is half that of scale 1 and the number of samples at scale 3 is half that of scale 2, but the observation period is the same for all scales as in figure 1.11. The mother wavelet oscillates rapidly within a short period of time at scale 1. In this way the signal is dilated with different resolutions at different levels for better observation of the disturbance event. At higher scales due to the dilation of the signals, mother wavelet oscillates less. So mother wavelet become less localized in time at higher scales. For that reason, fast and short transient disturbances are detected at lower scales. Similarly, long and slow transient disturbances are detected at higher scales.

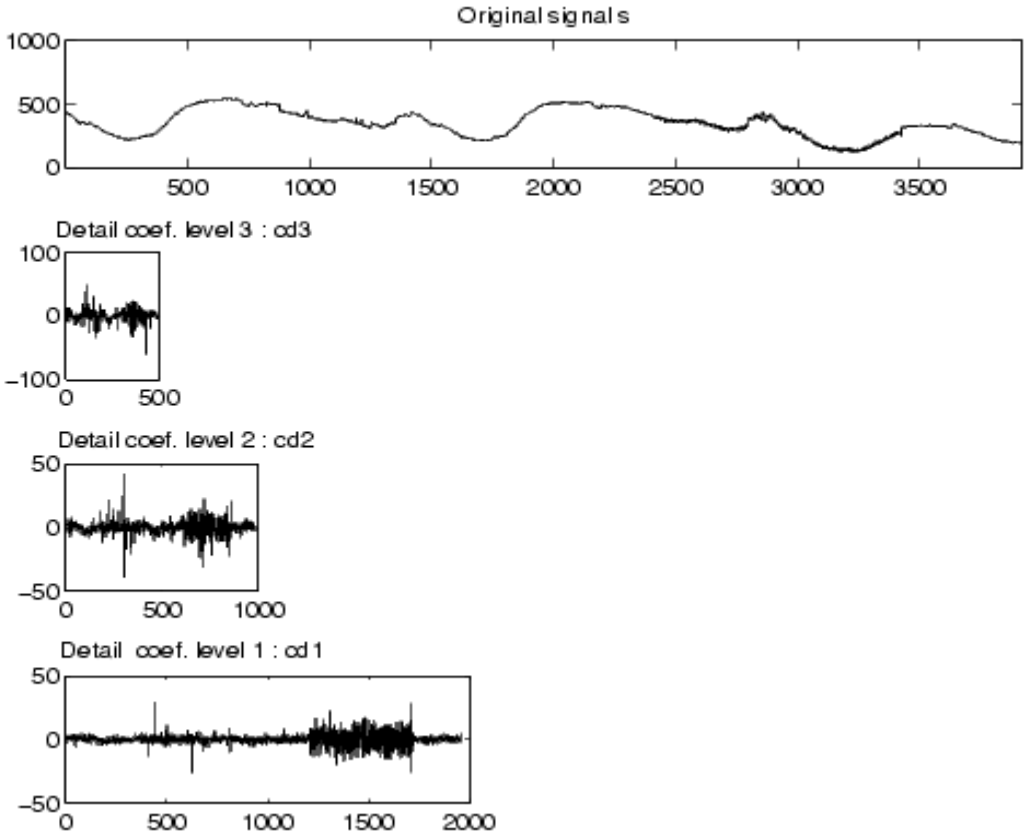

Figure 1.11: The top figure is the original signal. The figures demonstrate the decomposing of signal into three scales [42]

Figure 1.11 shows the decomposition of the original signals into three scale levels. At each scale, the number of samples is half that of the previous level. The original signal has 4000 samples. At level 1 there are 2000 samples. At level 3 there are 1000 and 500 at level 3.

.

Chapter 2

Review of existing fault distance calculation on transmission lines

Faults on transmission lines need be found out as quickly as possible otherwise they can destroy whole power systems. Generally, fault location methods can be classified into traveling-wave technique, knowledge based technique and impedance based technique.

In this research, only two methods were discussed. They are traveling wave and impedance based method. Results from both methods were compared. In this chapter, past published papers used to calculate the fault distance on a transmission line based on above methods were discussed.

2.1 Review of existing fault distance calculation using impedance based method

Impedance based method uses the fundamental frequency of voltage and current phasors from installed transducers such as numerical relays and fault recorders. Under this technique, phasor voltage and current can be taken from both terminals or from single terminal of a transmission line. Two-terminal algorithm provide more accurate results compared to single-end algorithm because this two-terminal algorithm is not affected by fault resistance and reactance. Phasor voltage and current data can be collected from two-ends of a transmission line either by synchronized or unsynchronized. Synchronized data can be collected using GPS, PMU. For the unsynchronized data, users have to first compute the synchronization error and fault location is calculated. Since the synchronized method has to use the communication device, it is more expensive than the unsynchronized method.

Impedance based method is widely used because of its simplicity and low cost. M.T. Sant et al. in 1979 introduced the online digital fault locator which measures the ratio of reactance of the line from the device to fault point [46]. After calculating the line impedance per unit length, the fault distance on the line is calculated. If fault distance is calculated on the measurement of reactance from one end of the line, accurate fault location cannot be determined because of fault resistance. If the fault is ungrounded, fault resistance will be small and it does not affect the precision of the fault location. In case of grounded fault, fault resistance will be high and it will affect the fault location. Wiszniewski in 1983 presented the

new method which eliminate above error [15]. Fault distance is calculated by measuring the reactance at one end of the line. The author calculates the phase shift between the total current at one end of the line and current flowing through fault resistance. T. Takagi et al. in 1981 developed a new method which used current and voltage data from one terminal to calculate fault distance on lines [53, 18]. A similar technique was proposed in [46, 47, and 53]. This method turned out to be inaccurate when fault resistance was present and fault currents were contributed from both ends of the line. In 1988, M.S. Sachdev and R. Agarwal proposed new fault location technique [4]. This method used post fault voltage and current from two end terminals which were not required to be synchronized. The same technique was proposed by D. Novosel et al. in 1996 [8]. Similarly, the author of [22] proposed a method for multi-terminal single transmission lines using asynchronous samples from each terminal. In 1992, the author of [19] proposed a fault location technique for multi-terminal two parallel transmission lines. In 1981 the author of [16] and in 1982 the author of [17] suggested a fault location method using synchronized voltage and current from both end terminals of lines. Later on, more papers [7, 20, and 52] were issued following the same techniques for fault location calculation. M. Kezunovic et al. in 1996 introduced new fault location method. A digital fault recorder was equipped with Global Positioning System (GPS) to retrieve synchronized data from two end terminals [5]. This reduced the computational burden. The solution was found to be more accurate. The voltage and current samples from both ends were taken at a sufficiently high sampling rate. Fault location technique proposed in [6] used Phasor Measurement Unit (PMU) at both ends of a line to get synchronized voltage and current data from both ends. In 1992, Adly A. Girgis et al. [7] proposed fault location algorithm applicable for two and three terminal lines. In this method they considered synchronization errors in sampling the voltage and current from two ends of the line. The author of [21] developed a fault location algorithm based on voltage and current data from single-end terminals and two-end terminals of transmission lines. In [8] data were taken from unsynchronized two-terminal lines to calculate fault location on a line. In [9] the samples of voltages and currents at both ends of line were taken synchronously and used to calculate fault location. In [10], fault location algorithm was based on synchronized samples of voltage and current data from two ends of the line. [11]

presented a new fault location algorithm based on phasor measurement units (PMUs) for series compensated lines. The technique used in [12,13,15,18,47,51,53] used voltage and current samples from one end of the line and the technique used in [4,7,20,49,52] used voltage and current samples from both ends of the line. These techniques were dependent on types of fault. Fault resistance and line capacitance were neglected, and balanced pre-fault loading condition were considered. The author of [23] proposed a new concept called 'distance factor'. The algorithm he used to calculate fault location was independent of fault, pre-fault currents, fault type, fault resistance, synchronization of fault locator placed at both ends of the line and pre-fault condition either balanced or not. The procedure was based on fundamental components of fault and pre-fault voltage at two ends of a transmission line. The author of [20] described a very accurate fault location technique which used post-fault voltage and current from both terminals. This technique was applicable to untransposed lines. [4, 48-51] techniques were applicable for the transposed lines. The author of [24] proposed fault location algorithms which used data from one end of the transmission line. This algorithm required only current signals as input data.

2.2 Review of existing fault distance calculation using traveling wave method

The traveling wave fault location method is known as the most accurate method currently in use. Fault location on transmission lines using traveling wave was first proposed by Röhrig in 1931 [25]. In this method, when faults occur on transmission lines, an electrical pulse originating from the fault propagates along the transmission line on both sides away from the fault point. The time of pulse return indicates the distance to the fault point. This method is suitable for a long and homogenous line. The disadvantage of the traveling wave method is that propagation can be significantly affected by system parameters and network configuration [26]. It is also difficult to locate faults near the bus or faults that occurred near zero voltage inception angle [27]. Under this method, we have single-ended fault location algorithm and double-ended fault location algorithm. In single-ended algorithm, traveling time of the first wave away from the fault point to terminal and the arrival of same wave after reflecting back from fault point is always proportional to fault distance [28, 29]. In single-ended algorithm, fault location is proportional to the first two consecutive transient arrival time. From measurements of the first

two consecutive transient arrival times, fault location can be calculated. This algorithm is consider to be erroneous because one should be precise in differentiating the wavefront. Sometimes it is hard to identify the wavefront when wave is being lost due to disturbance.

The double ended algorithm was developed by Dewe et al. [30] in 1993. In double-ended algorithm, fault location is proportional to the arrival time of waves at each end away from the faults. This method needs communication link to get information from both ends so that the data is at a common time base. This turns out to be expensive and complex compared to single-ended algorithm. This method does not depend on reflections of wave from the fault point to the terminal.

To analyze transient wave, fourier transform is used [34]. In Fourier transform, the signal is decomposed into a summation of periodic and sinusoidal functions. The time and frequency resolutions are both fixed. This analysis is suitable for slowly varying periodic stationary signal. Traveling wave signal is always non-periodic and transient in nature. Fourier Transform doesn't work well on discontinuous signals. Because of that limitation, wavelet transform has developed by Magnago et al. in [31]. The author of [37] made a comparison between fourier transform and wavelet transform. In wavelet transform, dilation of a single wavelet is done for analysis. It uses short windows at high frequencies and long windows at low frequencies [32]. It can represent signal both in time and frequency domain, which helps to figure out sharp transitions and fault location. The ability of wavelet transform to locate both time and frequency makes it possible to simultaneously determine sharp transitions of signals and location of their occurrence [31].

Chapter 3

In this chapter, methodology which were followed to calculate the fault distance is discussed. Single-ended traveling wave method and double ended impedance based method were used to calculate the fault distance. For impedance based method principles used by the author [8] were followed. For traveling wave, principle used by author [31] were followed.

Methodology

Tests were done on figure 3.1. Figure 3.1 is a single three phase transmission line system having two generators. Phasor voltage and current are assumed to be available from both ends of a single transmission line. This method is suitable for transposed and untransposed transmission lines. It does not depends on fault resistance and source impedance.

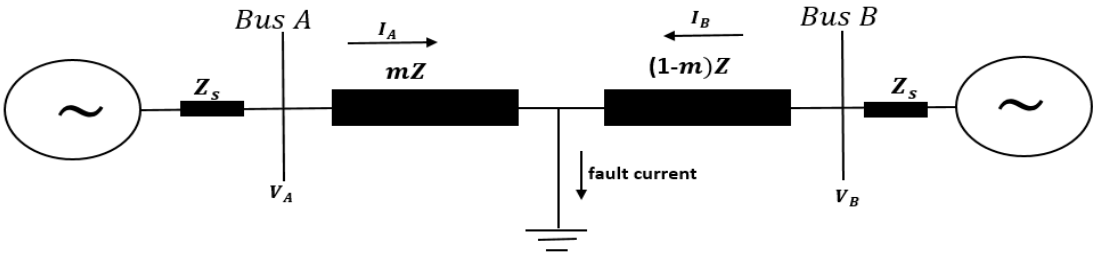

Figure 3.1: Faulted three phase transmission line

Fault locators are assumed to be located on both ends of the transmission line. When faults occurred, recorded phasor voltages and currents were taken from both ends. Fault distance is calculated using impedance based and traveling based method. The power system was designed in EMTP (Electromagnetic Transient Program), special software for simulation and analysis of transient in power system [44]. Algorithms of the traveling wave and the impedance based method were written in MATLAB. Different fault types were made at different locations on transmission lines. Fault voltages and fault currents from EMTP were taken and given as input to MATLAB which gives the fault distance.

3.1 Impedance based Method

The algorithm used in this paper follows the work of [8]. This method uses fault voltage and current from both terminal ends of transmission lines. Both ends are not synchronized. Fault currents and voltages are taken from fault recorder such as relays placed at the end on a

transmission line. This method is applicable for transposed and untransposed lines. It is not dependent upon fault types, load currents, source impedance and fault resistance [8].

3.1.1 Transmission line without shunt capacitance

Let's suppose fault occurs at some point which is m distance away from terminal A.V_f is fault voltage. The fault voltage is given by:

$$(V_f)_i = (V_A)_i - mZ_i * (I_A)_i \quad (3.1)$$

$$(V_f)_i = (V_B)_i - (1-m)Z_i * (I_B)_i \quad (3.2)$$

Where, i=0, 1, 2 is the zero, positive and negative sequence

Z_s= source impedance

m=fault distance from terminal A on transmission line

V_A, V_B = Three phase fault voltages at terminal A and B respectively

I_A, I_B = Three phase fault currents at terminal A and B respectively.

Z= line impedance which is equal to $R + jX$

Equating equation (3.1) and (3.2)

$$(V_A)_i - (V_B)_i + Z_i(I_B)_i = m * Z_i * (I_{A_i} + I_{B_i}) \quad (3.3)$$

Data from Bus A and Bus B are not synchronized .So, synchronization angle δ is added to equation (3.3) to make the two terminals synchronized. So, terminal voltages at terminal A and B becomes

$$(V_A)_i = (V_A)_i \angle \alpha_i + \delta \quad (3.4)$$

$$(V_B)_i = (V_B)_i \angle \beta_i \quad (3.5)$$

Similarly, equation for current is

$$(I_A)_i = (I_A)_i \angle \gamma_i + \delta \quad (3.6)$$

$$(I_B)_i = (I_B)_i \angle \theta_i \quad (3.7)$$

Where,

$\alpha, \beta, \gamma, \theta$= measured angles

Equation (3.3) can be written as

$$(V_A)_i e^{j\delta} - (V_B)_i + Z_i(I_B)_i = m * Z_i * (I_{A_i} * e^{j\delta} + I_{B_i}) \quad (3.8)$$

Synchronization angle δ can be expressed as $\cos(\delta) + jsin(\delta)$. Equation (3.8) is expressed into real and imaginary components as:

$$Re(V_A)_i sin\delta + Im(V_A)_i cos\delta - Im(V_B)_i + (C_4)_i = m((C_1)_i sin\delta + (C_2)_i cos\delta + (C_4)_i) \quad (3.9)$$

$$Re(V_A)_i cos\delta - Im(V_A)_i sin\delta - Re(V_B)_i + C_{3_i} = m((C_1)_i cos\delta - (C_2)_i sin\delta + (C_3)_i) \quad (3.10)$$

Where,

$$(C_1)_i = R_i * Re(I_A)_i - X_i * Im(I_A)_i \quad (3.11)$$

$$(C_2)_i = R_i * Im(I_A)_i + X_i * Re(I_A)_i \quad (3.12)$$

$$(C_3)_i = R_i * Re(I_B)_i - X_i * Im(I_B)_i \quad (3.13)$$

$$(C_4)_i = R_i * Im(I_B)_i + X_i * Re(I_B)_i \quad (3.14)$$

To find δ,equation (3.9) is divided by (3.10) and removing a number of terms, following equations are developed:

$$a_i * sin\delta + b_i cos\delta + c_i = 0 \quad (3.15)$$

Where,

$$a_i = -(C_3)_i Re(V_A)_i - (C_4)_i Im(V_A)_i - (C_1)_i Re(V_B)_i - (C_2)_i Im(V_B)_i + (C_1)_i (C_3)_i + (C_2)_i (C_4)_i \quad (3.16)$$

$$b_i = -(C_4)_i Re(V_A)_i - (C_3)_i Im(V_A)_i - (C_2)_i Re(V_B)_i + (C_1)_i Im(V_B)_i + (C_2)_i (C_3)_i + (C_1)_i (C_4)_i \quad (3.17)$$

$$c_i = -(C_2)_i Re(V_A)_i - (C_1)_i Im(V_A)_i - (C_4)_i Re(V_B)_i + (C_3)_i Im(V_B)_i \quad (3.18)$$

The synchronization angle δ is determined by an iterative Newton –Raphson Method. The equation for the iteration are

$$\delta_{k+1} = \delta_k - \frac{F(\delta_k)}{\acute{F}(\delta_k)} \quad (3.19)$$

$$F(\delta_k) = b_i * cos\delta_k + a_i * sin\delta_k + c_i \quad (3.20)$$

$$\acute{F}(\delta_k) = a_i * cos\delta_k - b_i * sin\delta_k \quad (3.21)$$

This method requires initial guess for δ. The iteration is terminated when the difference between $\delta_{k+1}$and δ_k is smaller than the specified tolerance. Once the synchronization angle is determined fault location m is calculated from equations (3.9) and (3.10).

If equation (3.9) is used, fault distance is:

$$m = \frac{Re(V_A)_i sin\delta + Im(V_A)_i cos\delta - Im(V_B)_i + (C_4)_i}{(C_1)_i sin\delta + (C_2)_i cos\delta + (C_4)_i} \quad (3.22)$$

If equation (3.10) is used, fault distance is:

$$m = \frac{Re(V_A)_i cos\delta - Im(V_A)_i sin\delta - Re(V_B)_i + (C_3)_i}{(C_1)_i cos\delta - (C_2)_i sin\delta + (C_3)_i} \quad (3.23)$$

Transmission lines are modeled according to their line length. Transmission lines shorter than 50miles are considered to be short transmission lines. They are modeled by lumped parameters as series resistance and inductance. Shunt capacitance is neglected. Transmission lines more than 50 miles but less than 150 miles are considered as medium transmission lines. Lines more than 150 miles are considered as long transmission lines. For medium and long transmission lines shunt capacitance should be taken into account. These line are modeled by distributed π or T model.

3.1.2 Transmission line with shunt capacitance

Shunt capacitance is modeled as shown in the figure below.

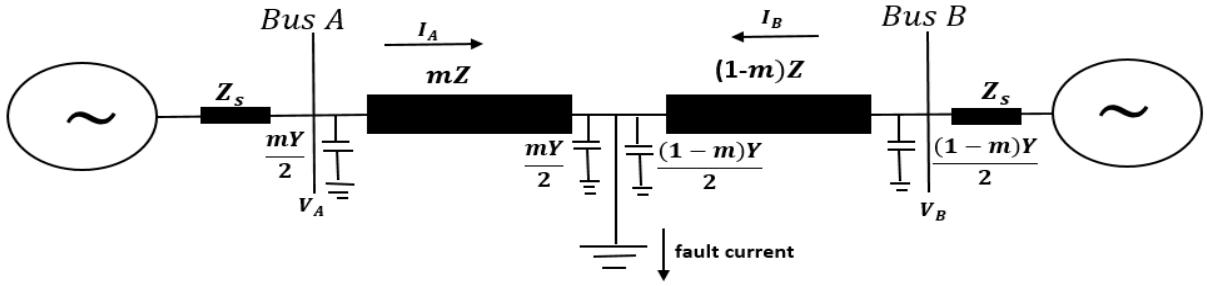

Figure 3.2: Faulted system with shunt capacitance

Series impedance and shunt admittance is

$$Z_{ld} = Z_l \left[\frac{\sinh(v*l*m)}{v*l*m}\right] \quad (3.24)$$

$$\frac{Y_d}{2} = \frac{Y}{2}\left[\frac{tanh\left(\frac{v*l*m}{2}\right)}{\frac{v*l*m}{2}}\right] \quad (3.25)$$

Where,

$v = \sqrt{zy}$ is the propagation constant.

$l = \frac{x}{m}$ is a line length.

z is the series impedance in ohms per mile and y is the shunt admittance in mhos per mile.

3.2 Traveling wave method

Based on the traveling wave theory on [25], when fault occurs on transmission lines, a wave will travel in both directions away from the fault point. It will continue to bounce back and forth between the fault point and two-terminal bus until it reached the post fault steady state. Traveling wave recorders (TWR) are assumed to be placed at the end of the line. From the recorded fault voltages and currents, transient time taken by surge to travel from the fault point to TWR is known. If the propagation velocity of the wave is known, distance to fault from any station can be calculated. The propagation velocity of the wave depends on the value of line parameter such as (inductance (L) and capacitance(C)). The fault location is greatly dependent on propagation speed of the traveling waves [38-40]. Wave velocity is determines by using the formula in (1.60). The transient wave might have other frequency components that propagate along the line. To find the dominant frequency two methods are used widely [35]. The first approach is spectrum estimation [36] and second is wavelet transform [31]. In this research, wavelet transform was used to extract the dominant frequency from the transient wave. Daubechies wavelet is used to detect and locate the disturbance event [41-42]. Daubechies wavelet has many filter coefficients like Daub4, Daub6, Daub8, and Daub10.

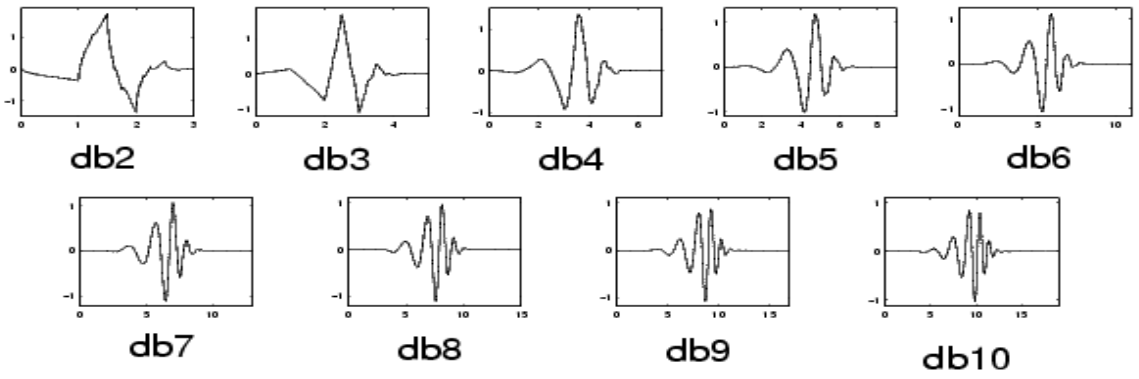

Figure 3.3: Nine members of Daubechies family [42]

The author of [43] presented that Daub4 and Daub6 wavelets are better for those power system disturbances which are short and fast. Daub8 and Daub10 wavelet are suitable for those disturbances which are slow transient. In this research, Daub4 wavelet was used.

In three phase transmission lines, traveling waves are mutually coupled, so there is no single traveling wave velocity. The phase domain signals are decomposed into their modal components by using modal transformation [31]. In this method, all transmission line are

assumed to be fully transposed and therefore the well-known Clarke's constant and real transformation matrix is used:

$$T = \begin{bmatrix} 1 & 1 & 1 \\ 2 & -1 & -1 \\ 0 & \sqrt{3} & -\sqrt{3} \end{bmatrix} \quad (3.26)$$

Where,

T is the transformation matrix. The phase signals are transformed into their modal components by using transformation matrix as follows:

$$\mathrm{S_{mode}} = \mathrm{TS_{phase}} \quad (3.27)$$

Where,

S_{mode} is the modal vectors and S_{phase} is the phase signals vectors (voltage or current). Equation (3.27) transformed the recorded phase signals into their modal components. There are two modes: ground mode and aerial mode. The ground mode is also called mode1 and the aerial mode is also called mode 2. The ground mode is suitable for grounded faults. So, this mode is not suitable for all types of faults. The aerial mode is suitable for both grounded and ungrounded faults.

Single-ended algorithm

In this method there is no need to synchronize with the remote end of transmission lines. Fault currents or voltages are taken from one end of the line and are transformed into their modal components using (3.27). Fault distance is calculated with the difference in the reflection time of two consecutive traveling waves from the fault point to that end.

3.2.1 Ungrounded fault

The ungrounded fault involves no significant reflection from the remote end bus. So fault distance is calculated by taking the product of wave velocity and half of the time delay between two consecutive peaks in the wavelet transform coefficient. Fault distance is calculated using the below equation:

$$x = \frac{vt_d}{2} \quad (3.28)$$

Where v is the wave velocity of the traveling waves

t_d is the time difference of the first two peaks of aerial mode wavelet transform coefficient in scale 1.

3.2.2 Grounded fault

In the grounded fault, reflection from the remote-end bus should be considered depending upon the location of the fault on the line. The reflected wave from the remote end bus may arrive after and before the reflected wave from the fault point. This can be verified using Lattice diagram.

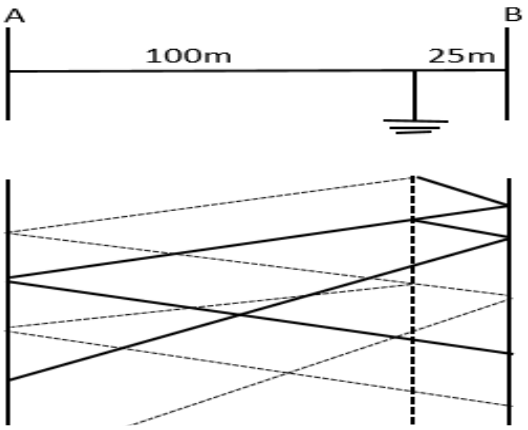

Figure 3.4 Lattice diagram of remote-end fault

From the figure 3.4, at terminal A the first peak is the wave away from fault point. Second wave is the reflected wave from terminal B.

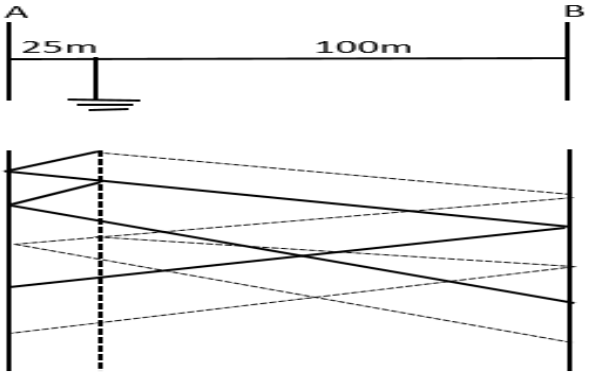

Figure 3.5 Lattice diagram of close-in fault

If fault occurs at first half of length of the line, wave from the remote end bus arrive before the reflected wave from fault point. From the above close-in and remote-end fault, it is clear that reflected wave from the remote-end bus always arrive after the reflection from the fault point, if and only if, fault occurs at close half of length of the line. If fault occurs at remote-end of the line, t_d in equation (3.28) is the difference of first two peaks in scale 1. The two

peaks are wavelet transform coefficient of aerial mode [31]. If the fault occurs within second half of the line, t_d is replaced by equation (3.29)

$$t_d = 2\tau - t_x \tag{3.29}$$

Where:

τ is the travel time for entire line length.

t_x= the time difference between the first two peaks of aerial mode wavelet transform coefficient in scale 1.

Chapter 4

This chapter compares the results we get from traveling wave method and impedance based method.

4.1 Results of traveling wave method for various fault types

Faults were made at different locations on a transmission line. Recorded fault current were transformed into their modal components: ground mode and aerial mode. Ground mode is significant only in grounded faults whereas aerial mode is significant for all types of faults. The speed of the wave is nearly equal to the speed of the light. So, high sampling frequency 100MHz was used for accuracy. Sampling frequency of 100MHz was considered to be high enough to capture the traveling waves. The transmission lines of length 46 miles were modeled in EMTP. The aerial mode current samples waveform was given as input to MATLAB. In MATLAB, the sampled waveform are decomposed into detail and approximation coefficients wavelets using high pass filter and low pass filters respectively. The approximation coefficient of wavelet transform is the smoothed version of the original signal. The detail coefficient has the detailed occurrence of disturbances. Sampled waveform was broken down in scale 1,2,3,4 using Daubechies4 filter. In this research, aerial mode detail coefficient at scale 1 was used to localize the disturbances for all fault types made at different locations on lines. Figure 4.1 is one example of fault distance calculations for close in fault. Similarly, figure 4.2 is an example of fault distance calculations for remote-end fault. MATLAB codes to find the fault distance is in Appendix C.

Figure 4.1 is the detail coefficient wavelet in scale 1 during phase a to ground. Phase a to ground fault was made at 8 miles away from Bus B. In order to calculate the fault distance, first current samples from Bus B was transformed into their aerial mode and wavelet transform was done in scale 1. Since, fault was grounded and fault occurred in close half end of the line, fault location was calculated by using equation (3.28).

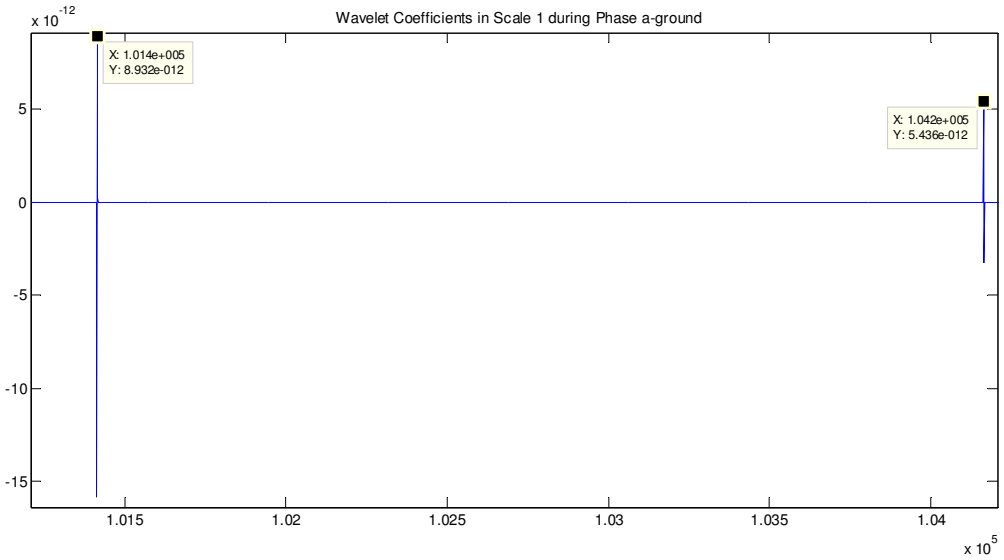

Figure 4.1: Phase a to ground at 8 miles away from Bus B.

$$\boldsymbol{x = \frac{vt_d}{2}}$$

Where,

$$v = \frac{1}{\sqrt{LC}}$$

$$v = \frac{1}{\sqrt{1.578*10^{-3}*7.894*10^{-9}}} miles/sec$$

$$= 283333.50\ miles/sec$$

t_d = The time difference between the first two consecutive peaks for grounded faults. From the figure 4.1, the first peak appear at time 2.028315ms and the second peak appear at time 2.084755ms.

$$x = \frac{283333.50(2.084755-2.028315)*10^{-3}}{2} = 7.997 miles$$

Figure 4.2 is an example for remote-end fault. Phase a to ground fault was made at 35miles away from Bus B. In order to calculate the fault distance, first current samples from Bus B was transformed into their aerial mode and wavelet transform was done in scale 1. Since, fault was grounded and fault occurred in remote-end of the line, t_d of equation (3.28) was replaced by equation (3.29).

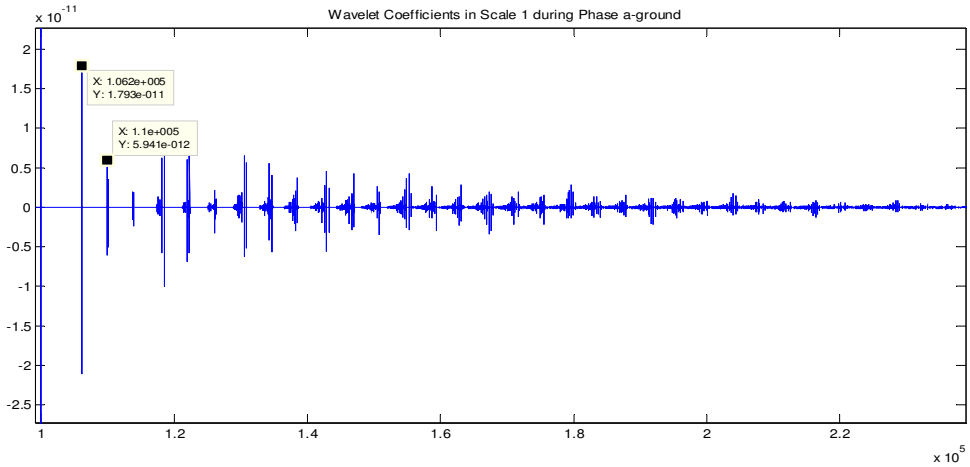

Figure 4.2: Phase a to ground at 35 miles away from Bus B.

Since fault is in the remote half of the line, equation (3.29) is used.

$$t_d = 2\tau - t_x$$

Where,

$$\tau = \frac{46}{283333.50} = 1.623528 * 10^{-4} sec$$

In figure 4.2, first peak appear at time 2.12359ms and second peak appear at time 2.201215ms.

$$t_d = 2 * 1.623528 * 10^{-4} - (2.201215 - 2.12359) * 10^{-3}$$
$$= 2.470806 * 10^{-4}$$
$$x = \frac{283333.50 * 2.470806 * 10^{-4}}{2} = 35.003 miles\ .$$

Table 4.1 shows fault distance calculations for all fault types when faults were at middle of the transmission line. All the figures of detail wavelet coefficient at scale 1 of all fault types are in Appendix B.

Table 4.1: Fault calculations for various fault types at 23 miles from Bus B

Fault Types	Actual Fault distance(mile)	Calculated Fault Distance(x)mile
Phase a to Ground	23	22.425
Phase b to Ground	23	22.425
Phase c to Ground	23	22.425
Line ab to Ground	23	22.425
Line ac to Ground	23	22.425
Line bc to Ground	23	22.425
Line a-Line b	23	22.995
Line b-Line c	23	22.995
Line a-Line c	23	22.995
3 Phase	23	22.995
3 Phase to Ground	23	22.995

Similarly, four types of fault were made at 8,12,24,35 miles away from Bus B and fault distance is calculated which is shown in Table 4.2.

Table 4.2: Fault calculations for various fault types at various locations on transmission lines

Method	Fault Types	Actual Distance(mile)	Calculated Distance(mile)
Traveling wave method	Phase a to ground	8	7.783
		12	11.676
		24	24.584
		35	35.003
	Line a –Line b	8	7.999
		12	12.004
		24	24.004
		35	35.003
	Line a –Line b to ground	8	7.783
		12	11.679
		24	24.584
		35	35.003
	3 Phase Fault	8	7.997
		12	12.002
		24	24.004
		35	35.003

4.2 Results of Impedance based method for various types of fault

Likewise in the traveling wave method, various types of faults were made at different locations on a transmission line. Recorded fault currents and voltages were transformed into

their modal components. Fault voltages and currents from both terminals were transformed into positive and negative sequence. Zero sequence voltages and currents calculation is not recommended because zero sequence parameters are considered as uncertainties [8]. Negative sequence voltages and currents can be used for all fault types [8]. However, it is not suitable for balanced fault like three phase fault [8]. Positive sequence values can be used for all fault types [8]. In this research, positive sequence was used for phase to phase fault and three phase fault. For grounded faults, negative sequence parameters are used. The negative sequence and the positive sequence parameters were taken from EMTP and given as input to MATLAB. Bus A and Bus B were not synchronized. To synchronize the two Bus, Bus B was taken as a reference Bus and the synchronization angle δ is added to Bus A. The synchronized angle is determined by iterative Newton-Raphson method in MATLAB. MATLAB codes used for this method is in the Appendix C. Faults were made at 8, 12,23,24,35 miles away from Bus B. Figure 4.3 shows the voltages and currents waveform at terminal B during three Phase fault at 35 miles away from Bus B.

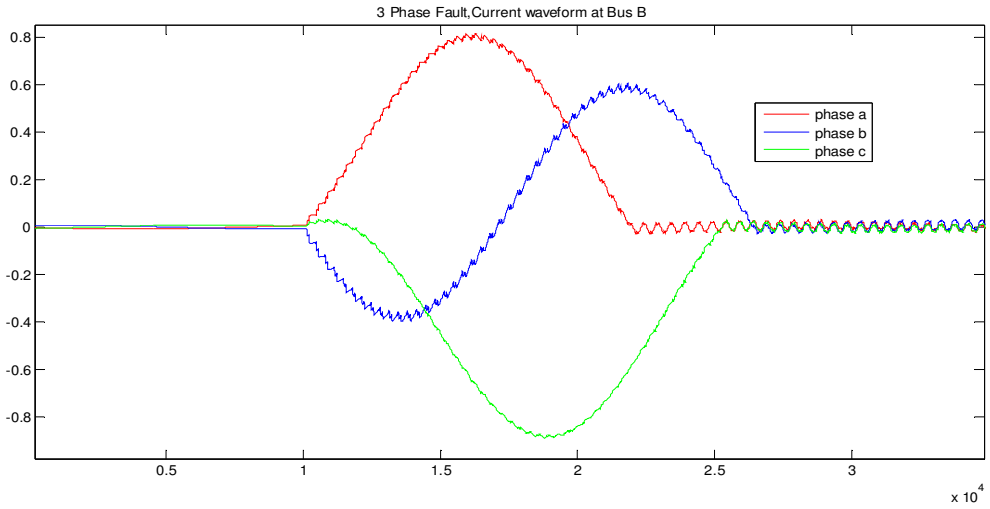

Figure 4.3: 3 Phase fault at 35 miles away from Bus B

Figure 4.3 shows the current waveform at terminal B during three phase fault. Current waveform was stable until the fault occurred. The fault occurred at 10ms. After the fault, the current increased which is clear from the figure 4.3.

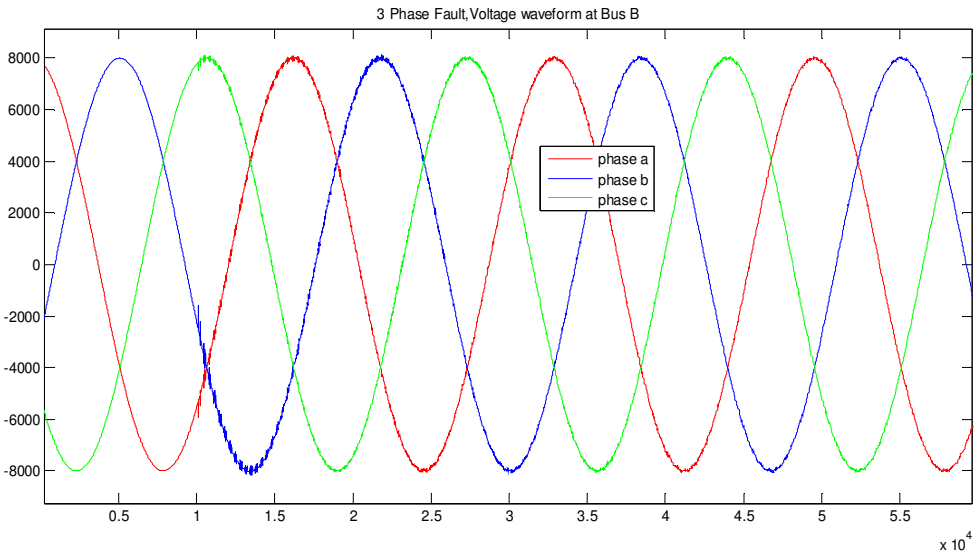

Figure 4.4: 3 Phase fault at 35 miles away from Bus B

Figure 4.4 shows the voltage waveform at terminal B during a three phase fault. Voltage waveform was stable until fault occurred. The fault occurred at 10ms. Voltage waveform decreased after the fault occurred. Since the source in EMTP was ideal source, it seems to be stable even after the fault occurred. Voltage waveform and current waveform of terminal A and B for all fault types at distance 35 miles away from Bus B is in Appendix B.

Fault distance calculations for various types of faults at 23 miles away from Bus B are shown in Table 4.3.Table 4.3 presented both the magnitude and phase of fault voltages and currents at both terminals A and B.

Table 4.3: Voltage and Current values of both terminals for various fault types at 23 miles from Bus B using impedance based method

Fault types	Bus A				Bus B				Actual Distance (mile)	Estimated Fault Distance (mile)
	Voltage		Current		Voltage		Current			
	Magnitude	Phase	Magnitude	Phase	Magnitude	Phase	Magnitude	Phase		
Phase a to ground	0.46523	3.11793	0.00015097	3.14133	0.516667	3.13257	0.00014765	3.14078	23	23
Phase b to ground	0.55068	3.13240	0.00024047	3.12488	0.554245	3.13224	0.00024975	3.13042	23	23.06
Phase c to ground	0.80216	3.13190	0.00031175	3.14039	0.804974	3.13212	0.00030479	3.13717	23	23.00
Phase ab to ground	0.55152	3.14005	0.00020086	3.13547	0.552370	3.13440	0.00020534	3.13757	23	22.85
Phase ac to ground	0.99684	3.13741	0.00035623	3.14083	0.995795	3.13741	0.00035441	3.13956	23	22.98
Phase bc to ground	0.78365	3.11447	0.00033022	3.13505	0.779452	3.13055	0.00033022	3.13926	23	23.00
Phase ab fault	8000.20	4.461E-06	0.00547054	1.56925	8000.20	0.17453	0.00548613	1.74664	23	23.00
Phase ac fault	8000.20	2.709E-06	0.00547157	1.56939	8000.20	0.17453	0.00548960	1.74558	23	23.33
Phase bc fault	8000.20	2.431E-06	0.00547501	1.56906	8000.20	0.17452	0.00548337	1.74609	23	23.00
3 Phase fault	8000.20	1.349E-05	0.00546668	1.57451	8000.22	0.17453	0.00548565	1.74797	23	23.00
3 phase to ground	0.97686	3.13421	0.00038635	3.13972	0.966179	3.13297	0.00038512	3.13505	23	22.81

Similar calculations were done for four types of faults which were made at different locations on lines shown by Table 4.4.

Table 4.4: Fault calculations for various fault types at various locations on transmission lines using impedance based method

Method	Fault Types	Actual Fault Distance(mile)	Calculated Fault Distance(mile)
Impedance based method	Phase a to ground	8	8.74
		12	13.8
		24	23.30
		35	34.84
	Phase ab fault	8	8.74
		12	13.8
		24	24.90
		35	35.88
	Phase ab to ground	8	8.74
		12	13.8
		24	23.50
		35	35.88
	3 Phase fault	8	8.234
		12	13.8
		24	24.90
		35	35.88

4.3 Accuracy of impedance based method and traveling wave method

Fault location accuracy is measured by the percentage error calculation as below:

$$\%error = \frac{|Actual\ length - Estimated\ location|}{Total\ length\ of\ line} * 100$$

Table 4.5: percentage error in fault calculations using impedance based method and traveling wave method

Fault types	Actual Distance (mile)	Calculated Distance Impedance based method (mile)	Calculated Distance Traveling wave method (mile)	% error (Impedance based method)	% error (Traveling wave method)

Phase a to ground	8	8.234	7.783	0.5087	0.4717
	12	13.8	11.676	3.9130	0.7043
	23	23	22.425	0.0000	1.2500
	24	23.30	24.584	1.5217	1.2696
	35	34.84	35.003	0.3478	0.0065
Phase ab fault	8	8.74	7.999	1.6087	0.0022
	12	13.8	12.004	3.9130	0.0087
	23	23	22.995	0.0000	0.0109
	24	23.90	24.004	0.2174	0.0087
	35	35.88	35.003	1.9130	0.0065
Phase ab to ground	8	8.74	7.783	1.6087	0.4717
	12	13.8	11.679	3.9130	0.6978
	23	22.85	22.425	0.3261	1.2500
	24	23.50	24.584	1.0870	1.2696
	35	34.57	35.003	0.9348	0.0065
3 phase fault	8	8.234	7.997	0.5087	0.0065
	12	13.8	12.002	3.9130	0.0043
	23	23	22.995	0.0000	0.0109
	24	24.90	24.004	1.9565	0.0087
	35	35.88	35.003	1.9130	0.0065

4.4 Summary

Table 4.5 shows the percentage error in fault calculation for various types of faults at various location using both methods. The impedance based method has the highest error compared to traveling wave method. Impedance method has the highest error at 12 miles and least error when faults were at middle of the transmission line. The error in traveling wave method is nearly zero. Traveling wave method has zero percentage of error for ungrounded fault and has highest percentage of error for grounded fault.

Chapter 5

CONCLUSION

Fault on the transmission line needs to be restored as quickly as possible. The sooner it is restored, the less the risk of power outage, damage of equipment of grid, loss of revenue, customer complaints and repair crew expenses. Rapid restoration of service can be achieved if precise fault location algorithm is implemented.

Many algorithms have been developed to calculate the fault distance on the transmission line. This paper gives the general overview of fault location calculation on transmission line using impedance based method and traveling wave method. It discussed the transmission line model, its sequence components, symmetrical components for fault analysis, fundamental principal of travelling wave. Finally, results from both methods were compared.

The percentage error due to traveling wave method was zero but impedance based method had the highest error of 3.91%. However, traveling wave method has many disadvantages. Since fault location is half of the product of velocity of wave and time difference between the first two peaks of the wave, transmission line might have multiple reflections from bus and transformers. This might create difficulties in identifying the actual reflection from the fault location.

Both methods have few advantages and disadvantages. The traveling wave method is accurate and can calculate the fault location within a couple of seconds after a fault. But to monitor the wideband transient signal and to process such signal to locate time, requires expensive technological tools. Traveling wave speed is close to speed of light. So high sampling frequency should be used to capture such fast waves. Therefore, it requires complex and expensive equipment. Impedance based method is known to be simple and low cost. It does not require the communication channel to exchange information between relays. Due to limited measurement, this method usually has error in fault locating. It can provide precise results only when fault is present for couple of cycles. Hence, this method is not suitable for fault locating in EHV and UHV where faults are cleared in less than two cycles. This method also causes issue for series compensated line.

Both methods have few pros and cons. If relays that include both impedance based method and traveling wave method are used to detect fault location, it would provide the best responses under all fault conditions. When fault occurs at zero voltage, there will be no wave or traveling wave amplitude might be too low for detection. In such situation, relays can identify fault location using line impedance and current and voltage samples from local and remote terminals of a line.

Bibliography

[1]Paul M. Anderson, “Analysis of Faulted Power Systems”, the Institute of Electrical and Electronics Engineers, Inc., 1995

[2]Arthur R.Bergen, Vijaya Vittal, “Power Systems Analysis”

[3]H. Mokhlis1, Hasmaini Mohamad, A. H. A. Bakar1, H. Y. Li, “Evaluation of Fault Location Based on Voltage Sags Profiles: a Study on the Influence of Voltage Sags Patterns”, 2011

[4]M.S Sachdev, FIEEE, R.Agarwal, St. MIEEE, “ A Technique for estimating transmission line fault locations from digital impedance relay measurements”,1998

[5] M. KezunoviC, B. PeruniEiC, “Automated Transmission line fault analysis using synchronized sampling at two ends ", 1996

[6] Joe-Air Jiang, Jun-Zhe Yang, Ying-Hong Lin, Chih-Wen Liu,” An Adaptive PMU Based Fault Detection/Location Technique for Transmission Lines”, 2000

[7] A. A. Girgis, D. G. Hart, and W. L. Peterson, “A New Fault Location Technique For Two-and Three-Terminal Lines,” IEEE Transactions on Power Delivery, vol. 7, no. 1, pp. 98–107, January 1992

[8] D. Novosel, D. G. Hart, E. Udren, and J. Garitty, “Unsynchronized Two- Terminal Fault Location Estimation,” IEEE Transactions on Power Delivery, vol. 11, no. 1, pp. 130–137, January 1996

[9] Javad Sadeh, N. Hadjsaid, A. M. Ranjbar, and R. Feuillet, “Accurate Fault Location Algorithm for Series Compensated Transmission Lines”, July 2000

[10] A. Gopalakrishnan, M. Kezunovic, S. M. McKenna, and D. M. Hamai, “Fault Location Using the Distributed Parameter Transmission Line Model”, October 2000

[11] Chi-Shan Yu, Chih-Wen Liu, Member, IEEE, Sun-Li Yu, and Joe-Air Jiang, “A New PMU-Based Fault Location Algorithm for Series Compensated Lines”, January, 2002

[12] Waikar, D.L., Elangovan, S., and Liew, A.C.: ‘Fault impedance estimation algorithm for digital distance relaying’, IEEE Trans., July 1994, PWRD-9, (3), pp. 1375-1383

[13]Girgis, A.A., and Makram, E.B., “Application of adaptive Kalman filtering in fault classification, distance protection, and fault location using microprocessors”, IEEE Trans., February 1982, PWRS-3, (I), pp. 301-309

[14] Wen-Chun Shih, “Time Frequency Analysis and Wavelet Transform Tutorial Wavelet for Music Signal Analysis”

[15] A. Wiszniewski, “Accurate fault impedance locating Algorithm”, Nov 1983

[16]E.O. Schweitzer and J.K. Jachinowski, "A Prototype Microprocessor-Based System for Transmission Line Protection and Monitoring”, presented at the Eighth Annual Western Protective Relay Conference, Spokane, Washington, October 1981

[17] Edmund 0. Schweitzer 111, "Evaluation and Development of Transmission Line Fault-Locating Techniques which uses Sinusoidal Steady-State Information”, presented at the Ninth Annual Western Protective Relay Conference, Spokane, Washington, October 1982

[18] T. Takagi, Y. Yamakoshi, J. Baba, K. Uemuraand, and T. Sakaguchi, “A New Algorithm of an Accurate Fault Location for EHV/UHV Transmission Lines: Part Il- Laplace Transform Method,” IEEE Transactions on Power Apparatus and Systems, vol. PAS-101, no. 3, pp. 564–573, March 1982

[19] T. Nagasawa, M. Abe, N. Otsuzuki, T. Emura. Y. Jikihara, M. Takeuchi, “Development of a New Fault Location Algorithm for Multi-Terminal

[20] Prof. A.T. Johns, DSC, PhD, C.Eng, FlEE, S. Jamali, BSc, MSc, “Accurate fault location technique for power transmission lines”, November 1989

[21] David J. Lawrence, Luis Z. Cabeza, Lawrence T. Hochberg, “Development of an advanced transmission line fault location system Part 1- Algorithm development and simulation”, October 1992

[22] Masayuki Abe and Nobuo Otsuzuki, Tokuo Emura and Masayasu Takeuchi, “Development of a new fault location system for multi terminal single transmission lines”, 1994

[23] I. Zamora,J.F. MiAambres,A.J. Mazon,R. Alvarez-lsasi,J. Laza ro, “Fault location on two-terminal transmission lines based on voltages”, January 1996

[24] M.B. Djuri6, Z.M. Radojevi6 and V.V. Terzija, Member IEEE, “Distance Protection and Fault Location Utilizing Only Phase Current Phasors”, October 1998

[25] J. Röhrig, “Location of faulty places by measuring with cathode ray oscillographs”, Elektrotech Zeits, 8, 241-242 (1931)

[26] M. H. Idris, Member, IEEE, M. W. Mustafa, Member, IEEE and Y. Yatim, “Effective Two-Terminal Single Line to Ground Fault Location Algorithm”, June 2012

[27] T. Kawady and J. Stenzel. “Investigation of practical problems for digital fault location algorithms based on EMTP simulation”, Asia-Pacific Transmission and Distribution Conference and Exhibition, 2002, Vol. 1, pp.118-123

[28] M. Ando, E. Schweitzer, R. Baker, “Development and Field-Data Evaluation of Single-End Fault Locator for Two-Thermal HVDC Transmission Lines,” Part I: Data Collection System and Field Data, IEEE Transactions on Power Apparatus and Systems, PAS-104, 3524-3530 (1985)

[29] M. Ando, E. Schweitzer, R. Baker, “Development and Field-Data Evaluation of Single-End Fault Locator for Two-Terminal HVDC Transmission Lines, “Part 2: Algorithm and Evaluation, IEEE Transactions on Power Apparatus and Systems, PAS-104, 3531-3537 (1985)

[30] M. Dewe, S. Sankar, J. Arrillaga, “The Application of Satellite Time References to HVDC Fault Location”, IEEE Transactions on Power Delivery, 8, 1295-1302 (1993)

[31] F. H. Magnago, A. Abur, “Fault location using wavelets ,” IEEE Transactions on Power Delivery, 13, 1475-1480 (1998)

[32] S. Sajedi, F. Khalifeh, Z. Khalifeh, T. karimi, “Application of Wavelet Transform for Identification of Fault Location on Transmission Lines,” 2011

[33] P. Murthy, J. Amarnath, S. Kamakshiah, B. Singh, “Wavelet Transform Approach for Detection and Location of Faults in HVDC System,” in IEEE Third international Conference on Industrial and Information Systems, Region 10, 1-6 (2008)

[34] G. Ban, L.Prikier, “Fault Location on EHV Lines Based On Electromagnetic Transients”, IEEE/NTUA Athens Power Tech Conference, 1993, pp. 936 - 940

[35] Emmanouil Styvaktakis, Mathias H.J. Bollen, Irene Y.H. Gu , “A Fault Location Technique Using High Frequency Fault Clearing Transients”, 1999

[36] S.M. Kay, S.L. Marple, “Spectrum Analysis: A Modem Perspective,” Proceedings of the ZEEE, vol. 69, no. 11, hov. 1981, pp. 1380- 14 1 9

[37] D. C. Robertson, 0. I. Camps, J. S. Mayer, and W. B. Gish, “Wavelets and Electromagnetic Power System Transients”, IEEE Transactions on Power Delivery, Vol.11, No.2, pp. 1050-1058, April 1996

[38] C. Ping, X. Bingyin, L. Jing, “A Traveling Wave Based Fault Locating System for HVDC Transmission Lines”, in International Conference on Power System Technology, 1-4 (2006)

[39]. K. Young-Jin, K. Sang-Hee, L. Dong-Gyu, K. Hyung-Kyu, “ Fault Location Algorithm Based on Cross Correlation Method for HVDC Cable Lines”, in IET 9th International Conference on Developments in Power System Protection, 360-364 (2008)

[40] T. Kawady, J. Stenzel, “ Investigation of practical problems for digital fault location algorithms based on EMTP simulation”, in IEEE/PES Transmission and Distribution Conference and Exhibition 2002: Asia Pacific, 1, 118-123 (2002)

[41] S. Santoso, E. Powers, W. Grady, and P. Hoffmann, “Power Quality Assessment via Wavelet Transform Analysis”, IEEE Transactions on Power Delivery, Vol.11, N0.2, pp. 924-930, April1996

[42] MATLAB User’s Guide, the Math Works Inc. and Natick, MA

[43] S.Santoso, E.J. Powers, and W.M. Grady, “Electric power quality disturbance detection using wavelet transform analysis,” in Proceedings of the IEEE-SP International Symposium on Time-Frequency and Time- Scale Analysis, Philadelphia, PA, Oct. 25-28, 1994, pp. 166-169

[44] H.W. Dommel, "Digital Computer Solution of Electromagnetic Transients in Single-and Multiphase Networks." IEEE Trans. Power Apparatus and Systems, vol. PAS-88, pp. 388-399, April 1969

[45] Y.Liao and S.Elangovan “Unsynchronized two-terminal transmission line fault location without using line parameters”, Nov 2006

[46] M.T. Sant, Y.G. Paithankar, “Online digital fault locator for overhead transmission line,” Nov, 1979

[47]Erikson, L., Saha,M.M and Rockfeller, “An accurate fault locator with compensation for apparent reactance in the fault resistance resulting from remote end infeed”, IEEE Trans., PAS-104, 1985, pp. 424435

[48] Scheweitzer, E.O., 111, “Evaluation and development of transmission line fault locating techniques which use sinusoidal steady state information”, Computers & Elec. Engng USA, 1983, IO, (4), pp. 269-218

[49]Cook,V,“Fundamental aspects of fault location algorithms used in distance protection”, IEE Proc. C, 1986, 133, (6), pp. 359-368

[50]Jeyasurya, B., Rahman,M.A, “Accurate fault location of transmission line using microprocessors”, IEE Conf. Publ. 302, 1989

[51]Lawrence, D.J., and Waser, D.L, “Transmission line fault location using digital fault recorder”, IEEE Trans., 1988, PWRD-3, (2). pp. 496-502

[52] M. Kezunovit, J. Mrkic, B. PeruniEiC, “An Accurate Fault Location Algorithm Using Synchronized Sampling,” May 1994

[53] T. Takagi, Y. Yamakoshi, J. Baba, K. Uemura, and T. Sakaguchi, “A New Algorithm of an Accurate Fault Location for EHV/UHV Transmission Lines: Part I- Fourier Transformation Method,” IEEE Transactions on Power Apparatus and Systems, vol. PAS-100, no. 3, pp. 1316–1323, March 1981

Appendix A

A1.Test System Data

In this appendix, the system parameters used for both methods were presented.

Table A1 Transmission lines of 46 miles is used to test and its parameters are presented below:

Parameters	Sequence +,-	Sequence 0
Resistance(Ω/mile)	0.0350	0.0225
Inductance(mH/mile)	1.578	1.738
Capacitance(nF/mile)	7.894	6.794

Table A2 Power System Data

Date	Bus A	Bus B
Voltage(v)	8000	8000
Frequency(Hz)	60	60
Inductance (H)	0.001194	0.001194

Appendix B

B1.Voltages and Currents waveform at Bus A and Bus B for various fault types at 35miles away from Bus B using Impedance based method

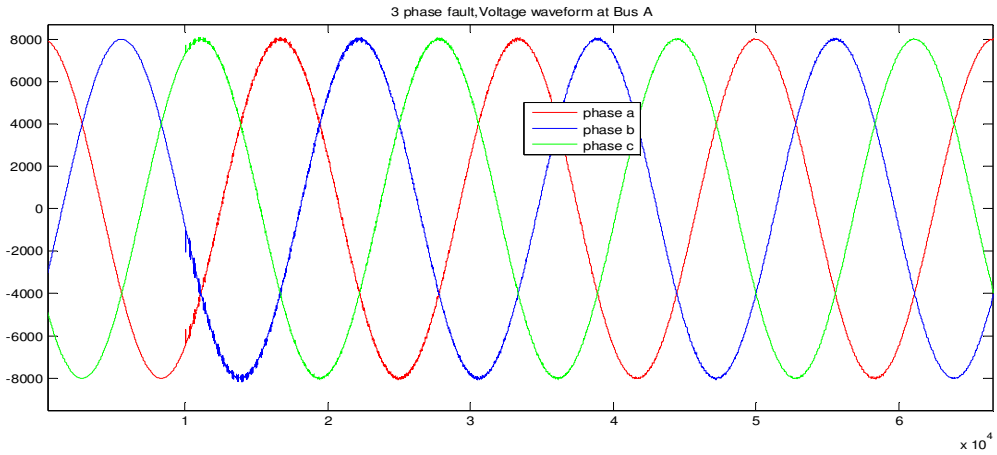

Figure 4.5: Voltage Waveform at Bus A during 3 phase fault

Figure 4.5 is the voltage waveform at Bus A during 3 phase fault. The total length of line between Bus A and Bus B is 46 miles. Fault occurred at 35 miles away from Bus B. Voltage waveforms were stable until the fault occurred at 10ms, then voltage decreased. Since the source was ideal, it was not clear in figure 4.5

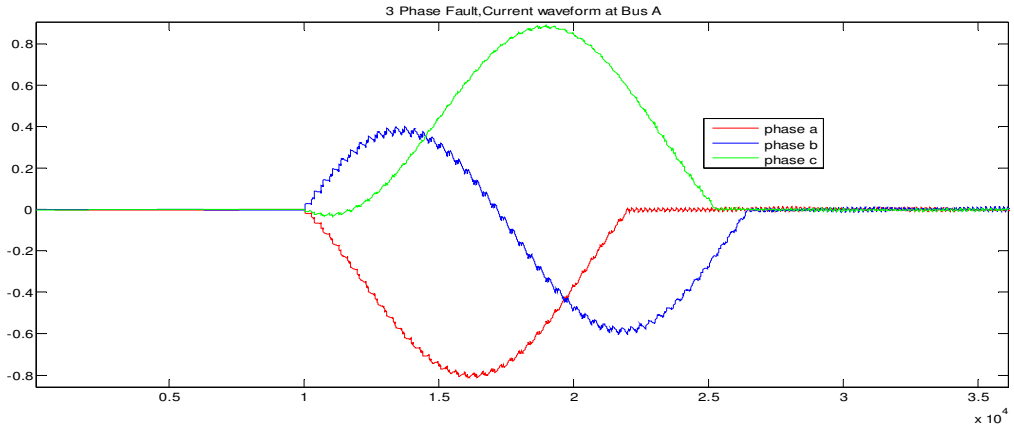

Figure 4.6: Current Waveform at Bus A during 3 phase fault

Figure 4.6 is the current waveform at Bus A during 3 phase fault. The total length of line between Bus A and Bus B is 46 miles. Fault occurred at 35 miles away from Bus B. Current waveforms were stable until the fault occurred at 10ms, then current increased.

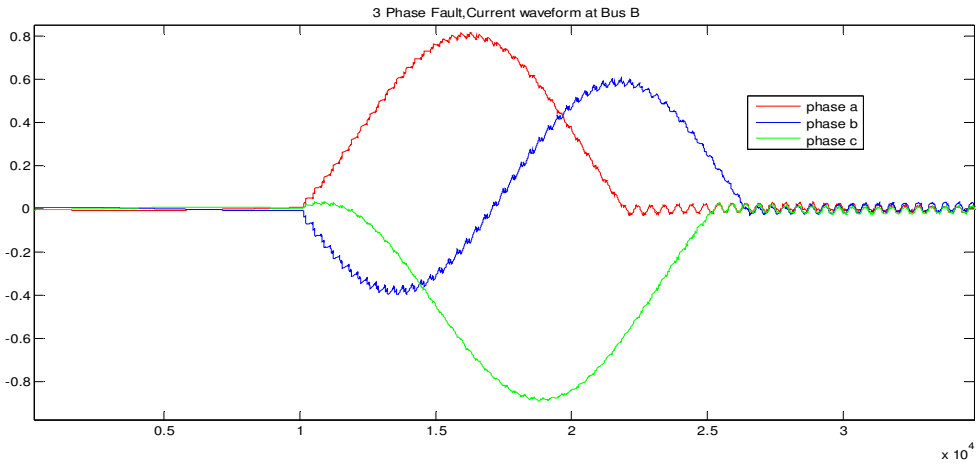

Figure 4.7: Current Waveform at Bus B during 3 phase fault

Figure 4.7 is the current waveform at Bus B during 3 phase fault. The total length of line between Bus A and Bus B is 46 miles. Fault occurred at 35 miles away from Bus B. Current waveforms were stable until the fault occurred at 10ms, then current increased.

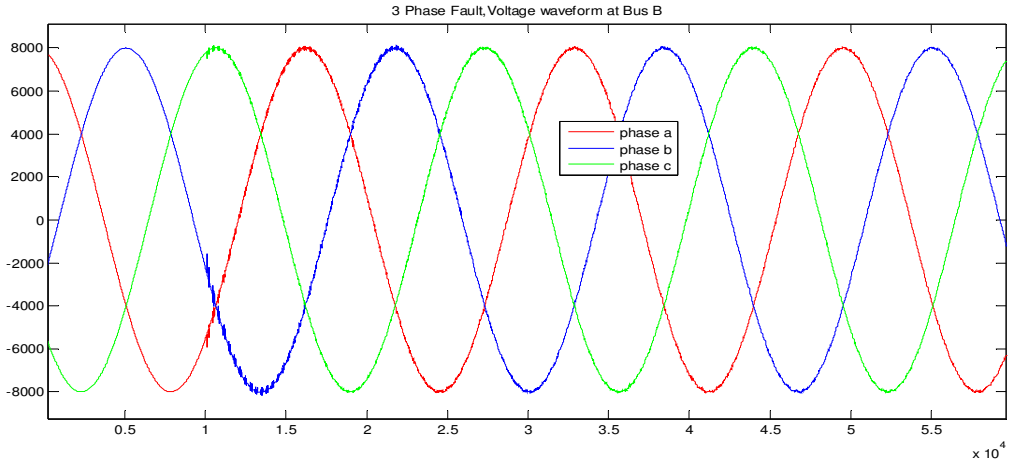

Figure 4.8: Voltage Waveform at Bus B during 3 phase fault

Figure 4.8 is the voltage waveform at Bus B during 3 phase fault. The total length of line between Bus A and Bus B is 46 miles. Fault occurred at 35 miles away from Bus B. Voltage waveforms were stable until the fault occurred at 10ms, then voltage decreased. Since the source was ideal, it is not clear in figure 4.8.

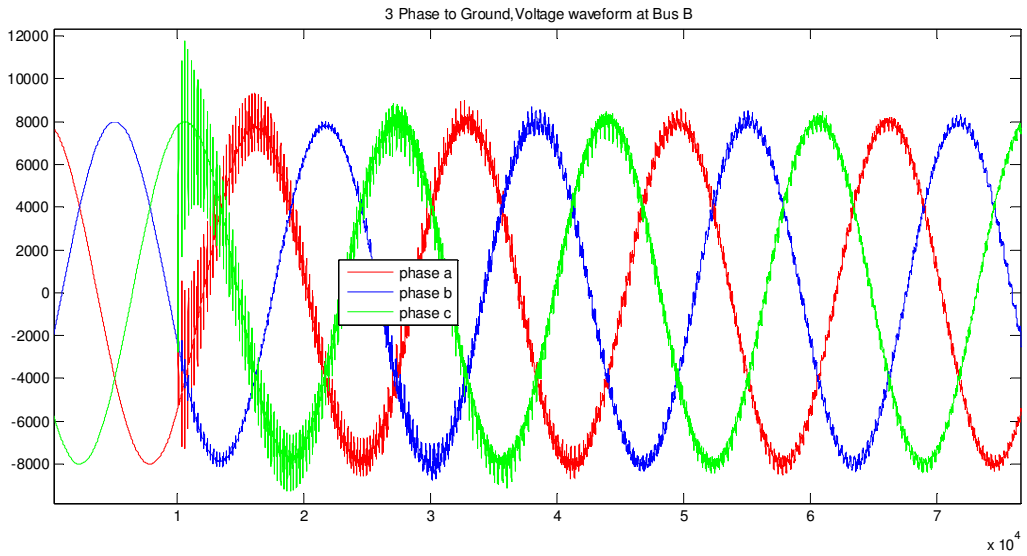

Figure 4.9: Voltage Waveform at Bus B during 3 phase to ground

Figure 4.9 is the voltage waveform at Bus B during 3 phase to ground fault. The total length of line between Bus A and Bus B is 46 miles. Fault occurred at 35 miles away from Bus B. Voltage waveforms were stable until the fault occurred at 10ms, then voltage decreased. Since the source was ideal, it is not clear in figure 4.9.

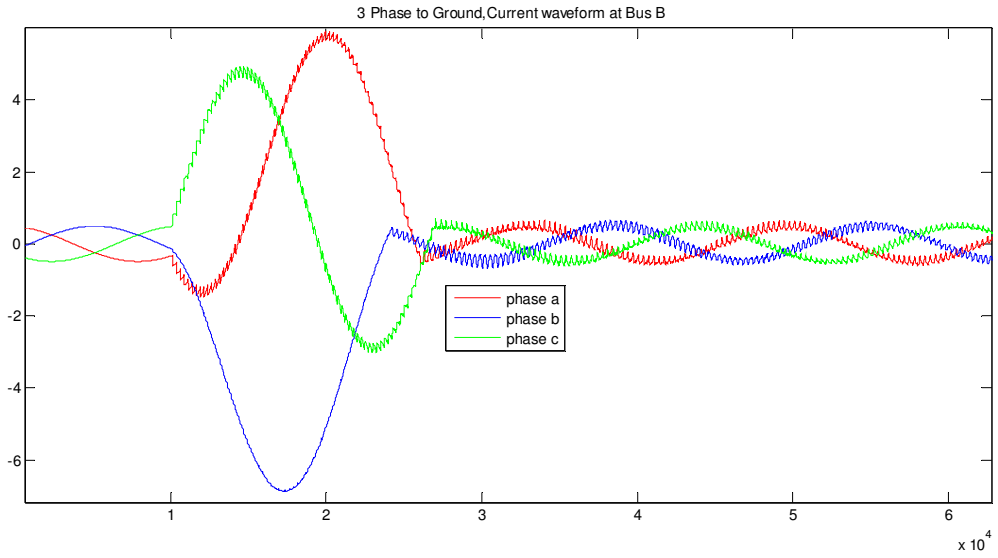

Figure 4.10: Current Waveform at Bus B during 3 phase to ground

Figure 4.10 is the current waveform at Bus B during 3 phase fault to ground. The total length of line between Bus A and Bus B is 46 miles. Fault occurred at 35 miles away from Bus B. Current waveforms were stable until the fault occurred at 10ms, then current increased.

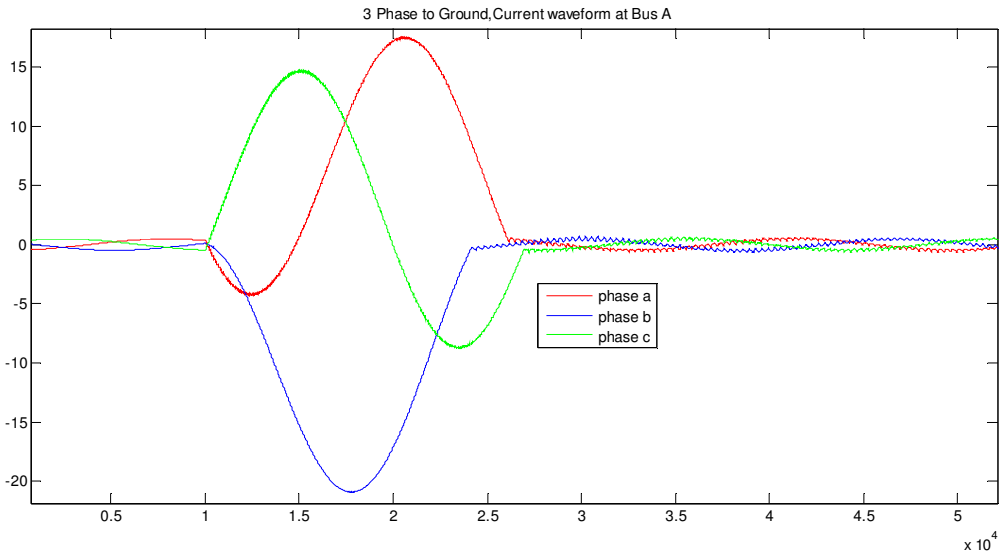

Figure 4.11: Current Waveform at Bus A during 3 phase to ground

Figure 4.11 is the current waveform at Bus A during 3 phase fault to ground. The total length of line between Bus A and Bus B is 46 miles. Fault occurred at 35 miles away from Bus B. Current waveform was stable until the fault occurred at 10ms, then current increased.

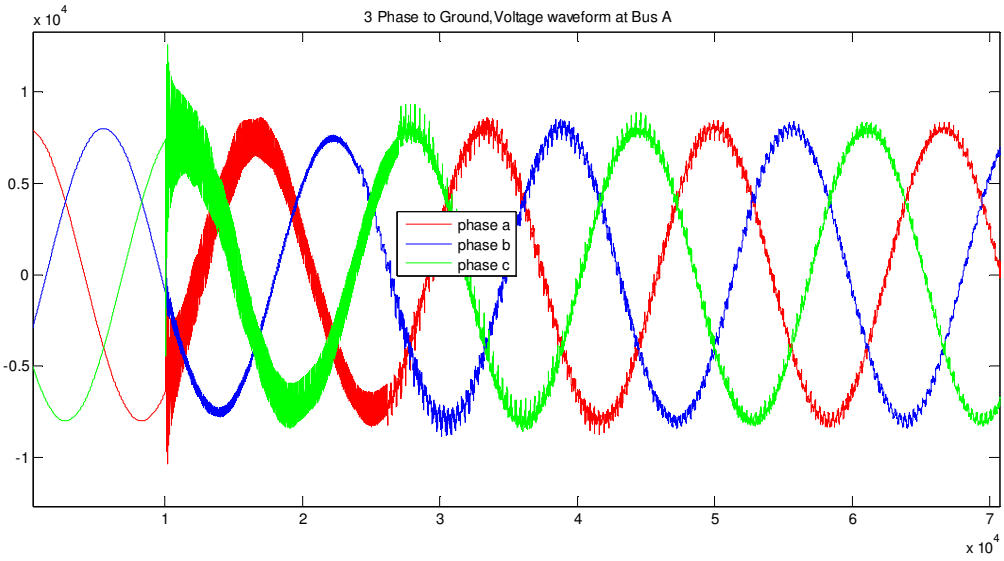

Figure 4.12: Voltage Waveform at Bus A during 3 phase to ground

Figure 4.12 is the voltage waveform at Bus A during 3 phase to ground fault. The total length of line between Bus A and Bus B is 46 miles. Fault occurred at 35 miles away from Bus B. Voltage waveforms were stable until the fault occurred at 10ms, then voltage decreased.

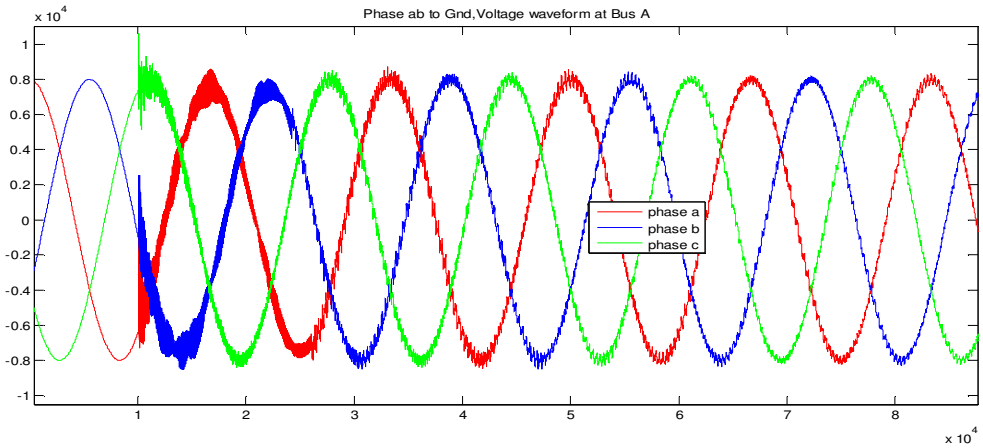

Figure 4.13: Voltage Waveform at Bus A during Phase ab to ground fault

Figure 4.13 is the voltage waveform at Bus A during phase a and phase b to ground fault. The total length of line between Bus A and Bus B is 46 miles. Fault occurred at 35 miles away from Bus B. Voltage waveforms were stable until the fault occurred at 10ms, then voltage decreased.

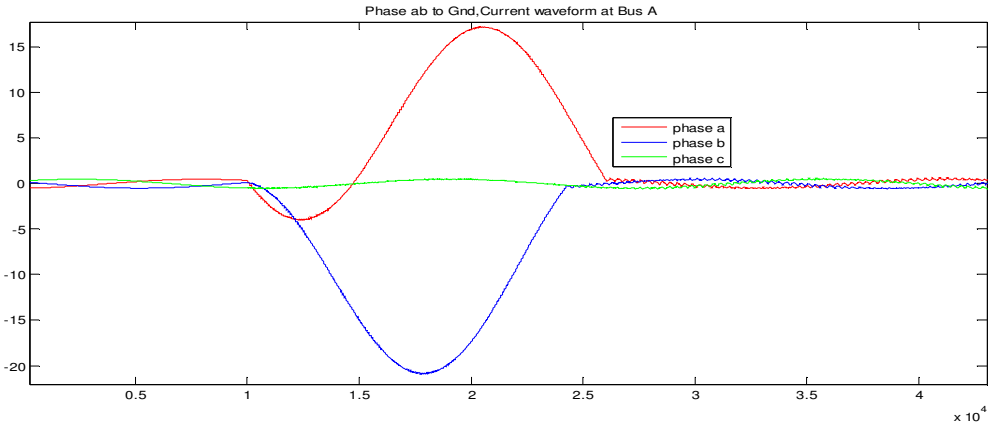

Figure 4.14: Current Waveform at Bus A during Phase ab to ground fault

Figure 4.14 is the current waveforms at Bus A during phase a and phase b to ground fault. The total length of line between Bus A and Bus B is 46 miles. Fault occurred at 35 miles away from Bus B. Current waveforms were stable until the fault occurred at 10ms, then current increased.

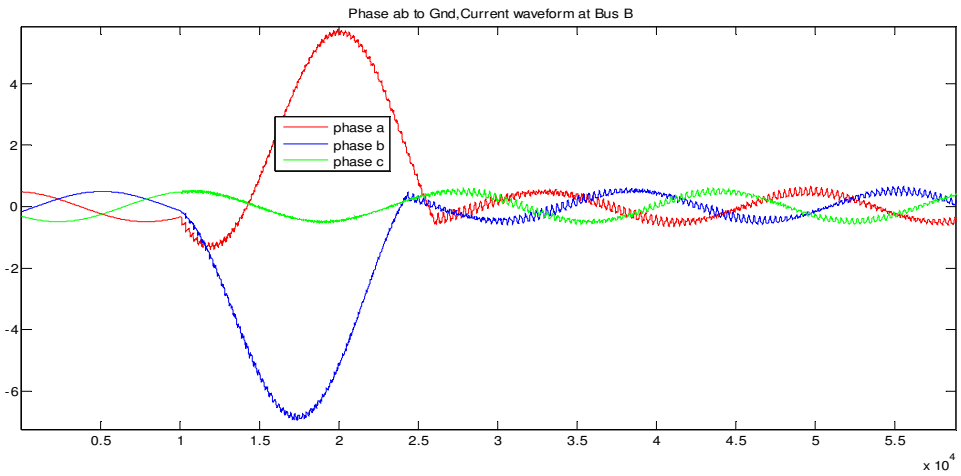

Figure 4.15: Current Waveform at Bus B during Phase ab to ground fault

Figure 4.15 is the current waveform at Bus B during phase a and phase b to ground fault. The total length of line between Bus A and Bus B is 46 miles. Fault occurred at 35 miles away from Bus B. Current waveforms were stable until the fault occurred at 10ms, then current increased.

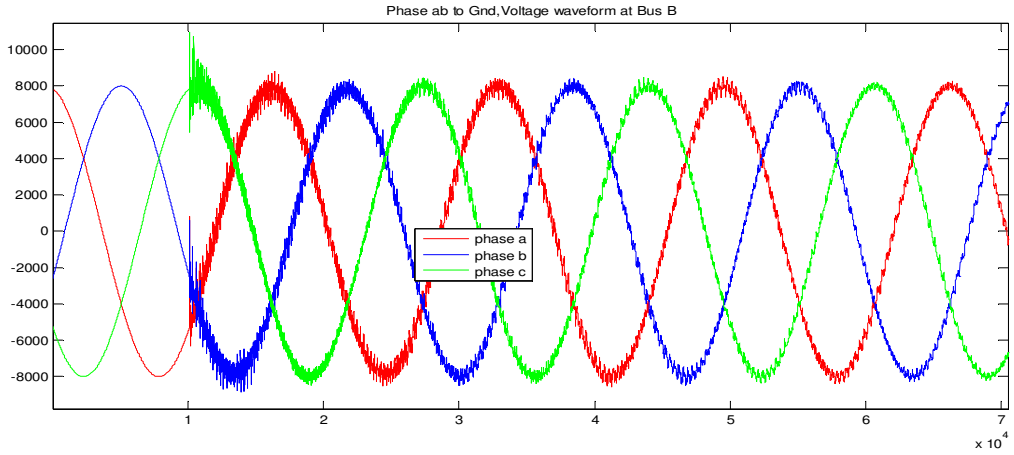

Figure 4.16: Voltage Waveform at Bus B during Phase ab to ground fault

Figure 4.16 is the voltage waveform at Bus B during phase a and phase b to ground fault. The total length of line between Bus A and Bus B is 46 miles. Fault occurred at 35 miles away from Bus B. Voltage waveform were stable until the fault occurred at 10ms, then voltage decreased.

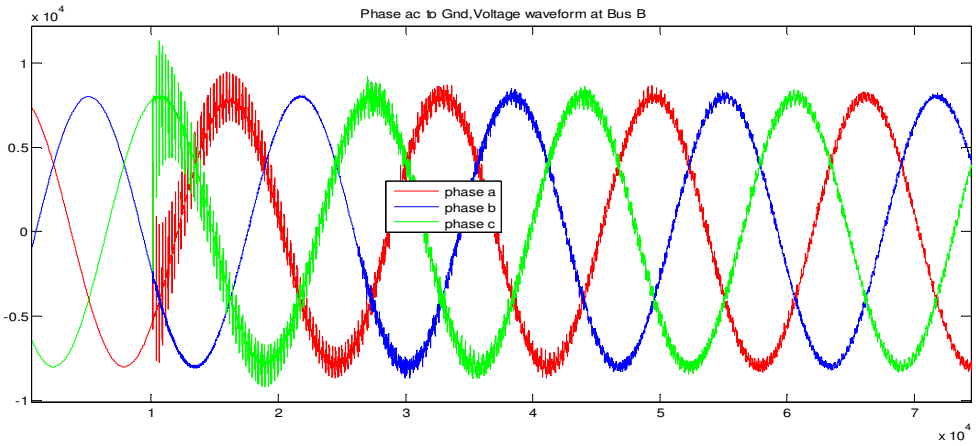

Figure 4.17: Voltage Waveform at Bus B during Phase ac to ground fault

Figure 4.17 is the voltage waveform at Bus B during phase a and phase c to ground fault. The total length of line between Bus A and Bus B is 46 miles. Fault occurred at 35 miles away from Bus B. Voltage waveforms were stable until the fault occurred at 10ms, then voltage decreased. At 10ms, disturbance on phase a and phase c is seen in the figure 4.17.

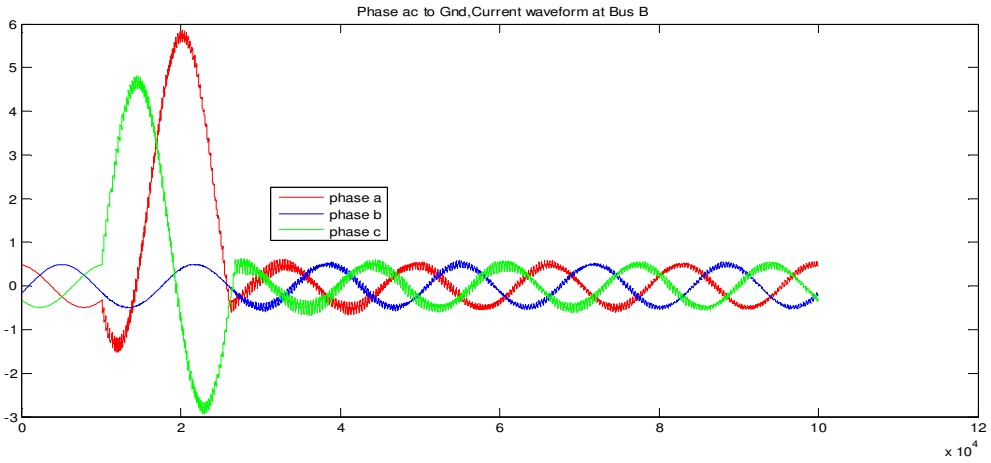

Figure 4.18: Current Waveform at Bus B during Phase ac to ground fault

Figure 4.18 is the current waveform at Bus B during phase a and phase c to ground fault. The total length of line between Bus A and Bus B is 46 miles. Fault occurred at 35 miles away from Bus B. Current waveforms were stable until the fault occurred at 10ms, then current increased.

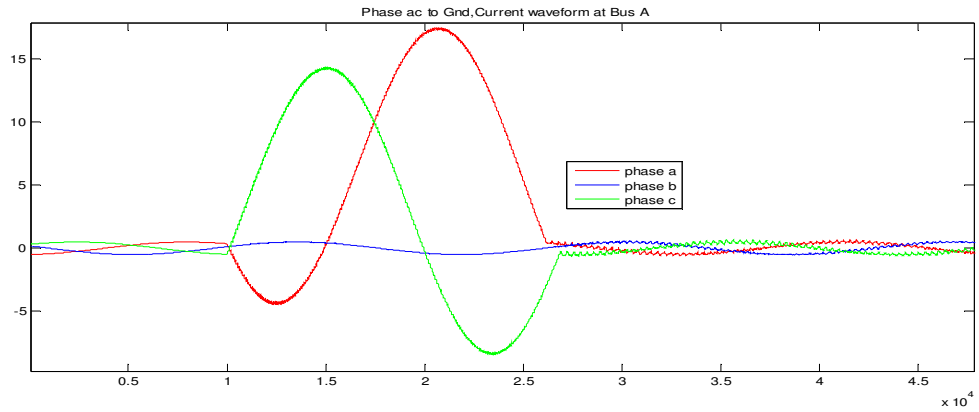

Figure 4.19: Current Waveform at Bus A during Phase ac to ground fault

Figure 4.19 is the current waveform at Bus A during phase a and phase c to ground fault. The total length of line between Bus A and Bus B is 46 miles. Fault occurred at 35 miles away from Bus B. Current waveforms were stable until the fault occurred at 10ms, then current increased.

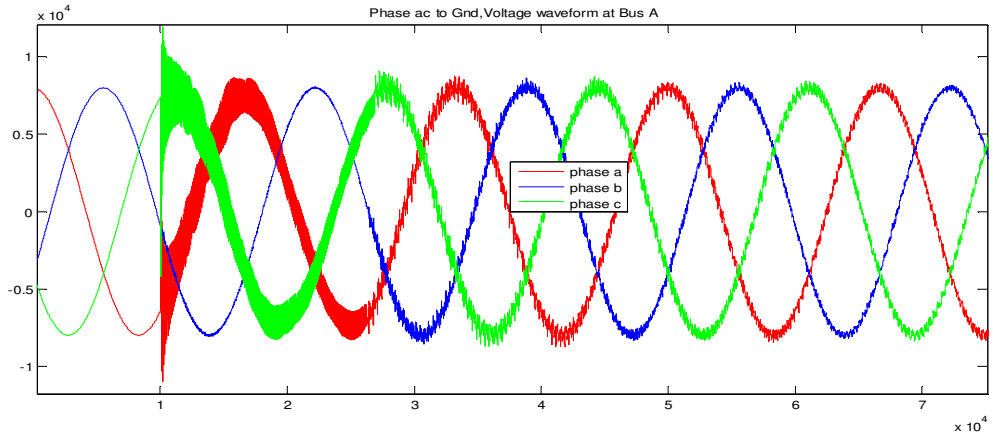

Figure 4.20: Voltage Waveform at Bus A during Phase ac to ground fault

Figure 4.20 is the voltage waveform at Bus A during phase a and phase c to ground fault. The total length of line between Bus A and Bus B is 46 miles. Fault occurred at 35 miles away from Bus B. Voltage waveforms were stable until the fault occurred at 10ms, then voltage decreased.

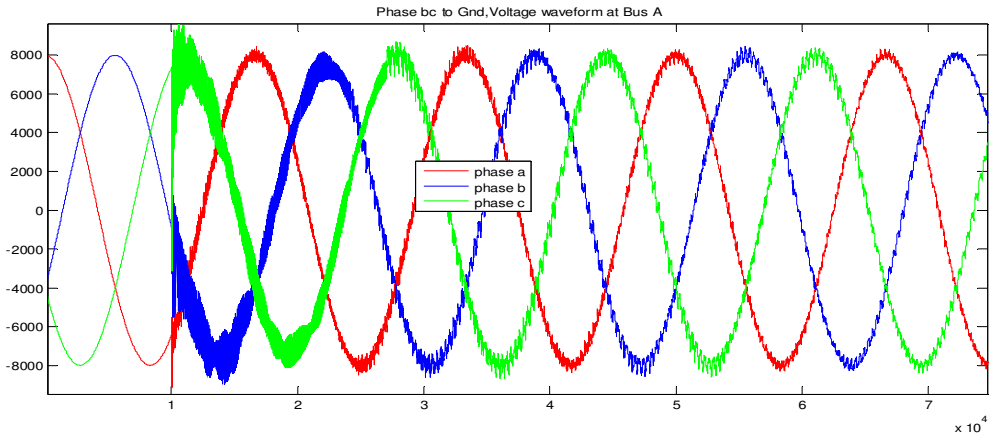

Figure 4.21: Voltage Waveform at Bus A during Phase bc to ground fault

Figure 4.21 is the voltage waveform at Bus A during phase b and phase c to ground fault. The total length of line between Bus A and Bus B is 46 miles. Fault occurred at 35 miles away from Bus B. Voltage waveforms were stable until the fault occurred at 10ms, then voltage decreased.

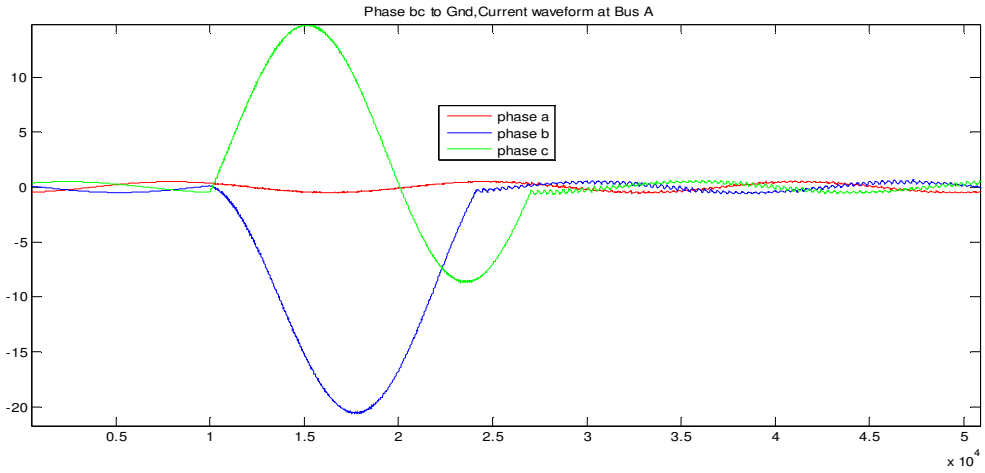

Figure 4.22: Current Waveform at Bus A during Phase bc to ground fault

Figure 4.22 is the current waveform at Bus A during phase b and phase c to ground fault. The total length of line between Bus A and Bus B is 46 miles. Fault occurred at 35 miles away from Bus B. Current waveforms were stable until the fault occurred at 10ms, then current increased.

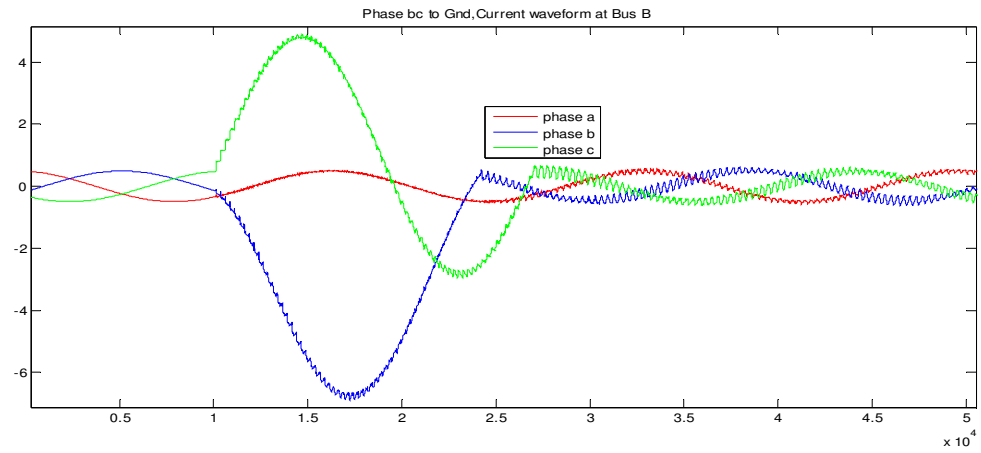

Figure 4.23: Current Waveform at Bus B during Phase bc to ground fault

Figure 4.23 is the current waveform at Bus B during phase b and phase c to ground fault. The total length of line between Bus A and Bus B is 46 miles. Fault occurred at 35 miles away from Bus B. Current waveforms were stable until the fault occurred at 10ms, then current increased.

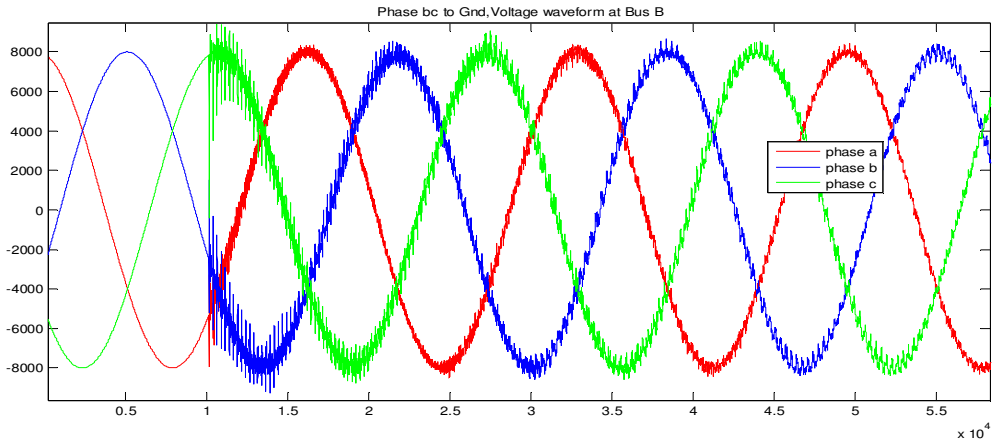

Figure 4.24: Voltage Waveform at Bus B during Phase bc to ground fault

Figure 4.24 is the voltage waveform at Bus B during phase b and phase c to ground fault. The total length of line between Bus A and Bus B is 46 miles. Fault occurred at 35 miles away from Bus B. Voltage waveforms were stable until the fault occurred at 10ms, then voltage decreased.

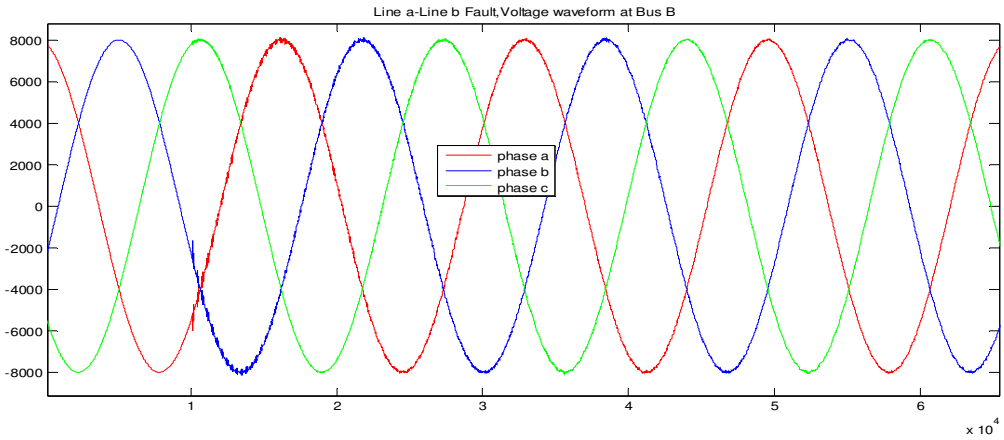

Figure 4.25: Voltage Waveform at Bus B during Phase a make connection with Phase b

Figure 4.25 is the voltage waveform at Bus B during phase a make connection with phase b. The total length of line between Bus A and Bus B is 46 miles. Fault occurred at 35 miles away from Bus B. Voltage waveforms were stable until the fault occurred at 10ms, then voltage decreased.

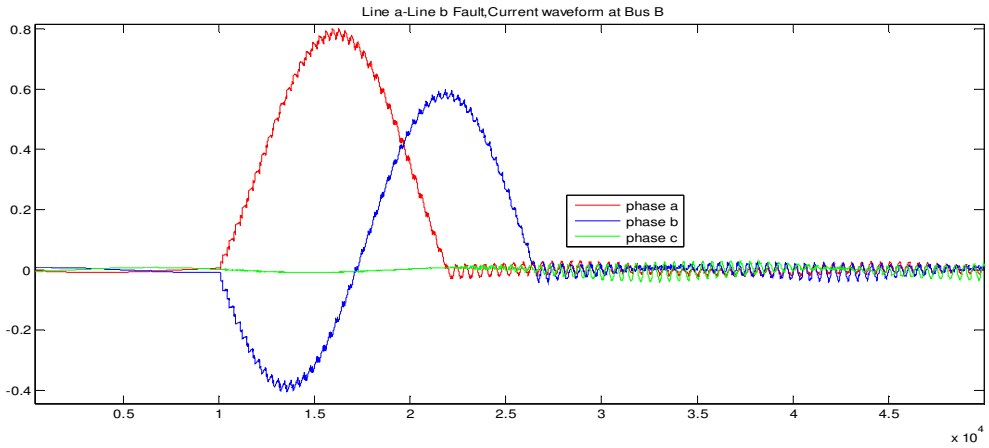

Figure 4.26: Current Waveform at Bus B during Phase a make connection with Phase b

Figure 4.26 is the current waveform at Bus B during 3 phase fault to ground fault. The total length of line between Bus A and Bus B is 46 miles. Fault occurred at 35 miles away from Bus B. Current waveforms were stable until the fault occurred at 10ms, then current increased.

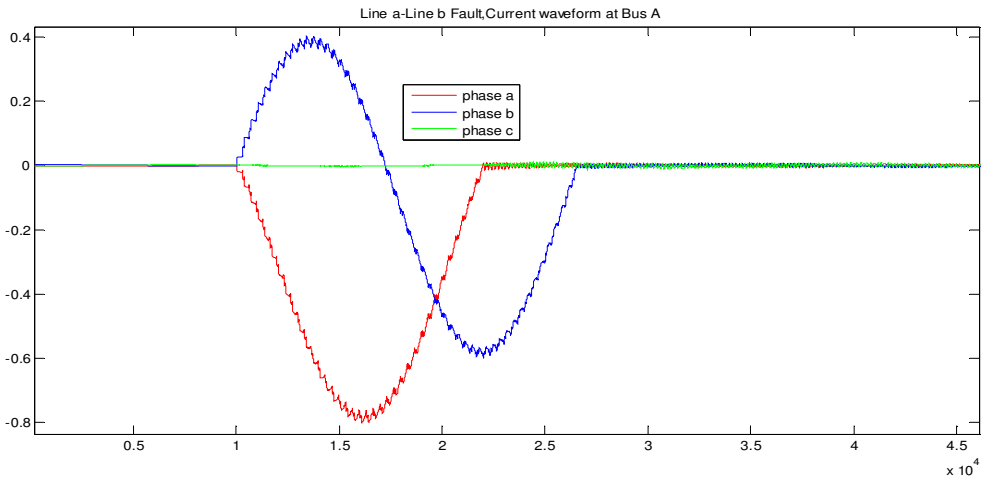

Figure 4.27: Current Waveform at Bus A during Phase a make connection with Phase b

Figure 4.27 is the current waveform at Bus A during phase a make connection with phase b. The total length of line between Bus A and Bus B is 46 miles. Fault occurred at 35 miles away from Bus B. Current waveforms were stable until the fault occurred at 10ms, then current increased.

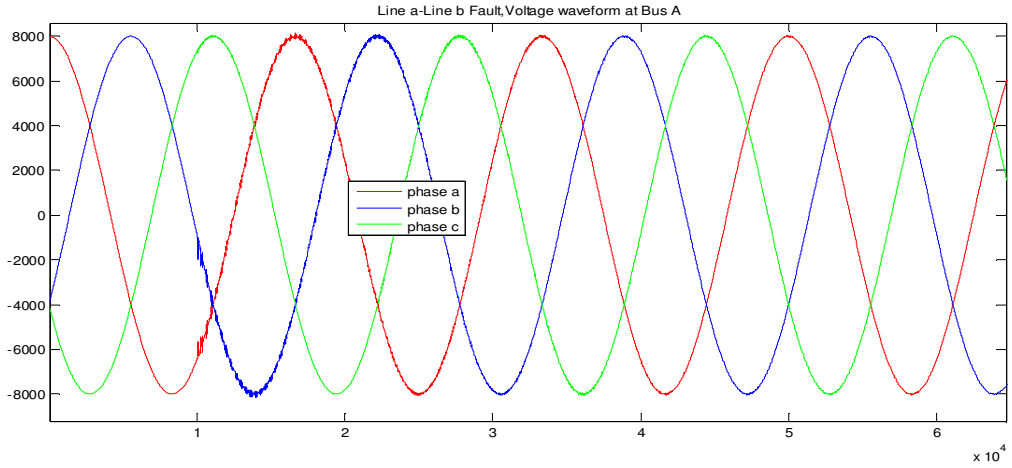

Figure 4.28: Voltage Waveform at Bus A during Phase a make connection with Phase b

Figure 4.28 is the voltage waveform at Bus A during phase a make connection with phase b. The total length of line between Bus A and Bus B is 46 miles. Fault occurred at 35 miles away from Bus B. Voltage waveform were stable until the fault occurred at 10ms, then voltage decreased.

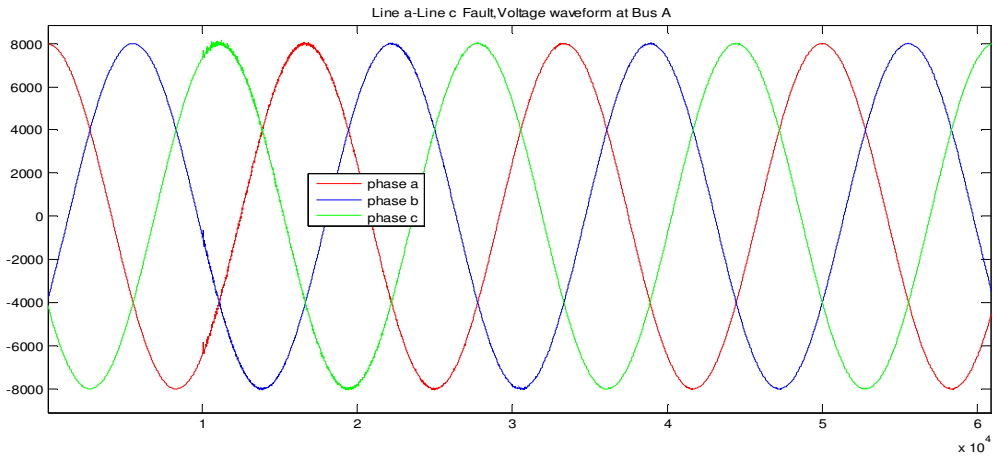

Figure 4.29: Voltage Waveform at Bus A during Phase a make connection with Phase c

Figure 4.29 is the voltage waveform at Bus A during phase a make connection with phase c. The total length of line between Bus A and Bus B is 46 miles. Fault occurred at 35 miles away from Bus B. Voltage waveforms were stable until the fault occurred at 10ms, then voltage decreased.

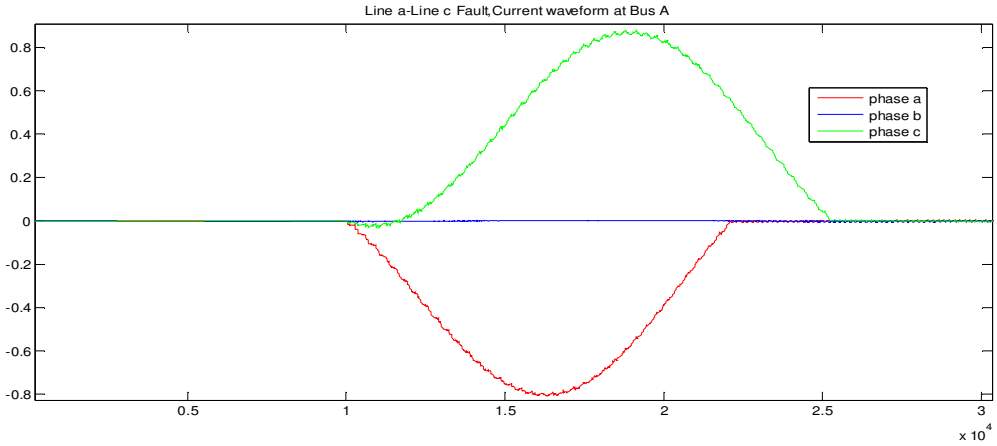

Figure 4.30: Current Waveform at Bus A during Phase a make connection with Phase c

Figure 4.30 is the current waveform at Bus A during phase a make connection with phase c. The total length of line between Bus A and Bus B is 46 miles. Fault occurred at 35 miles away from Bus B. Current waveforms were stable until the fault occurred at 10ms, then current increased.

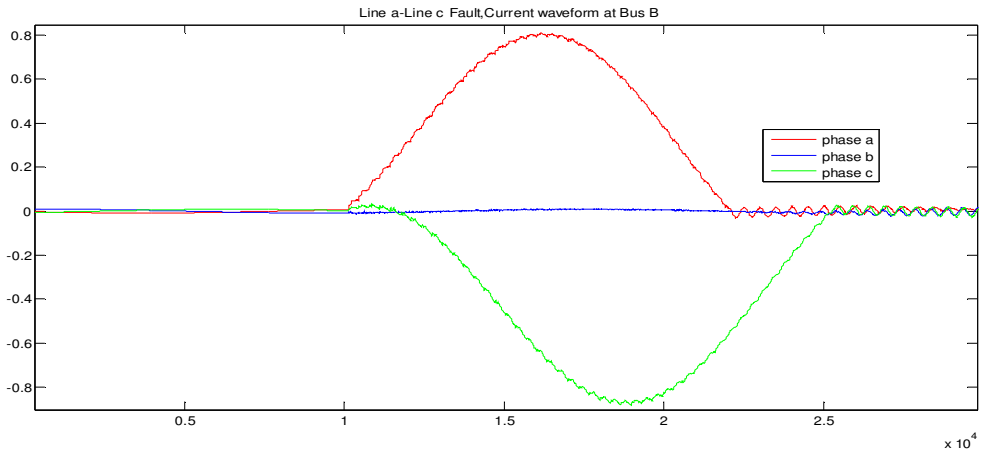

Figure 4.31: Current Waveform at Bus B during Phase a make connection with Phase c

Figure 4.31 is the current waveform at Bus B during phase a make connection with phase c. The total length of line between Bus A and Bus B is 46 miles. Fault occurred at 35 miles away from Bus B. Current waveforms were stable until the fault occurred at 10ms, then current increased.

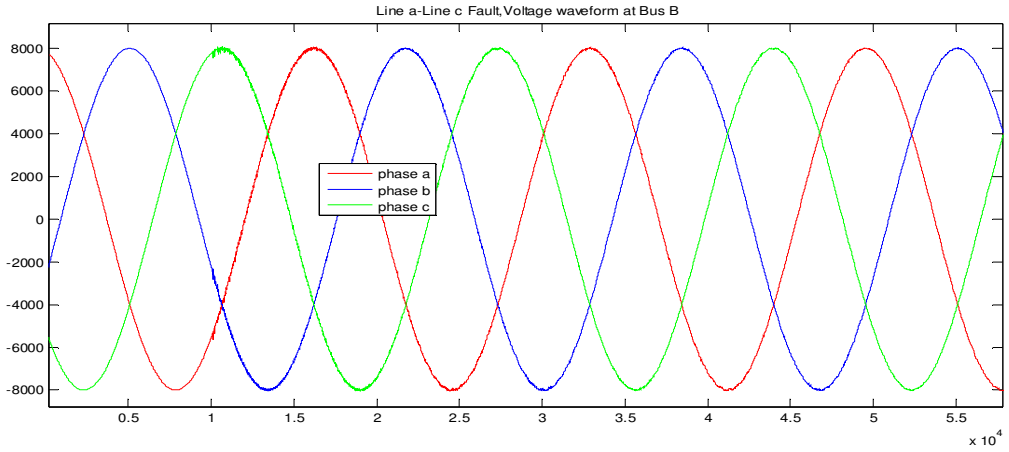

Figure 4.32: Voltage Waveform at Bus B during Phase a make connection with Phase c

Figure 4.32 is the voltage waveform at Bus B during phase a make connection with phase c. The total length of line between Bus A and Bus B is 46 miles. Fault occurred at 35 miles away from Bus B. Voltage waveforms were stable until the fault occurred at 10ms, then voltage decreased.

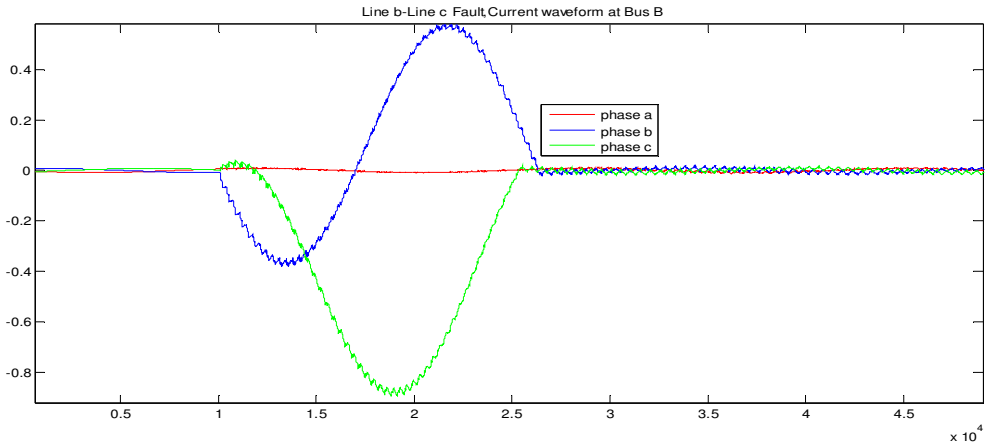

Figure 4.33: Current Waveform at Bus B during Phase b make connection with Phase c

Figure 4.33 is the current waveform at Bus B during phase b make connection with phase c. The total length of line between Bus A and Bus B is 46 miles. Fault occurred at 35 miles away from Bus B. Current waveforms were stable until the fault occurred at 10ms, then current increased.

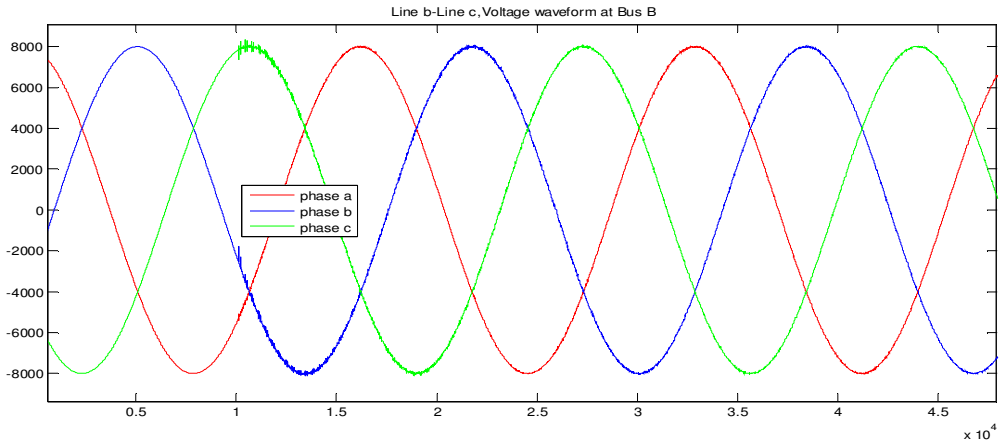

Figure 4.34: Voltage Waveform at Bus B during Phase b make connection with Phase c

Figure 4.34 is the voltage waveform at Bus B during phase b make connection with phase c. The total length of line between Bus A and Bus B is 46 miles. Fault occurred at 35 miles away from Bus B. Voltage waveforms were stable until the fault occurred at 10ms, then voltage decreased.

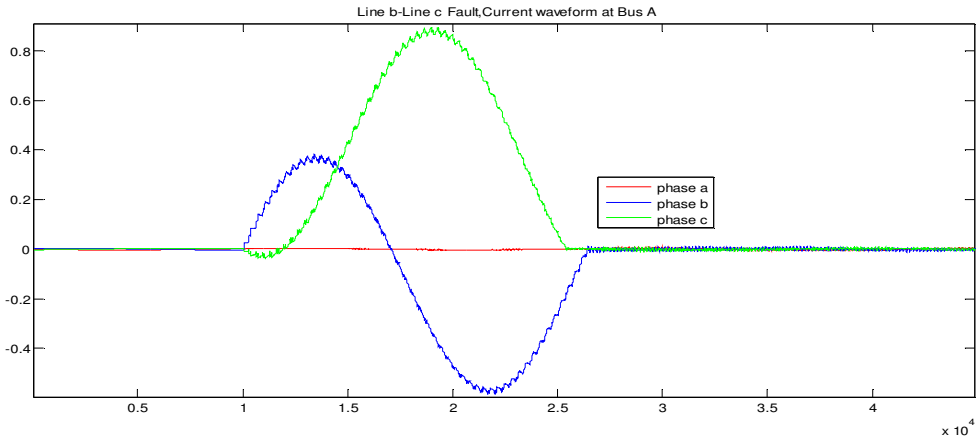

Figure 4.35: Current Waveform at Bus A during Phase b make connection with Phase c

Figure 4.35 is the current waveform at Bus A during phase b make connection with phase c. The total length of line between Bus A and Bus B is 46 miles. Fault occurred at 35 miles away from Bus B. Current waveforms were stable until the fault occurred at 10ms, then current increased.

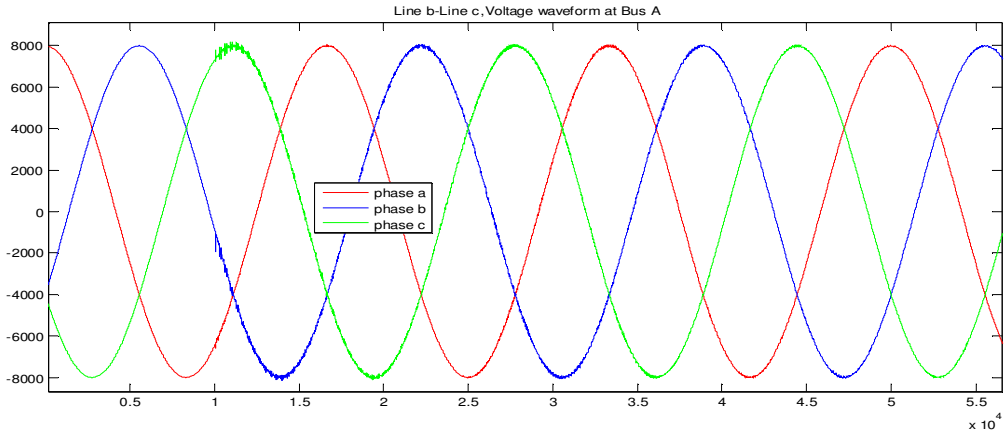

Figure 4.36: Voltage Waveform at Bus A during Phase b make connection with Phase c

Figure 4.36 is the voltage waveform at Bus A during phase b make connection with phase c. The total length of line between Bus A and Bus B is 46 miles. Fault occurred at 35 miles away from Bus B. Voltage waveforms were stable until the fault occurred at 10ms, then voltage decreased.

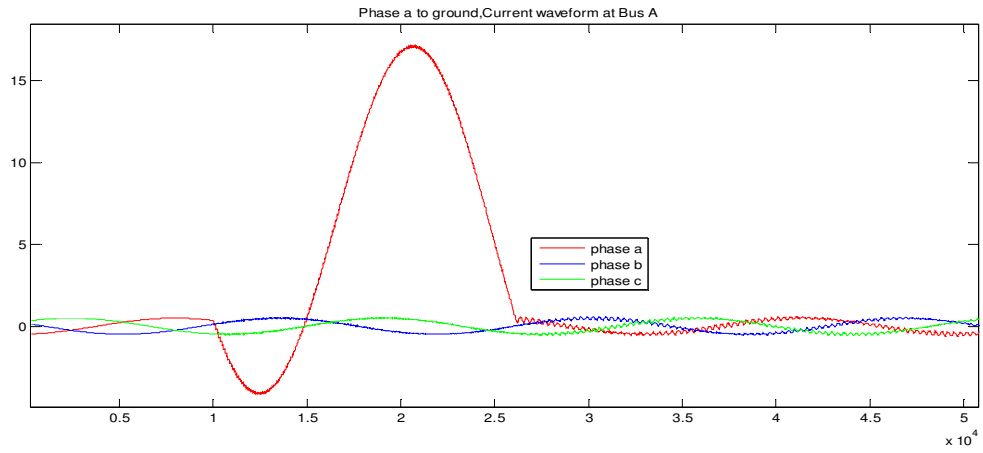

Figure 4.37: Current Waveform at Bus A during Phase a to ground fault

Figure 4.37 is the current waveform at Bus A during phase a to ground fault. The total length of line between Bus A and Bus B is 46 miles. Fault occurred at 35 miles away from Bus B. Current waveforms were stable until the fault occurred at 10ms, then current increased.

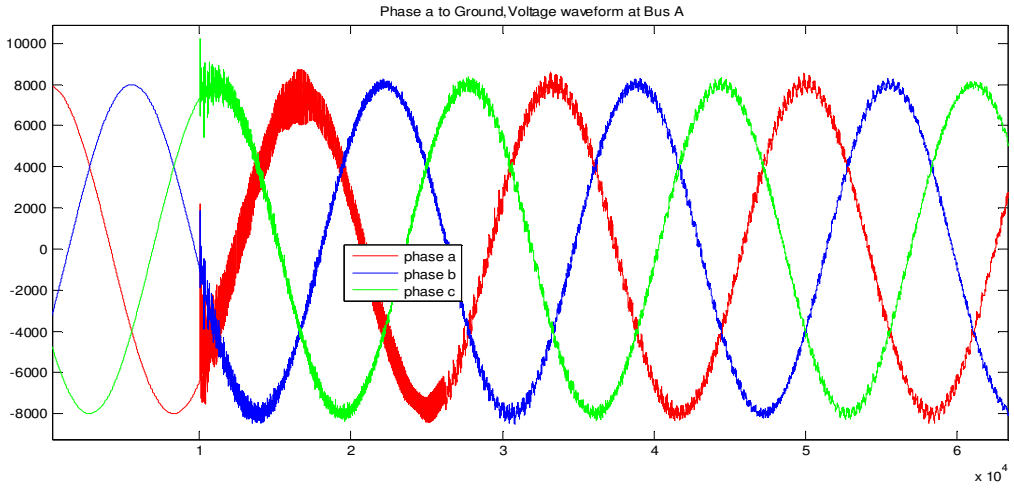

Figure 4.38: Voltage Waveform at Bus A during Phase a to ground fault

Figure 4.38 is the voltage waveform at Bus A during phase a to ground fault. The total length of line between Bus A and Bus B is 46 miles. Fault occurred at 35 miles away from Bus B. Voltage waveforms were stable until the fault occurred at 10ms, then voltage decreased.

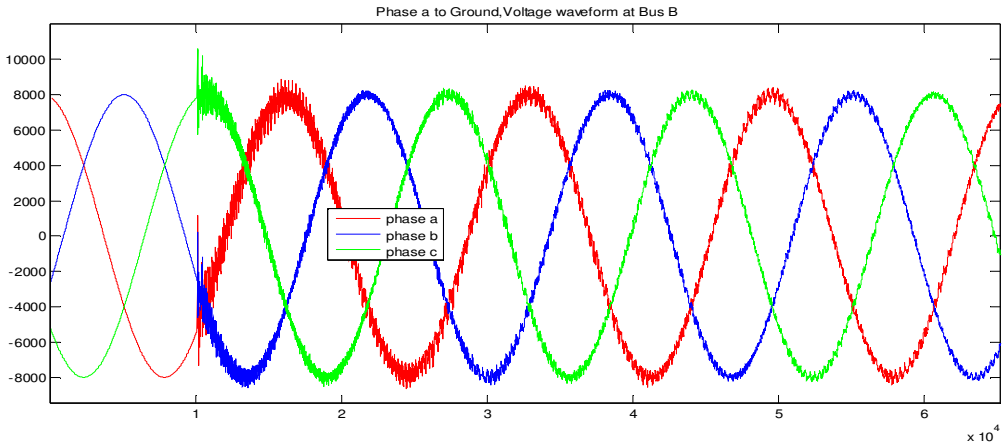

Figure 4.39: Voltage Waveform at Bus B during Phase a to ground fault

Figure 4.39 is the voltage waveform at Bus B during phase a to ground fault. The total length of line between Bus A and Bus B is 46 miles. Fault occurred at 35 miles away from Bus B. Voltage waveforms were stable until the fault occurred at 10ms, then voltage decreased.

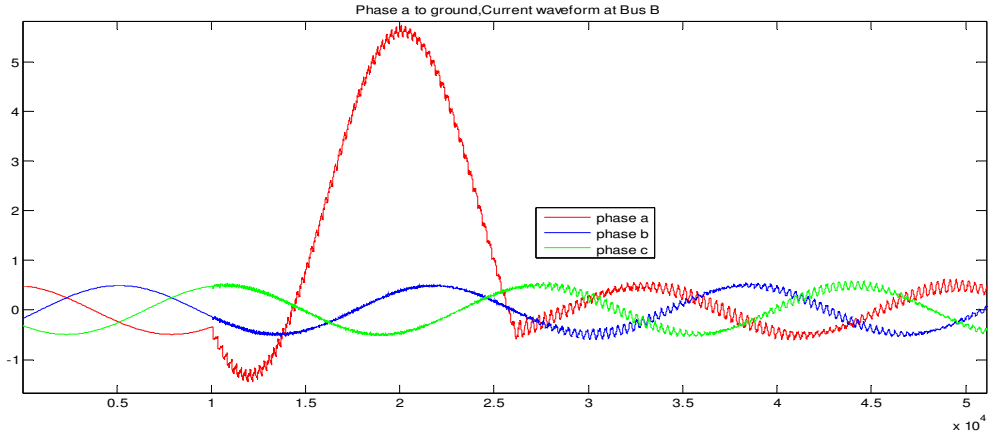

Figure 4.40: Current Waveform at Bus B during Phase a to ground fault

Figure 4.40 is the current waveform at Bus B during phase a fault to ground fault. The total length of line between Bus A and Bus B is 46 miles. Fault occurred at 35 miles away from Bus B. Current waveforms were stable until the fault occurred at 10ms, then current increased.

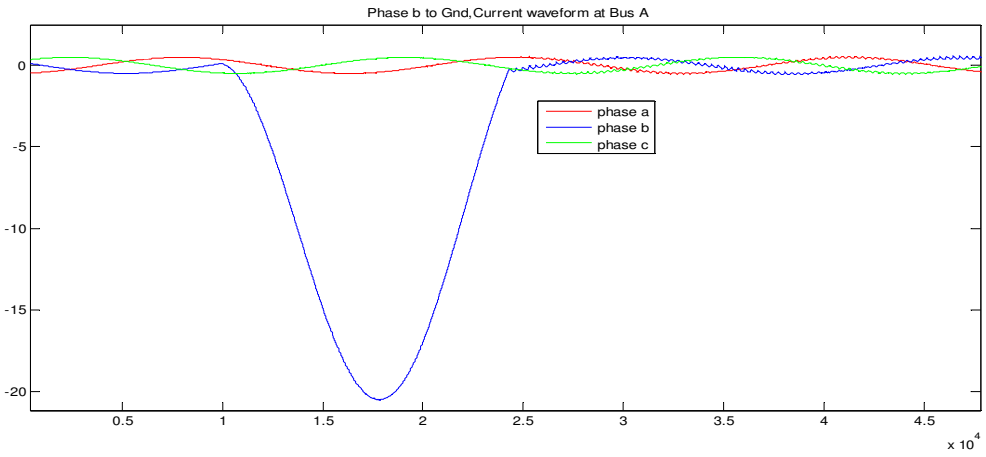

Figure 4.41: Current Waveform at Bus A during Phase b to ground fault

Figure 4.41 is the current waveform at Bus A during phase b to ground fault. The total length of line between Bus A and Bus B is 46 miles. Fault occurred at 35 miles away from Bus B. Current waveforms were stable until the fault occurred at 10ms, then current increased.

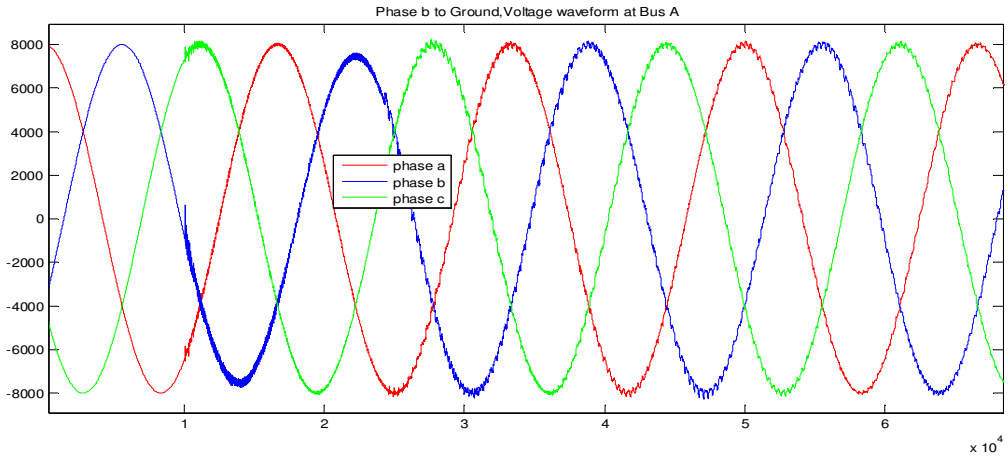

Figure 4.42: Voltage Waveform at Bus A during Phase b to ground fault

Figure 4.42 is the voltage waveform at Bus A during phase b to ground fault. The total length of line between Bus A and Bus B is 46 miles. Fault occurred at 35 miles away from Bus B. Voltage waveforms were stable until the fault occurred at 10ms, then voltage decreased.

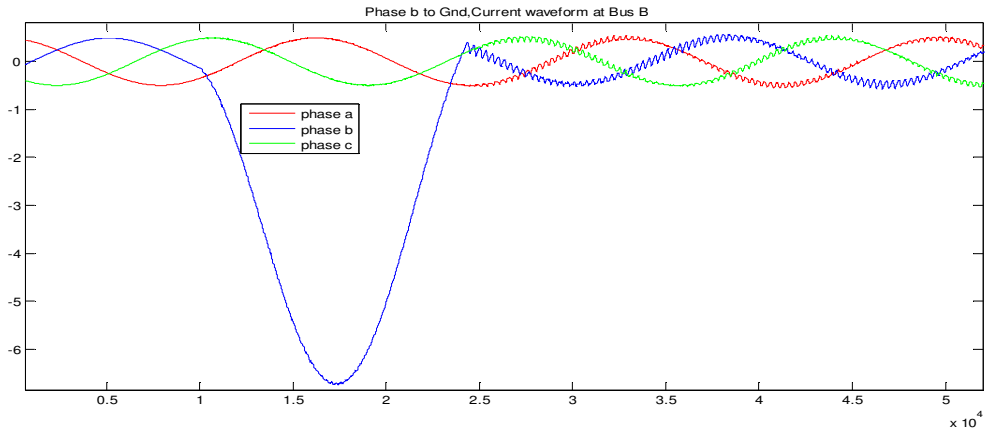

Figure 4.43: Current Waveform at Bus B during Phase b to ground fault

Figure 4.43 is the current waveform at Bus B during phase b to ground fault. The total length of line between Bus A and Bus B is 46 miles. Fault occurred at 35 miles away from Bus B. Current waveforms were stable until the fault occurred at 10ms, then current increased.

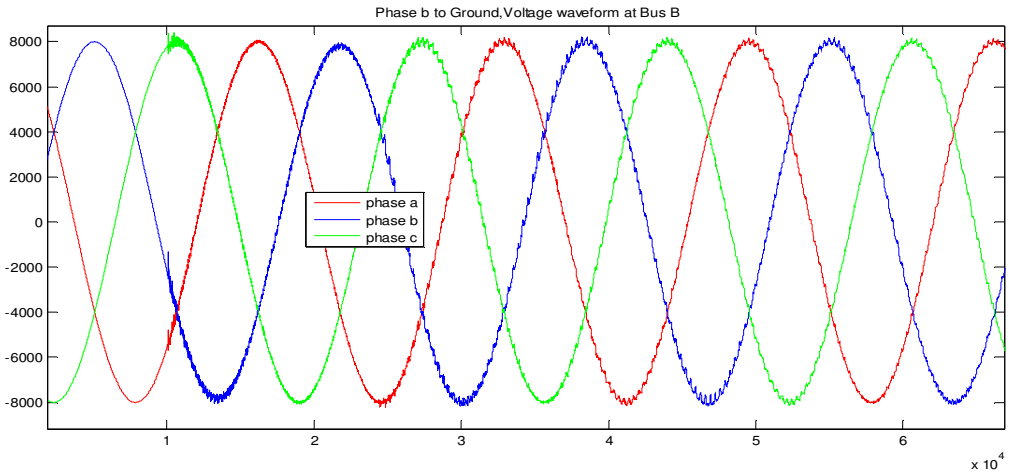

Figure 4.44: Voltage Waveform at Bus B during Phase b to ground fault

Figure 4.44 is the voltage waveform at Bus B during phase b to ground fault. The total length of line between Bus A and Bus B is 46 miles. Fault occurred at 35 miles away from Bus B. Voltage waveforms were stable until the fault occurred at 10ms, then voltage decreased.

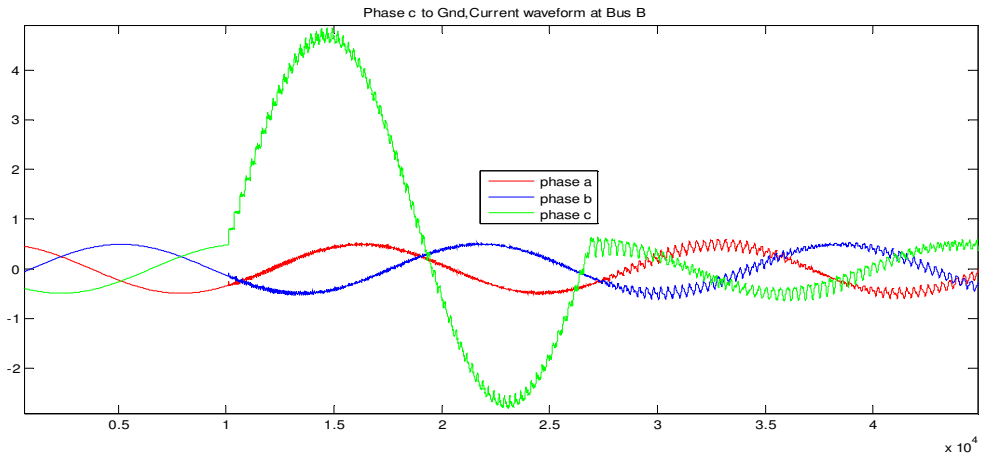

Figure 4.45: Current Waveform at Bus B during Phase c to ground fault

Figure 4.45 is the current waveform at Bus B during phase c to ground fault. The total length of line between Bus A and Bus B is 46 miles. Fault occurred at 35 miles away from Bus B. Current waveforms were stable until the fault occurred at 10ms, then current increased.

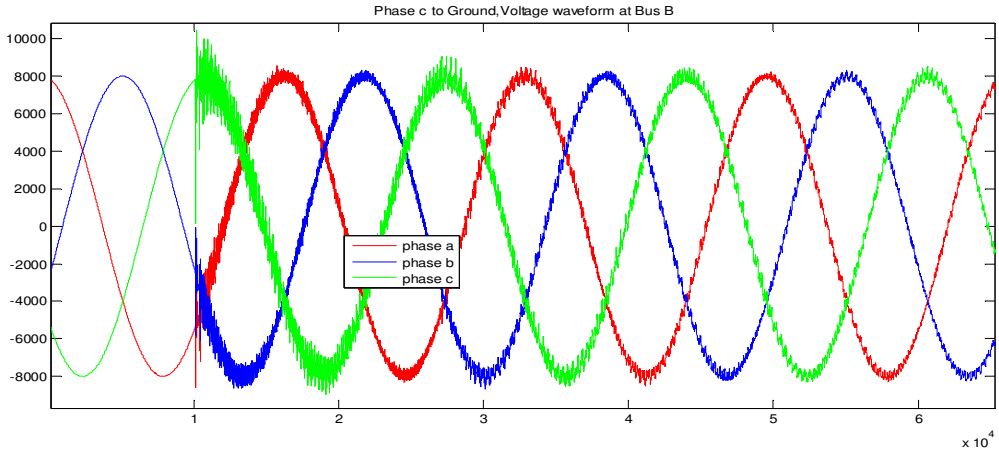

Figure 4.46: Voltage Waveform at Bus B during Phase c to ground fault

Figure 4.46 is the voltage waveform at Bus B during phase c to ground fault. The total length of line between Bus A and Bus B is 46 miles. Fault occurred at 35 miles away from Bus B. Voltage waveforms were stable until the fault occurred at 10ms, then voltage decreased.

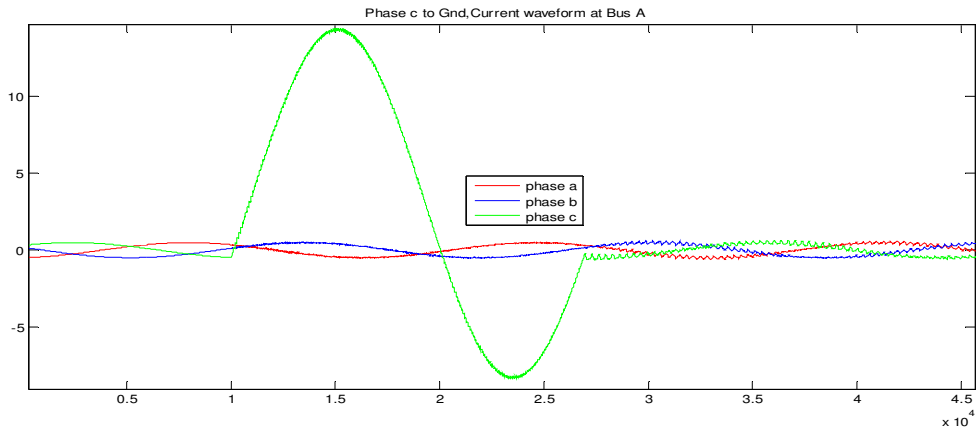

Figure 4.47: Current Waveform at Bus A during Phase c to ground fault

Figure 4.47 is the current waveform at Bus A during phase c to ground fault. The total length of line between Bus A and Bus B is 46 miles. Fault occurred at 35 miles away from Bus B. Current waveforms were stable until the fault occurred at 10ms, then current increased.

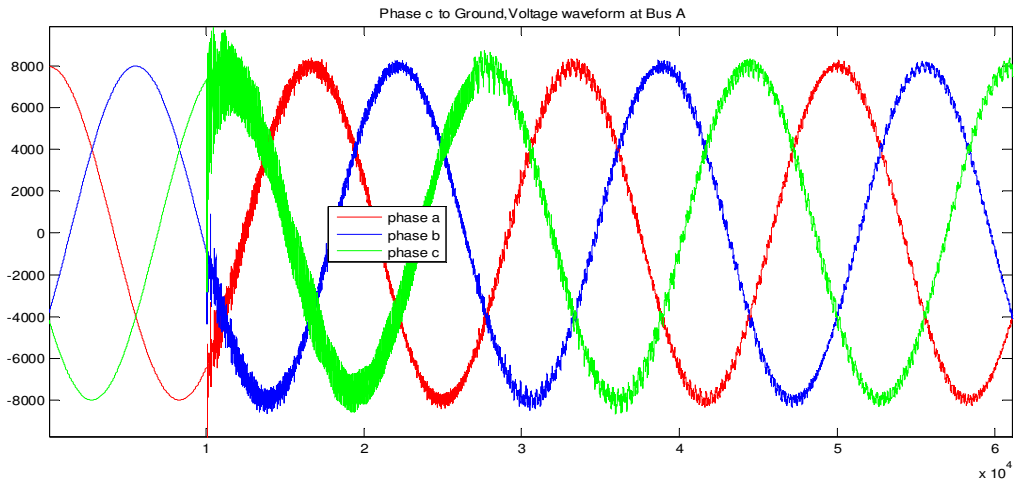

Figure 4.48: Voltage Waveform at Bus A during Phase c to ground fault

Figure 4.48 is the voltage waveform at Bus A during phase c to ground fault. The total length of line between Bus A and Bus B is 46 miles. Fault occurred at 35 miles away from Bus B. Voltage waveforms were stable until the fault occurred at 10ms, then voltage decreased.

B2.Wavelet coefficient of various fault types at 23 miles away from Bus B using traveling wave method:

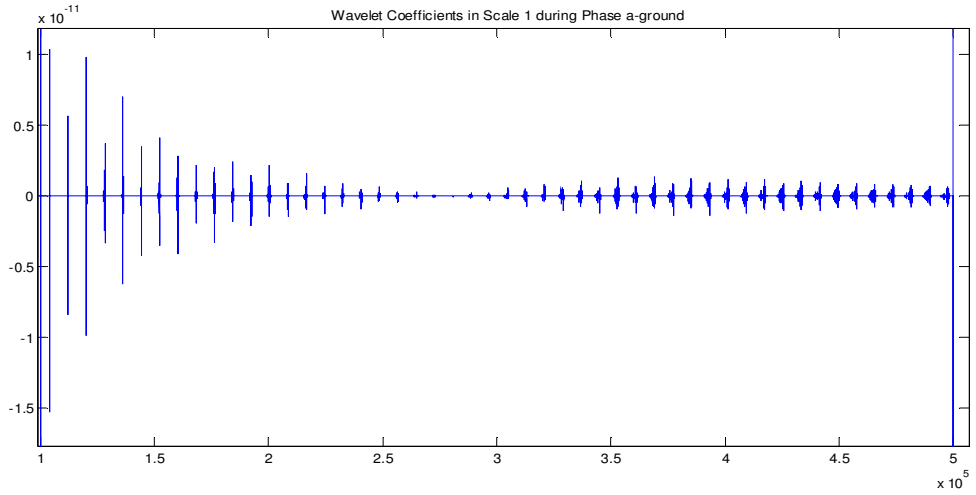

Figure 4.49: Detail coefficient of wavelets at terminal B during Phase a to ground fault

Figure 4.49 present the wavelet coefficient at Bus B during phase a to ground fault. Fault was 23 miles away from Bus B. The sampled signal from EMTP was decomposed into four scale levels using Daubechies4 filter. The distance between Bus A and Bus B is 46miles.

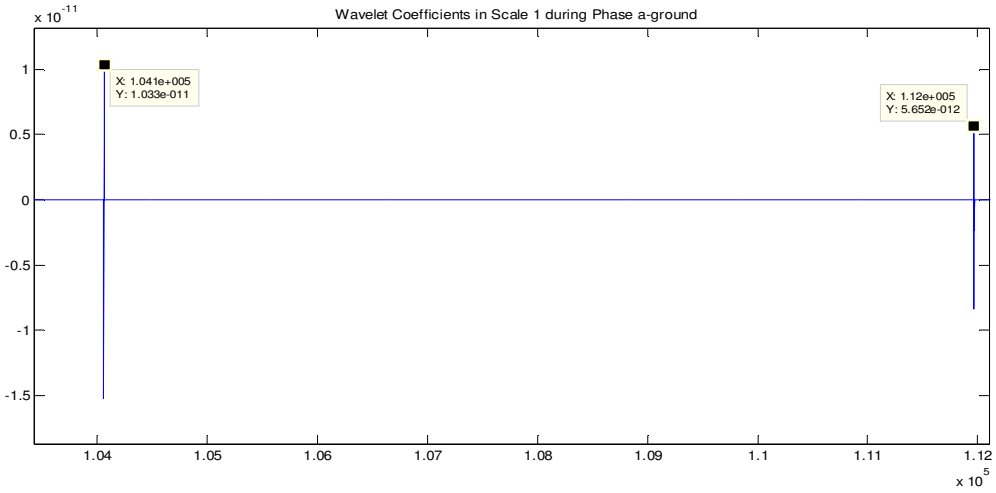

Figure 4.50: First two consecutive peaks

The first peak is the time taken by surge from fault location to Bus B. The second peak is the reflected wave from Bus B to fault location and back to Bus B. The first peak appeared at 2.0812558ms and the second peak appeared at 2.239295ms.

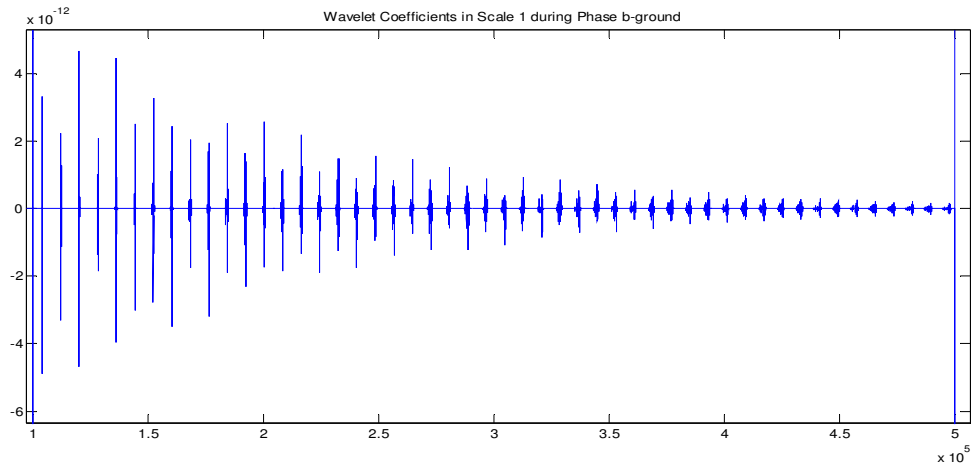

Figure 4.51: Detail coefficient of wavelets at terminal B during Phase b to ground fault

Figure 4.51 present the wavelet coefficient at Bus B during phase b to ground fault. Fault was 23 miles away from Bus B. The sampled signal from EMTP was decomposed into four scale levels using Daubechies4 filter. The distance between Bus A and Bus B is 46miles.

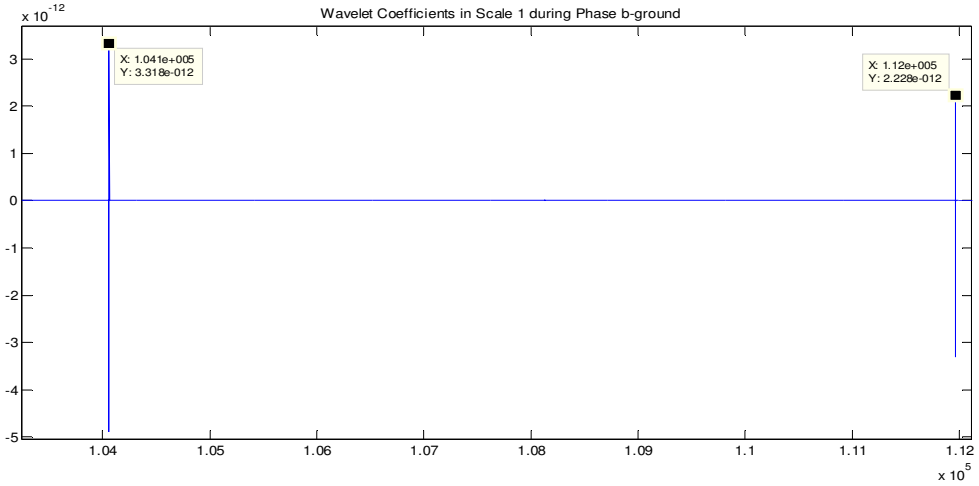

Figure 4.52: First two consecutive peaks

The first peak is the time take by surge from fault location to Bus B. The second peak is the reflected wave from Bus B to fault location and back to Bus B. The first peak appeared at 2.0812558ms and the second peak appeared at 2.239295ms.

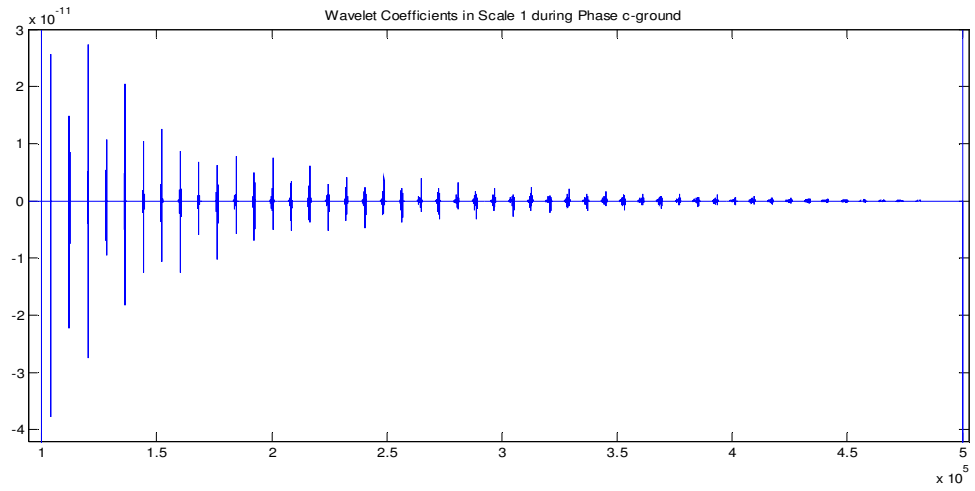

Figure 4.53: Detail coefficient of wavelets at terminal B during Phase c to ground fault

Figure 4.53 present the wavelet coefficient at Bus B during phase c to ground fault. Fault was 23 miles away from Bus B. The sampled signal from EMTP was decomposed into four scale levels using Daubechies4 filter. The distance between Bus A and Bus B is 46miles.

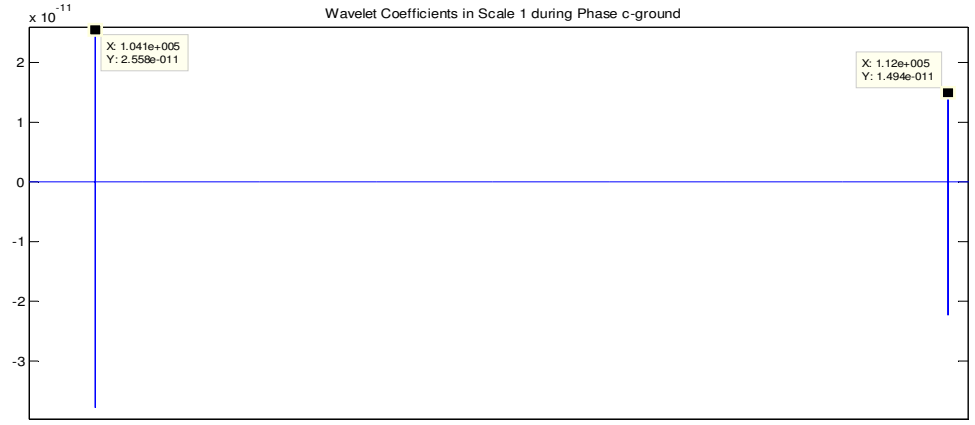

Figure 4.54: First two consecutive peaks

The first peak is the time taken by surge from fault location to Bus B. The second peak is the reflected wave from Bus B to fault location and back to Bus B. The first peak appeared at 2.0812558ms and the second peak appeared at 2.239295ms.

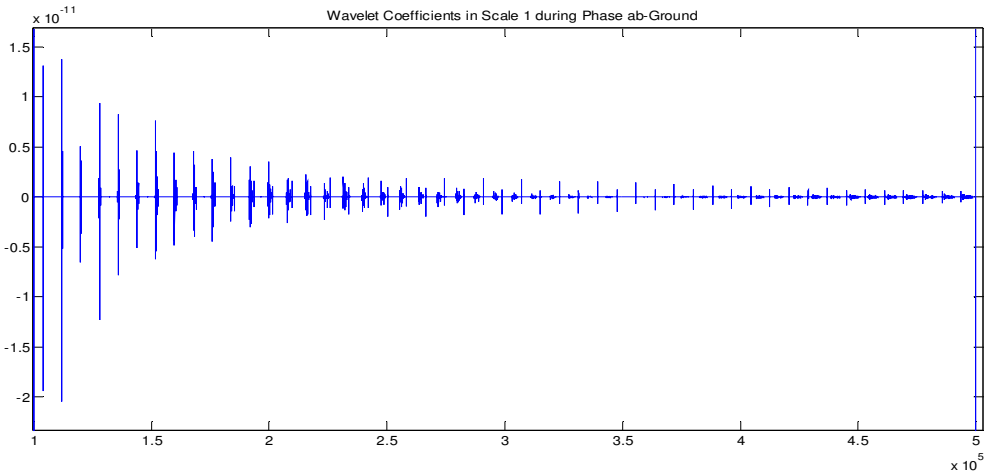

Figure 4.55: Detail coefficient of wavelets at terminal B during Phase ab to ground fault

Figure 4.55 present the wavelet coefficient at Bus B during phase a make connection with phase b fault. Fault was 23 miles away from Bus B. The sampled signal from EMTP was decomposed into four scale levels using Daubechies4 filter. The distance between Bus A and Bus B is 46miles.

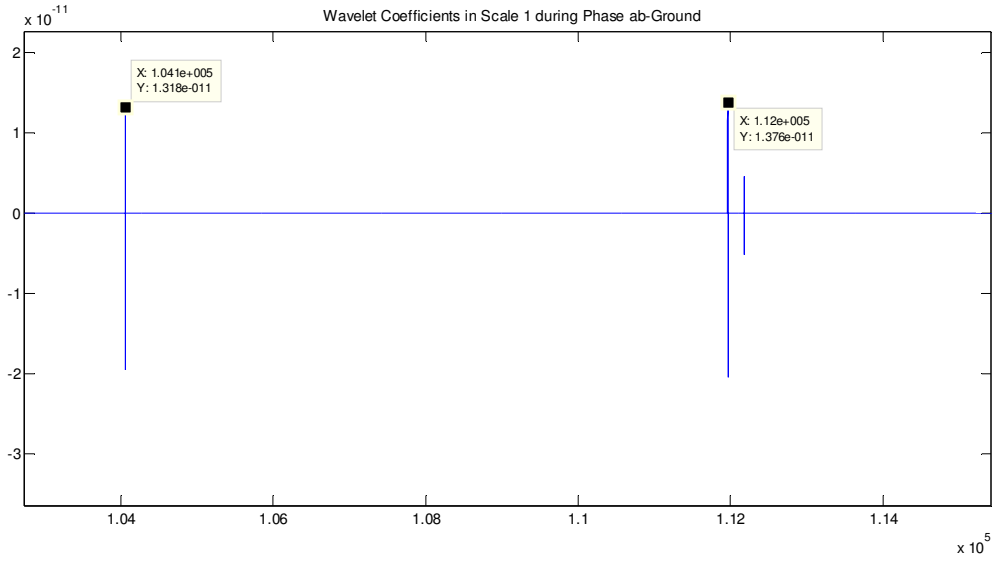

Figure 4.56: First two consecutive peaks

For ungrounded fault, time delay between any two consecutive peaks was taken. The first peak appeared at 2.0812558ms.The second peak appeared at 2.239295ms.

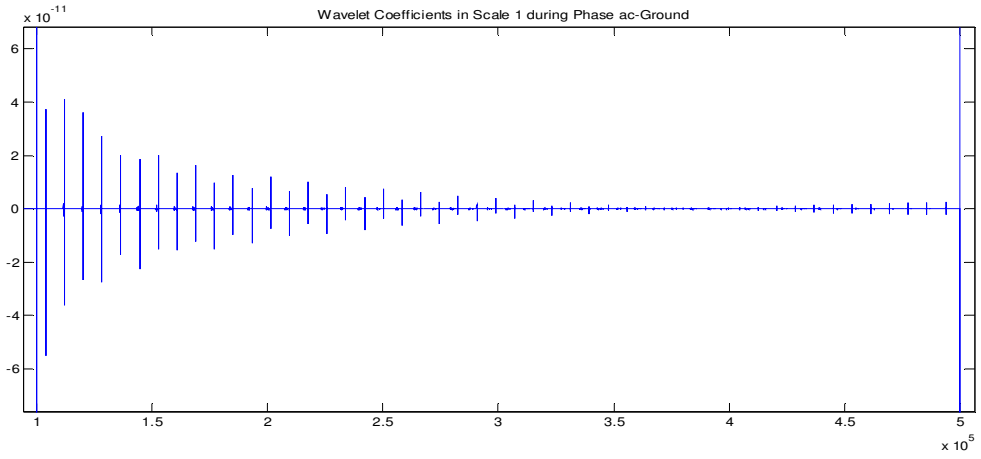

Figure 4.57: Detail coefficient of wavelets at terminal B during Phase ac to ground fault

Figure 4.57 present the wavelet coefficient at Bus B during phase a make connection with phase c. Fault was 23 miles away from Bus B. The sampled signal from EMTP was decomposed into four scale levels using Daubechies4 filter. The distance between Bus A and Bus B is 46miles.

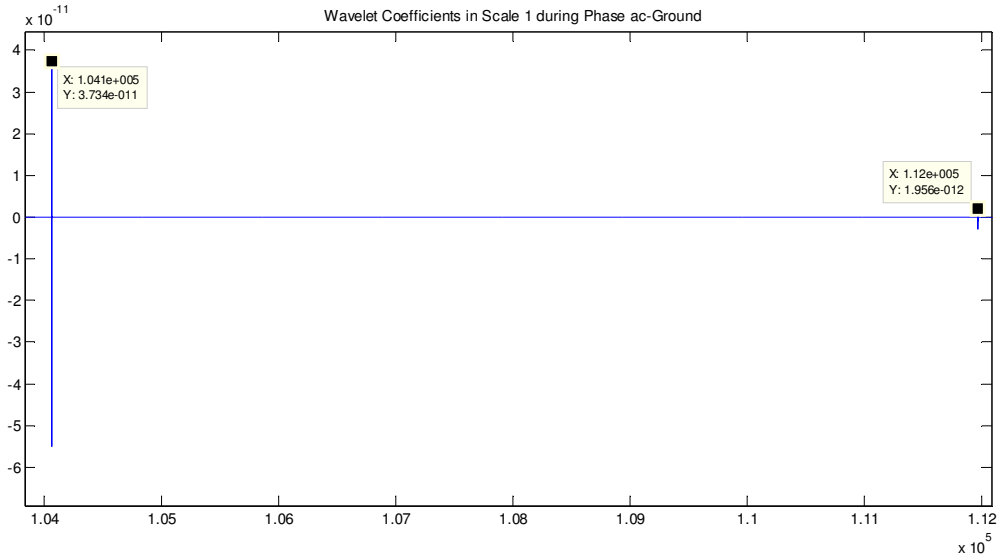

Figure 4.58: First two consecutive peaks

For ungrounded fault, time delay between any two consecutive peaks was taken. Here, the first two consecutive peak was taken. The first peak appeared at 2.081ms.The second peak appeared at 2.2392ms.

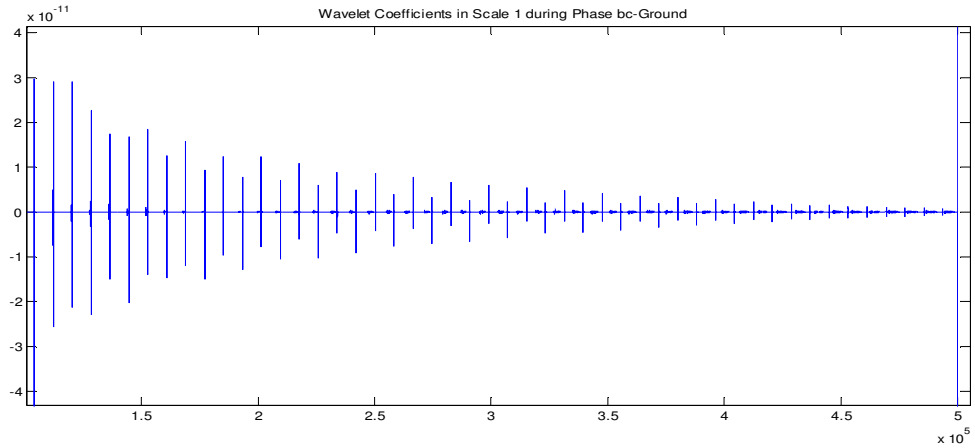

Figure 4.59: Detail coefficient of wavelets at terminal B during Phase bc to ground fault

Figure 4.59 present the wavelet coefficient at Bus B during phase b make connection with phase c. Fault was 23 miles away from Bus B. The sampled signal from EMTP was decomposed into four scale levels using Daubechies4 filter. The distance between Bus A and Bus B is 46miles.

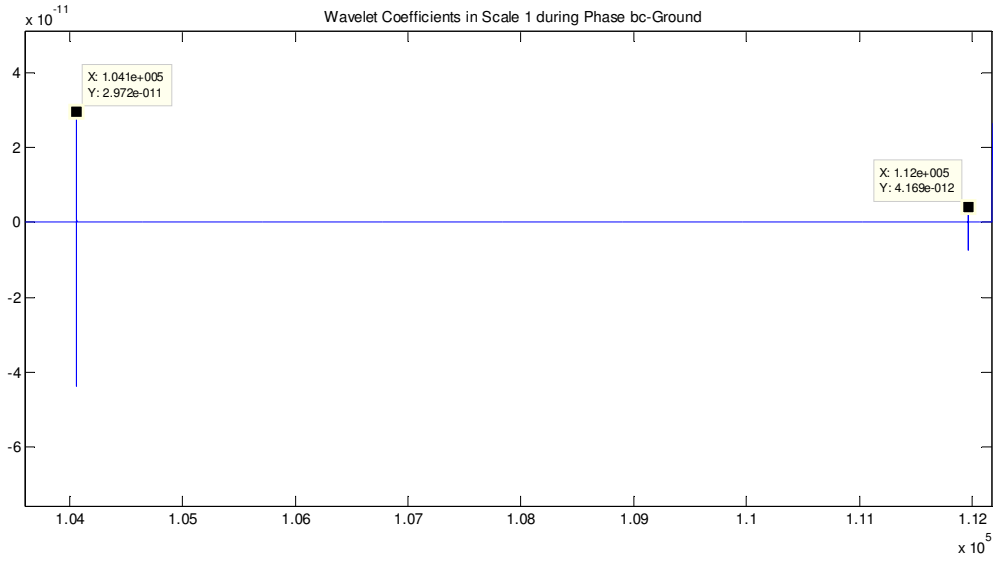

Figure 4.60: First two consecutive peaks

For ungrounded fault, time delay between any two consecutive peaks was taken. Here, the first two consecutive peak was taken. The first peak appeared at 2.081ms.The second peak appeared at 2.2392ms.

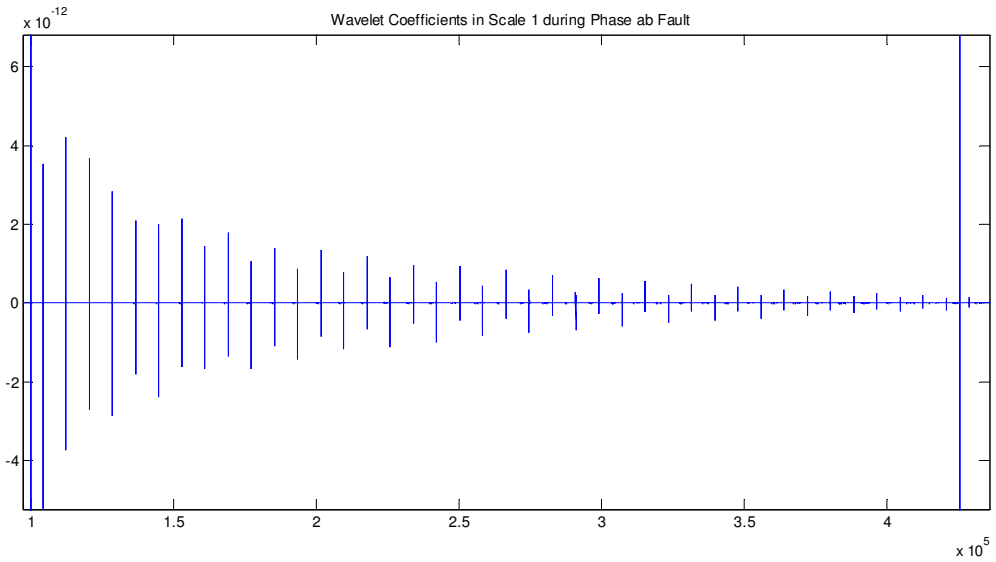

Figure 4.61: Detail coefficient of wavelets at terminal B during Phase ab fault

Figure 4.61 present the wavelet coefficient at Bus B during phase a make connection with phase b. Fault was 23 miles away from Bus B. The sampled signal from EMTP was decomposed into four scale levels using Daubechies4 filter. The distance between Bus A and Bus B is 46miles.

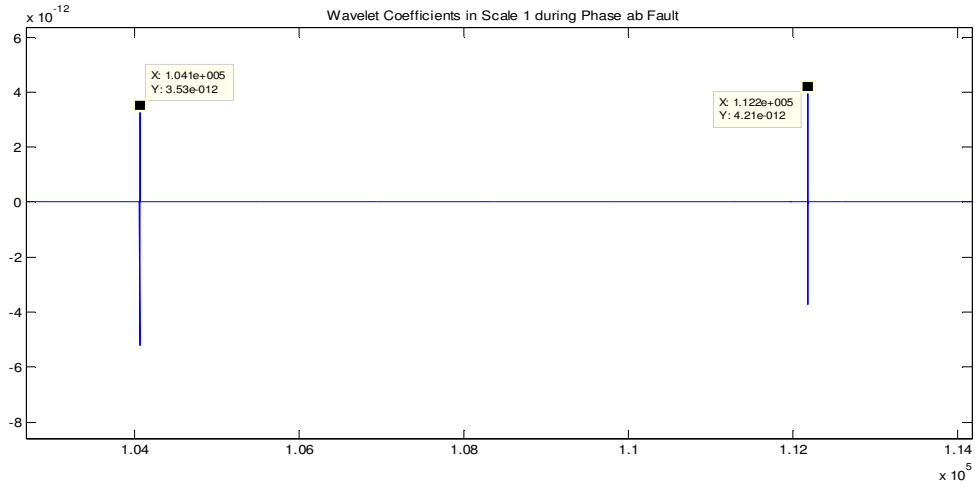

Figure 4.62: Two consecutive peaks

For ungrounded fault, time delay between any two consecutive peaks was taken. The first peak appeared at 2.0812558ms. The second peak appeared at 2.24357ms.

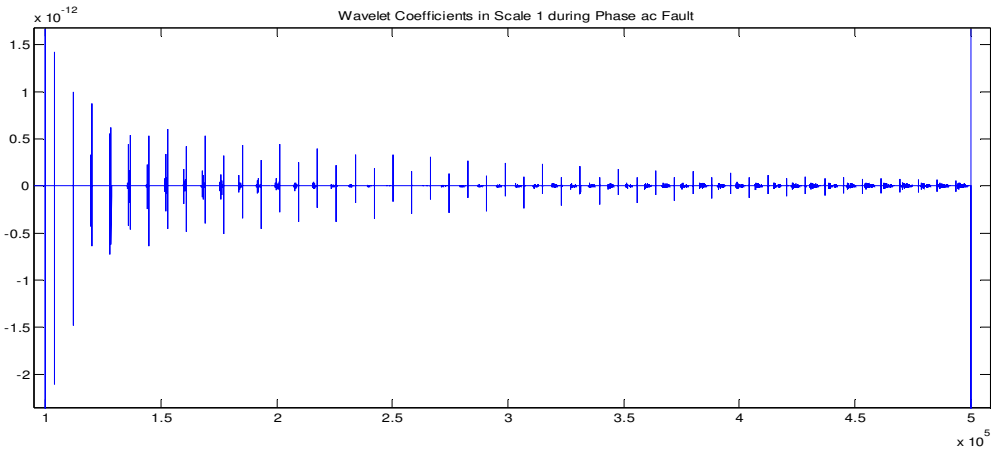

Figure 4.63: Detail coefficient of wavelets at terminal B during Phase ac fault

Figure 4.63 present the wavelet coefficient at Bus B during phase a make connection with phase c. Fault was 23 miles away from Bus B. The sampled signal from EMTP was decomposed into four scale levels using Daubechies4 filter.

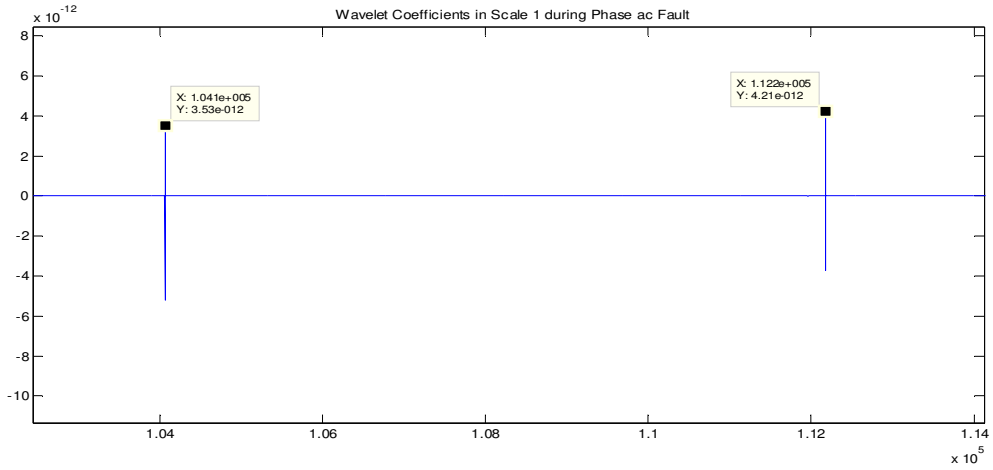

Figure 4.64: Two consecutive peaks

For ungrounded fault, time delay between any two consecutive peaks was taken. The first peak appeared at 2.0812558ms. The second peak appeared at 2.24357ms.

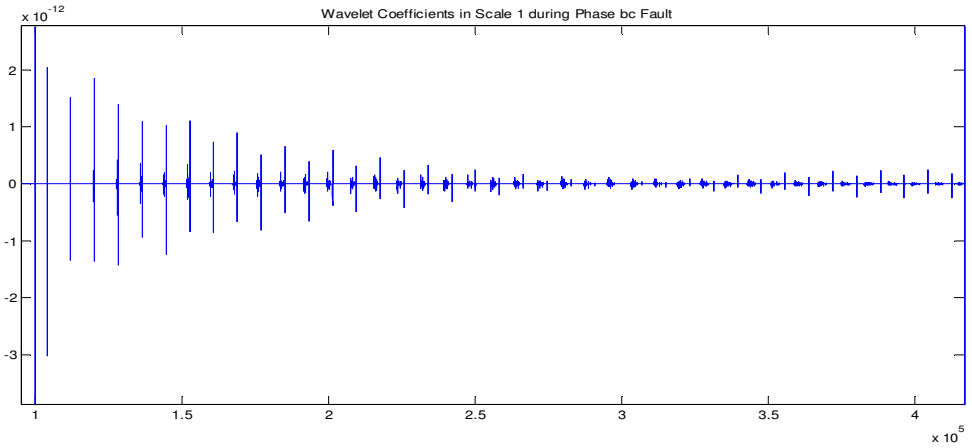

Figure 4.65: Detail coefficient of wavelets at terminal B during Phase bc fault

Figure 4.65 present the wavelet coefficient at Bus B during phase b make connection with phase c fault. Fault was 23 miles away from Bus B. The sampled signal from EMTP was decomposed into four scale levels using Daubechies4 filter. The distance between Bus A and Bus B is 46miles.

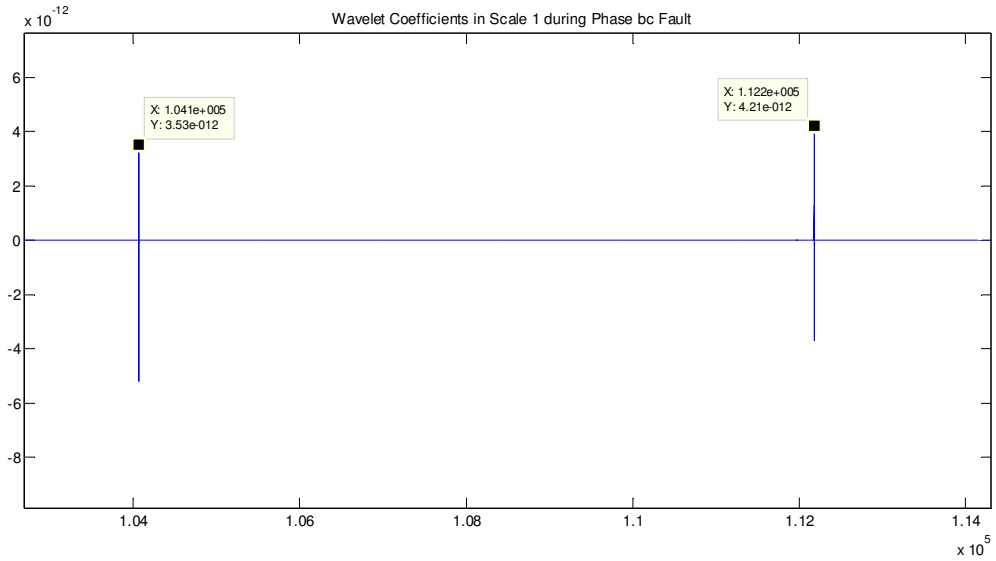

Figure 4.66: Two consecutive peaks

For ungrounded fault, time delay between any two consecutive peaks was taken. The first peak appeared at 2.0812558ms.The second peak appeared at 2.24357ms.

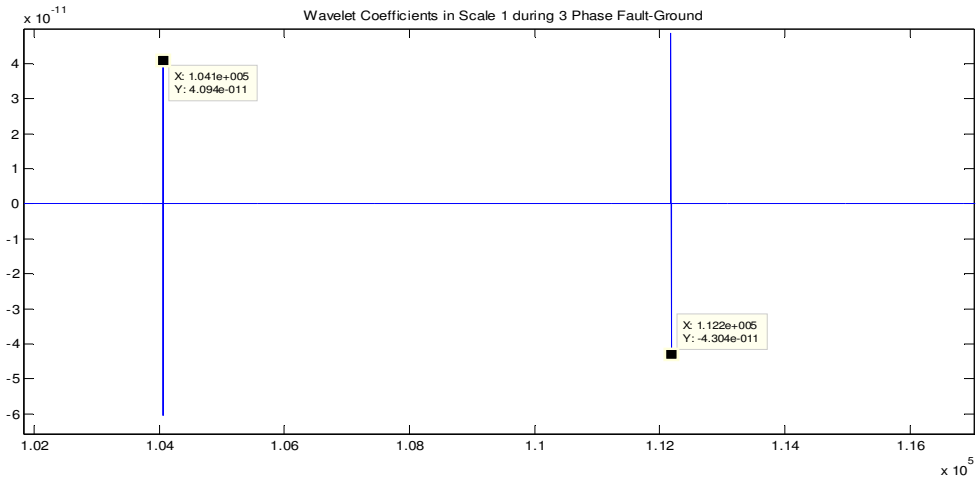

Figure 4.67: Detail coefficient of wavelets at terminal B during 3 phase to ground fault

Figure 4.67 present the wavelet coefficient at Bus B during 3 phase to ground fault. Fault was 23 miles away from Bus B. The sampled signal from EMTP was decomposed into four scale levels using Daubechies4 filter. The distance between Bus A and Bus B is 46miles.

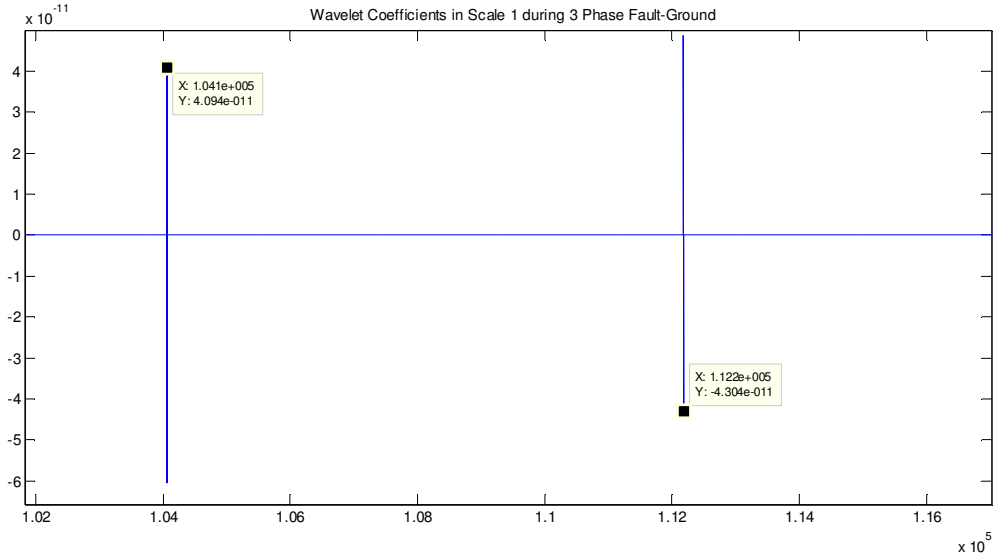

Figure 4.68: First two consecutive peaks.

Figure 4.68 shows the first two consecutive peaks during 3 phase to ground fault. The first peak appeared at 2.0812558ms. The second peak appeared at 2.24357ms.

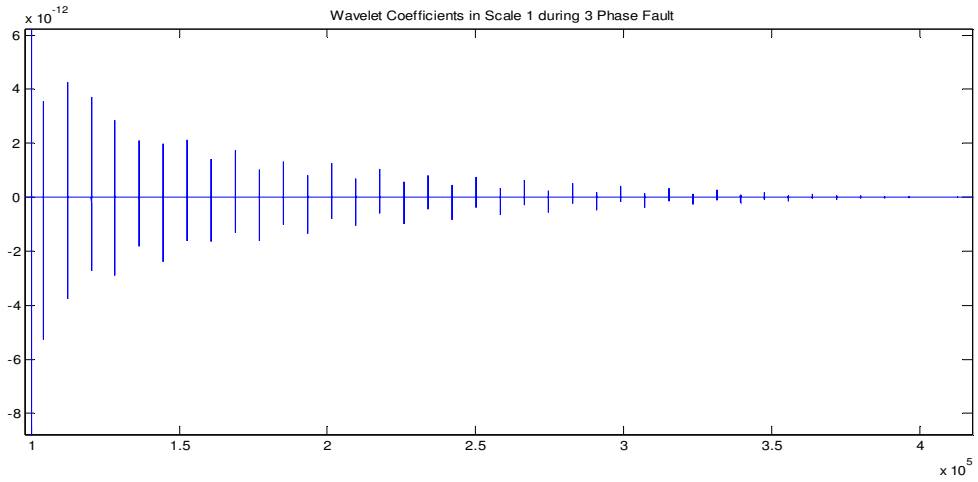

Figure 4.69: Two consecutive peaks of detail coefficients during 3 phase fault

Figure 4.69 present the wavelet coefficient at Bus B during 3 phase fault. Fault was 23 miles away from Bus B. The sampled signal from EMTP was decomposed into four scale levels using Daubechies4 filter. The distance between Bus A and Bus B is 46miles.

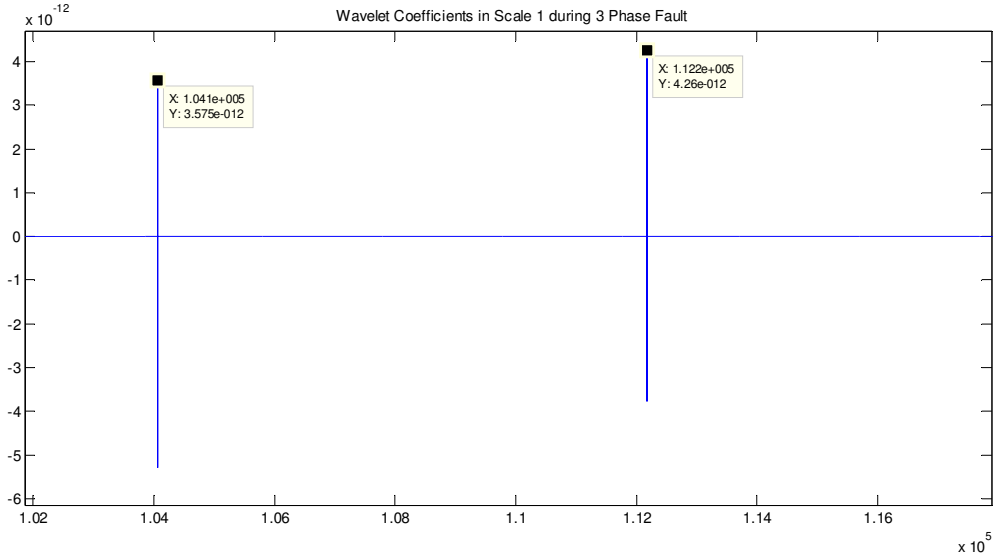

Figure 4.70: Two consecutive peaks of detail coefficients during 3 phase fault

For ungrounded fault, time delay between any two consecutive peaks was taken. Peak appeared at 2.081255ms and peak appeared at 2.24357ms was taken to calculate the fault distance.

Appendix C

C1. MATLAB code for travelling wave method

```
signal= scp16(:,2);%scp16 is sampled wave taken from EMTP
%decomposition filter using Daubechies4 wavelet
[Lo_D,Hi_D] = wfilters('db4','d');
%reconstruction filter
[Lo_R,Hi_R] = wfilters('db4','r');
%it decomposes the signal into 4 level using 'db4' wavelet
[c,l] = wavedec(signal,4,Lo_D,Hi_D);
% it extracts the detail coefficients at level 4 from the wavelet
% decomposition structure [c,l]
[cd1, cd2, cd3, cd4] = detcoef(c,l,[1 2 3 4]);
figure (1); plot (signal); title('Original signal');
figure (2); plot (cd1); title('Scale 1');
figure (3); plot (cd2); title('Scale 2');
figure (4); plot (cd3); title('Scale 3');
figure (5); plot (cd3); title('Scale 4');
```

C2. MATLAB code for impedance based method

The algorithm used by author [31] is followed in this research.

```
close all;
clc;
R= 0.035; %total resistance of transmission line
X= 0.594; %total inductance of transmission line
a1=.1838610; %magnitude of voltage at Bus A
b1=3.11045; % voltage phase at Bus A
a2=0.000238700; %current magnitude at Bus A
b2=3.13145; %current phase at Bus A
a3=0.951584; %magnitude of voltage at Bus B
b3=3.1467; % voltage phase at Bus B
a4=0.00035420187; %current magnitude at Bus B
b4=3.128703; %current phase at Bus B
c1= R*a2-X*b2; %coefficient
c2= R*b2 +X*a2; %coefficient
c3= R*a4- X*b4; %coefficient
c4= R*b4 +X*a4; %coefficient
a= -c3*a1-c4*b1-c1*a3-c2*b3+c1*c3+c2*c4;
b= c4*a1-c3*b1-c2*a3+c1*b3+c2*c3-c1*c4;
c= c2*a1-c1*b1-c4*a3+c3*b3;
del= zeros(30,1);%synchronization angle at k iteration
del1= zeros (31, 1); %synchronization angle at k+1 iteration
```

```
del1 (1) = 0;
for i= 1:30
del(i)= del1(i);
f1= b*cos (del (i)) +a*sin (del (i)) +c;
f2= a*cos (del (i))-b*sin (del (i));
del1 (i+1) =del (i)-(f1/f2);
diff= abs(del1(i+1)-del(i));
m1=(a1*sin(del1(i+1))+b1*cos(del1(i+1))-b3+c4)/(c1*sin(del1(i+1))+c2*cos(del1(i+1))+c4);
%fault distance in percentage from Bus B.
end
```

VITA

Sushma Ghimire was born in Kathmandu, Nepal. She completed her Bachelor of Science in Electronics and Communication Engineering from Tribuvan University, Kathmandu, Nepal in 2006. She worked as BSS engineer (Base Station Subsystem) in Ncell Pvt. Ltd, Nepal from May 2007- June 2010. Ncell is Telecom Company of Nepal. She joined University of New Orleans in Aug, 2011. She is expected to finish her Master of Science in Electrical Engineering from University of New Orleans in May 2014.